Impact of land-use and land-management on the water infiltration capacity of soils on a catchment scale

von der

Fakultät Architektur, Bauingenieurwesen und Umweltwissenschaften

der Technischen Universität Carolo-Wilhelmina

zu Braunschweig

zur Erlangung des Grades eines

Doktors der Naturwissenschaften (Dr. rer. nat.)

genehmigte

Dissertation

von

Mohamed Said Desoky Abu-Hashim

geboren am 10.06.1974

aus Sharkia, Ägypten

Eingereicht am 27. Januar 2011

Disputation am 07. März 2011

Berichterstatter Prof. Dr. Matthias Schöniger

Prof. Dr. Dr. Ewald Schnug

(2011)

Acknowledgement

It is with great pleasure to express sincere thanks and gratitude to Prof. Dr. Dr. habil. Dr. h.c. Ewald Schnug for the kind supervision of my thesis, and for his valuable guidance, support and encouragement.

I am highly indebted to Dr. Holger Lilienthal for his direct supervision, constant encouragement, fruitful suggestion, and critical interest during the preparation of the manuscript.

Many sincere thanks are also for Prof. Dr. Matthias Schöniger for agreeing to act as a second supervisor and for his cooperation and guidance. Similarly, I am so grateful and thankful to Prof. Dr. Rolf Nieder and Prof. Dr. Antje Schwalb for their cooperation and guidance.

Sincere thanks are due to the staff members of the Julius Kühn Institute for their help and encouragement, especially Frau Katrin Bittner for her “digitizing” assistance.

I would like to invest this opportunity to express my gratitude to my wife and my parents for their love and encouragement.

Abstract

Agriculture is the largest user of the resource soil. So, even small changes in certain soil properties can lead to huge effects on a regional scale. The infiltration capacity is as such an important soil parameter, and also a good indicator of soil quality and soil fertility. Silent sealing, as a result of a negative change in the infiltration capacity due to unfavourable land-use and management, will results in severe effects like faster runoff production and flooding on regional scale,.

The assessment of impacts due to land-use or land-management changes on a regional scale is difficult, because detailed information on soil properties and land-management are rarely available. The awareness of the effects of interference in ecosystems is extremely important to supply landscape planners and politicians with information about the impacts of their proposed plans.

The aim of this work is the assessment of the maximum water storage capacity of soils under different land-use and land-management situations in a real river catchment (Schunter). Based on field measurements of infiltration under several land-use and land-management situations, a modelling approach has been developed to determine the maximum potential water storage capacity (S_{max}). This maximum water storage capacity is closely related to the saturated hydraulic conductivity (K_s), and also a suitable indicator, which can be used to compare different land-use/land-management scenarios. S_{max} is a theoretical value describing the maximum potential of a given soil/land-use unit. Although, in reality, the water storage is highly variable due to different soils and land-uses on a catchment scale, S_{max} allows the direct comparison of different soil/land-use units.

Since the required input parameters for detailed process models are often not available at a regional scale, general assumptions and simplifications have to be applied in order to provide meaningful statements. In this special case an integrated measure is needed which takes the soil properties in combination to the land-use and the land-management into account. Such an integrated measure can be found as a part in the Curve Number (CN) from the “Curve Number Model" of the National Resource Conservation Service. The CN is a dimensionless value which has been experimentally identified for a variety of different soil, land-use and land-management situations for small scale catchments in the US. The CN is related to the

water retention potential (S), and S was originally used to compute the direct runoff from a precipitation event. Since this work addresses only the agricultural viewpoint of impacts of land-use and land-management, the main focus is on the relation of CN to the water retention potential and the computation of S_{max}. Final runoff computations were not the aim of this work. Knowing the limitations of the Curve Number Model for hydrological questions, runoff has been computed for the year 2002for demonstration purposes only.

The CN-Model has often been criticized for its obscure determination of the CN from precipitation/runoff relations, which have not been properly published, not even in the official handbooks. In this work new methods for the determination of the CN have been developed. Now the CN can be directly measured (CN_m)based on field infiltration measurements. Use of the saturated hydraulic conductivity allows the computation of the maximum water storage capacity (S_{max}) for a given soil, land-use and land-management combination. Since the maximum storage capacity is used, the prevailing wetting status of the soil can also be neglected.

On a catchment scale, only a subset of all soil, land-use and land-management situations can be covered by measurements. The remaining situations have to be estimated or be adapted from literature values. The use of pedotransfer functions allow the computation of soil properties (e.g., K_s) based on their textural composition. The performance of the pedotransfer functions in comparison to the field measurements have been tested, resulting in a poor capability of predicting correct values from the pedotransfer functions. The comparison of measured CNm with published values of the CN performed very well.

Based on the CNm-Model, scenarios of historic (1950), current (2009) and future (2070) land-uses for the Schunter catchment have been computed, showing the direct impact of different land-use situations to the maximum water storage capacity on a regional scale. Although the scenarios are just snapshots, not taking the temporal dimension of land-use changes into account, this method is useful to detect the impacts of land-use and land-management changes.

This work examined a new method to derive the CN_m by infiltration measurements in the field. The experimental determination of the CN_m allows the update of existing curve numbers

for special situations not covered in the handbook. Also, the application of the CN concept to German soils is now possible. The computation of the maximum potential storage capacity (S_{max}) is a useful measure to identify the impacts and to compare land-use and land-management scenarios.

The impact of land-use and land-management changes on a catchment scale has been clearly demonstrated. Compared to the situation in 1950, in the year 2009the maximum water storage capacity has decreased by 17 %. Projecting a similar land-use change of the past 60 years into the future will result in a loss of water storage capacity of 19 % compared to 1950. The model approach offers a useful tool for landscape analysis. Due to the manifold different land-management practices in agriculture, additional measurements should be performed in the future.

Glossary

Symbol	Description	Dimension
C_c	Clay content	M. M^{-1}
C	Cropland	-
C_{org}	Organic carbon content	L. L-1
E	Evapotranspiration	L
F	Forest	-
G	Grassland	-
h	Pressure head	L
H	Effective pressure head	L
Hs	Pressure value in the standpipe of the hood	L
I_a	Initial abstraction	-
K_s	Saturated hydraulic conductivity	L. T^{-1}
K_u	Unsaturated hydraulic conductivity	L. T^{-1}
n	Pore size distribution index	-
p	Porosity	M. L^{-3}
ρ_d	Dry bulk density	M. L^{-3}
P	Precipitation	L
P_e	Effective precipitation	L. L^{-2}
q_s	Steady state infiltration rate	$L.T^{-1}$
Q	Runoff depth	L
Q_s	Steady flow rate	$L^3.T^{-1}$
r	Radius of the hood	L
S	Potential storage capacity	L
Si	Sink term	$L^3.L^{-3}.T^{-1}$
Sa	Sand content	M. M^{-1}
t	Time	T
U	Urban area	-
Us	Pressure value in a U-pipe manometer	L
W	Water	-
x	Spatial coordinate	L
α	Soil sorptivity number	L^{-1}
θ	Volumetric water content	$L^3.L^{-3}$
θ_r	Residual water content	$L^3.L^{-3}$
θ_s	Saturated water content	$L^3.L^{-3}$

Abbreviation	Description
AGNPS	Agricultural Non-Point Source Pollution Model
AMC	Antecedent Moisture Condition
ATKIS	Amtliches Topographisch Kartographisches Information System
Bük50	Bodenkundliche Übersichtskartierung 1:50.000
CN	Curve Number
CN_m	Measured Curve Number
DEM	Digital elevation Model
DWD	German Metrological Service
eBD	Effective Bulk density
EPIC	Environmental Policy Integrated Climate
GIS	Geographic Information System
HOT-Model	Help of Organic against Torrents-Model
HRU	Hydrologic Response Unit
HSG	Hydrologic Soil Group
KA5	German manual for soil surveying
K_s-M	Measured saturated hydraulic conductivity
K_s-R	Saturated hydraulic conductivity calculated by ROSETTA model
K_s-C	Saturated hydraulic conductivity calculated by COSBY model
K_s-S	Saturated hydraulic conductivity calculated by SAXTON model
K_s-V	Saturated hydraulic conductivity calculated by VEREECKEN model
K_s-B	Saturated hydraulic conductivity calculated by BRACKENSIEK model
NRCS-CN	National Resource Conservation Service Curve Number
PTF	Pedo Transfer Function
SOM	Soil Organic Matter
SWAT	Soil and Water Assessment Tool
SCS	Soil Conservation Service
S_{max}	Maximum water storage capacity

Table of contents

List of figures

List of tables

1 Introduction

Water is vital for all living organisms on earth and the essential constituent of all life. However, it is simultaneously considered a source of death and destruction, mainly due to river floods which are related to heavy precipitation.
In recent years the number of devastating flood events has enormously increased in large parts of Europe. A most impressive example here is the large Elbe River flood in the year 2002, where large parts of eastern Germany were flooded. Major damage to private and public property not only has a negative economic effect but also strengthens the need for an appropriate flood forecasting system that takes into account a changing environment. Furthermore, floods cause great soil erosion resulting in pronounced losses in soils, as well as the deterioration of soil quality resulting in negative effects the yield production of the soils.
Thus the ability of soils to infiltrate water is an important property within the water cycle. The loss of soils due to sealing by buildings and traffic infrastructure is one important factor which influences the water cycle negatively.

The change of the soil infiltration capacity due to inadequate land-management also leads to a *silent sealing* (Schnug & Haneklaus, 2002), a deterioration of soil properties which results in negative impacts (e.g., faster runoff production). On a regional scale the assessment of the impacts which influence infiltration capacity is difficult, since only little information on infiltration properties is available.

The aim of this work is the identification of a parameter suitable to compare the impacts of different land-use/land-management situations to the water infiltration of soil. Within the framework of the well known Curve Number Model from the National Resource Conservation Service (1972), the determination of the water storage capacity (S) offers such a parameter. The assessment of the maximum water storage capacity of soils (S_{max}) under different land-use and land-management situations in a real river catchment (Schunter) has been investigated. Different approaches for the determination of S_{max} have been tested, e.g., based on field

measurements of infiltration under several land-use and land-management situations and computation of pedotransfer functions, and finally the measured values have been compared to published literature values.

This maximum water storage capacity is closely related to the saturated hydraulic conductivity (K_s), and is a suitable indicator, which can be used to compare different land-use/land-management scenarios. S_{max} is a theoretical value describing the maximum potential of a given soil/land-use unit. Although, in reality the water storage is highly variable due to different soil and land-uses on a catchment scale, S_{max} allows the direct comparison of different soil/land-use units.

With common soil maps and databases, soil properties based on the textural composition can be predicted. Mostly, these predictions are performed using pedotransfer functions based on standard laboratory methods derived on homogenized soils. An important soil property is the saturated hydraulic conductivity (K_s) which controls infiltration, but recent studies (Al-Hassoun, 2008, Hartmann et al., 2008) have shown that there are also other impacts:
The land-use (forest, grassland, cropland, urban area) and the land-management (i.e., conventional and organic farming) have different impacts on the infiltration capacity and water storage of the soils. The knowledge about these relationships is very important.
In comparison to conventional farming, with high inputs of fertilisers and the use of heavy machinery leading to soil compaction and a loss of soil biological activity, for example, organic farming produces a sustainable soil structure and high biological activity which enhances water infiltration rates and soil water-holding capacity (Poudel et al., 2001). Furthermore, soils under organic farming will support the biological activity and have plenty of bio-pores, which in turn enhance water infiltration rates into the soil (Schnug and Haneklaus, 2002). Consequently, organic farming can be adopted as a beneficial agronomic measure for improving soil properties and enhancing soil infiltration capacity.

In this work several field infiltration measurements have been performed under different land-use and land-management situations, combined with the measurement of additional soil properties (e.g., bulk density, texture, organic matter content). Also digital soil data are available for every field measurement.
The infiltration was measured by using a Hood-Infiltrometer (Schwärzel and Punzel, 2007). Furthermore, the hood infiltrometer is used for measuring the saturated soil hydraulic properties as integral information over the upper soil horizons, utilizing the equations of Wooding (1968) and Gardner (1958).

Since the required input parameters for detailed process models are often not available at a regional scale, general assumptions and simplifications have to be applied in order to obtain meaningful statements. In this special case, an integrated measure is needed which takes the soil properties in combination to the land-use and the land-management into account. Such an integrated measure can be found as a part of the Curve Number (CN) from the “Curve Number Model" of the National Resource Conservation Service (1972). The CN is a dimensionless value which has been identified experimentally for a variety of different soil, land-use and of land-management situations for small scale catchments in the US. The CN is related to the water retention potential (S), and S was originally used to compute the direct runoff from a precipitation event. Since this work addresses only the agricultural viewpoint of impacts of land-use and land-management, the main focus has been put on the relation of CN to the water retention potential and the computation of the maximum water storage capacity (S_{max}).
The CN-Model has often been criticized for its obscure determination of the CN from precipitation/runoff relations, which have not been properly published, not even in the official handbooks. In this work, new ways to determine the CN have been developed. Now the CN can be directly measured (CN_m) based on field infiltration measurements Using the saturated hydraulic conductivity allows the computation of the maximum water storage capacity (S_{max}) for a given soil, land-use and land-management combination. Since the maximum storage capacity is used, the prevailing wetting status of the soil can also be neglected.

On a catchment scale only a subset of all soil, land-use and land-management situations can be covered by measurements. The remaining situations have to be estimated or be adapted with literature values. The use of pedotransfer functions allow the computation of soil properties (e.g., K_s) based on their textural composition. The performance of the pedotransfer functions in comparison to the field measurements has been tested in this work, as well as the comparison of measured CN_m with published values of the CN.

Due to its simplicity, the Curve Number Model soon became one of the most popular techniques for engineers and practitioners, mainly for small catchment hydrology (Mishra and Singh, 2006). It has been in use for about 50 years, and is a popular, ubiquitous, and enduring means of estimating storm runoff from rainfall events. Since its inception, new applications and developments have emerged, and insights to general rainfall-runoff hydrology have been gained. It has to be stated again that this work addresses only the agricultural viewpoint of impacts of land-use and land-management, the main focus has been put on the relation of CN to the water retention potential and the computation of S_{max}. Final runoff computations were not the aim of this work!

Although the Curve Number Method was originally developed in the United States and is mainly for the evaluation of storm runoff in small agricultural watersheds, it soon evolved well beyond its original objective and was adopted for various land-uses such as urbanized and forested watersheds (Mishra and Singh, 1999).

It should be noted that much of the international interest is prompted by the wide array of agriculture and water quality models such as AGNPS: Agricultural Non-Point Source Pollution Model (Young et al., 1987), EPIC: Environmental Policy Integrated Climate (Williams, 1995), and SWAT: Soil and Water Assessment Tool (Arnold et al., 1996), which incorporated elements of the CN method for runoff generation and soil moisture management. In addition, these models seem to have achieved a life and a user group of their own, and the CN components are used as a fixed background technology.

The CN-Model has often been criticized for its obscure determination of the CN from precipitation/runoff relations, which have not been properly published, not even in the official handbooks. In this work, new ways to determine the CN have been developed. Based on field infiltration measurements, now the CN can be directly measured (CNm)! The use of the saturated hydraulic conductivity allows the maximum water storage capacity (S_{max}) to be computed for a given soil, land-use and land-management combination. Also, the performance of pedotransfer functions for the determination of the CN has been tested. Since the maximum storage capacity is used, the prevailing wetting status of the soil can also be neglected.

So far all computations are made on plot scale only, but with the availability of digital soil maps, the infiltration properties can be regionalised based on pedo-cells.
The modification of the classical CN approach and its application on a regional scale allows the impact of land-use change and different land-management on soil infiltration to be estimated. Land-use information from 1950 and 2009 is available for a test-site close to Braunschweig (Schunter catchment). Assuming that in 1950 agriculture was a low input system using fewer mineral fertilizers, and low weight machinery, the change of the infiltration capacity for the whole region can be estimated based on the change of land-management and the loss of soil due to soil sealing. Derived from the land-use changes between 1950 and 2009, a projection into the future can be made to estimate in which way the infiltration capacity might change. Although, the scenarios are just snapshots, not taking the temporal dimension of land-use changes into account, this method can be useful to detect the impacts of land-use and land-management changes.

Objectives of this work

Using the Curve Number to predict the maximum storage capacity as a measure of the watershed retention potential (Hawkins et al., 2009), it will be compared with the infiltration capacities measure (saturated hydraulic conductivity or K_s) as an alternative measure of retention ability closely linked to soil properties, profile, and land-use.

This leads to several hypotheses:

- The originally published CN values are still reliable without modification under different land-use and land-management situations.

- Different types of land-use and/or land-management have an impact on the water infiltration capacity of soils.

- The maximum storage capacity S_{max} is a suitable measure to compare the impact of different land-use and land-management.

- The determination of the Curve number (CN_m) by field infiltration measurements is a measure to explain the impact of different land-uses and land-management styles on the soil infiltration capacity.

- Based on S_{max}, scenarios can be developed for the impact of the land-use change between 1950 and 2009 on the infiltration capacity of the Schunter catchment area.

- The infiltration capacity on a catchment scale can be improved by a change in the land-management.

- The change of the agriculture management practices can be used for a preventive flood protection.

2 Relation between land-use/land-management and infiltration

"*Infiltration is the term applied to the process of water entry into the soil, generally by downward flow through all or part of the soil surface. The rate of this process determines how much water will enter the root zone and how much, if any, will run off" (Hillel 2004).*The infiltration is sensitive to the near surface conditions of the soil, as well as the antecedent water conditions. Soil can be an excellent temporary storage medium for water, depending on the type and the condition of the soil (USDA 1998), but if the rainfall intensity is greater than the infiltration rate, water will accumulate on the surface and runoff will begin. The rate of infiltration normally declines rapidly during the early stage of a rainstorm event and reaches a constant value after several hours of rainfall. This steady-state infiltration can be converted to the saturated hydraulic conductivity. This is the maximum infiltration rate a specific soil can reach.

In terms of time fist there is the filling of small pores on the soil surface with water reduces, which reduced the ability of capillary forces to actively move water into the soil. As the soil moistens, the structures of the clay particles absorb water causing them to expand. This expansion reduces the size of soil pores and reduces the infiltration. Also raindrops break large soil clumps into smaller particles. These particles then clog soil surface pores reducing the movement of water into the soil.

The location of a soil in the landscape (e.g. slope, crest, depression) has also an impact on the infiltration rate, since vertical water movement can turns into lateral movement depending on the slope. The infiltration should be measured as steady-state infiltration on flat terrain, in order to attribute the changes in infiltration on land-use, land-management and the soil. The temporal variability of the infiltration rate can be neglected using measurements under saturated conditions. In term soil quality, the infiltration should be high. Proper management of the soil can help to maximize the infiltration.

The land-use (e.g. forest, grassland, cropland, urban area) and the land-management (i.e. conventional and organic farming) have different impacts on the infiltration

capacity and water storage of soils. The knowledge about these relationships is very important to minimize soil water erosion impact and to guarantee high infiltration rates.

2.1 Impact of land-use on infiltration

It is generally accepted that changes in land-use patterns (e.g. expansion of settlements including deforestation, road-construction, distinct practices in arable land and grassland management) contribute to an increased frequency and severity of flood generation. For forest land-use, it has been stated that the promotion of sustainable forest management will considerably increase the water retention in landscapes (FAO, 2003).

The highest infiltration capacity noted in the forest soil was due to a higher content of soil organic matter and an improved soil structure as well as a high fraction of macro-pores produced by the root activity (Wahren et al., 2009; Mapa, 1995). Moreover, the study of Mann and Tolbert (2000) revealed that the presence of decayed root channels leading to spots with high infiltration rates, and the great development of roots at deeper depths in the soil provides higher soil stability and results in more pathways for water infiltration. Heermann and Duke (1983) reported that the presence of litter layers on the soil surface of forest retards the surface runoff and provides more time for water to infiltrate into the soil. Not only the macropores and the pre-event soil moisture are influenced by the land-use, but also the water retention characteristics due to a changed pore distribution (Wahren et al., 2007a). Thus, the change in land-use will have distinct effects on infiltration capacity and the water retention. Wood and Blackburn (1981), Schukla et al., (2003) and Fu et al., (2006) stated that change in land-use affect physical, chemical, and biological characteristics of the soil and the infiltration capacity influenced by the soil structure, and land-use.

Due to the development and the urbanization activity, land-use is subjected to changes causing soils to be impervious surfaces, which leads to decrease in the soil infiltration capacity and consequently increase the amount of runoff.

Grassland has a higher infiltration capacity compared to the arable land (Ernest and Tollner 2002, and Al-Hassoun 2009). These studies deduced that the infiltration rate is higher under grass compared to field crops. This could be attributed to the higher soil compaction in arable lands due to a high stress induced by field machinery leading to higher soil dry bulk density and decreased infiltration rates. The grassland is initially under no tillage or mechanical stress, and so has less compaction, a lower soil dry bulk density and increased infiltration rates. These results corresponded with Cameron et al., (1981). Tollner et al., (1990) and Broersma et al., (1995) who demonstrated that the land-use change from natural or semi-natural vegetation to continual tillage and grazing has a pronounced effect on the soil bulk density, porosity, infiltration, water storage, water transport characteristics, and runoff, and Hillel (1982) revealed that the compaction could reduce the largest soil pores resulting in a diminished infiltration rate.

In addition, grassland provides a permanent soil cover that could decreases the negative impact of raindrops on the soil surface and thus reduces the degradation of the aggregate stability, declines the surface runoff rate, and giving more time for infiltration (Laurance, 2007; Schüler, 2006; Armbruster et al., 2004; Bronstert, 2004).

On the other hand, the perennial grass produces a greater amount of plant biomass in the soil, leading to a higher accumulation of the surface organic matter, which in turn contributes to enhanced infiltration rates, compared to the annual vegetation (Wienhold and Tanaka, 2000).

The ability of the forest and the grassland to increase the water storage capacity in the watershed relay on their saturated hydraulic conductivity potential. This finding is proved by the work of Wahren et al., (2009), who pronounced that the higher small-scale heterogeneity under forest is mainly due to the presence of decayed root channels leading to spots with high infiltration rates. Obviously, the ploughed arable land has a destroyed macropores structure. After infiltration, water cannot further percolate into the subsoil because the macropores are cut at the lower boundary of the

plough horizon. Thus, the infiltration capacity at the arable plot is lower than at the forest plots and less variable.

The higher soil infiltration capacity and so the saturated hydraulic conductivity are associated with a higher content of the soil organic matter under the forest land-use and grassland compared to the agricultural land-use.

2.2 Impact of land-management on infiltration

The rate of water infiltration into the soil, its consequence movement in the soil matrix and surface runoff are important consideration in developing land-management practices which increase the efficiency of rainfall use and maintain a favourable soil water condition that is crucial for plant and soil health. Moreover, land-management alters infiltration and runoff through their effect on soil structure and micro-topographical modifications, as by providing physical barriers to runoff (Young, 1997).

Soil sealing is considered one of the main threats to soil as organic matter decline, flooding, erosion, soil biodiversity loss, contamination and landslides (Campbell, 2008). The problem of soil sealing intensified by inappropriate agronomic managements is qualified as “silent” sealing. It can also be expressed as a loss of the soil infiltration capacity induced by the soil surface sealing or the subsoil sealing (soil compaction).

Conventional farm management, including the removal of crop residues from the soil, leads to great damages to the soil aggregates, revealing a loss of mechanical stability (Unger, 1992; Hernanz et al., 2002; Rogasik et al., 2004). Numerous studies have demonstrated that the infiltration capacity of soils can be a good indicator of the soil quality and health (Wood and Blackburn, 1981; Mc Calla et al., 1984; Abdul-Megid et al., 1987; Shukla et al., 2003; Dexter, 2004). The results of Al-Hassoun (2009) revealed that the higher soil aggregate stability was related to a greater content of soil organic matter under conservation tillage in comparison to conventional tillage, and the higher infiltration rate was generated not only by larger numbers of soil macropores and biopores but also by a higher soil resistance to the surface sealing.

Many factors could contribute to the greater pore driven infiltration under these managements, including enhanced soil aggregation as a result of increasing the organic matter content, enhancing of percolation resulting from roots as channel for pass flow and increasing the number of flow paths resulting from the soil fauna populations (Bouma et al., 1982). The high soil aggregate stability can be achieved under tillage treatments, which guarantee no or minimum soil disturbance and contribute to higher inputs of surface crop residues as a resource of ecological management. The organic farm management, due to the improved soil structure and the higher biological activity, is a better strategy to guarantee higher infiltration capacity compared to the conventional management.

Mapa and Gunasena (1995) noted that the higher aggregate stability produces a higher macro-porosity in the soil, which in turn results in a higher soil infiltration capacity. On the other hand, it is well known that organic management never uses pesticides, which adversely affect earthworms. Therefore, organic management is more useful for earthworm populations in comparison to conventional management. This fact was associated with Schnug et al., (2004) who stated that organic management results in a greater number and biomass of earthworms producing more "biopores" in the soil, and hence higher infiltration capacity in comparison to conventional management.

Poudel et al., (2001) demonstrated that organic management leads to a better soil structure and higher biological activity and greatly infiltration capacity of soil. In addition, the work of Wuest (2001), Al-Hassoun (2009) and Hartmann et al., (2009) revealed that the different soil management and tillage intensities influenced the water infiltration capacity into the soil significantly. The differences observed in the infiltration rates were a consequence of the changes in soil physical, chemical and biological properties induced by different tillage treatments (Pelegrin et al., 1990). Furthermore, the influence of soil tillage on infiltration rates should be considered from the viewpoint of the loosening effect and the impact of earthworm abundance (Al-Hassoun, 2009). Soil tillage intensity affects the distribution of macropores resulting in changes in the soil infiltration potential (Logsdon et al., 1990).

On the other hand, it was pronounced that higher infiltration rates are due to a distinctly higher soil aggregate stability under shallow tillage, in contrast to deep tillage. This is predominant because shallow tillage results in the concentration of organic matter in the topsoil, producing a high soil aggregate stability (Kouwenhoven et al., 2002), which in turn enhances the soil porosity promoting more water infiltration through the soil.

Conservation tillage -maintaining the surface crop residue- can achieve a high soil structural stability, reduce the prospect of plough pans formation, enhance the water infiltration potential, and decrease the soil surface sealing (Rogasik et al., 2004). Otherwise, conventional tillage leads to a loss of the mechanical stability, a reduction of the soil organic matter content, and a soil compaction resulting in negative impacts on the soil water infiltration (Hermawan and Cameron, 1993).

Higher soil organic matter content increased the soil aggregate stability under organic management, as the soil aggregate stability is positively related to the soil organic matter content (Tisdall and Oades, 1980). Organic farming and conservation tillage, through enhancing the infiltration capacity, could offer means as alternative strategy for flood protection. It takes place because of the mechanical stress on the soil induced by heavy machinery loads (Etana and Håkansson, 1994), and due to intensive tillage operations (Gaultney et al., 1982). Soil compaction leads to a decrease of soil macropores, an increase of the soil dry bulk density and the penetration resistance and hence causes reductions of water infiltration rates (Hillel, 1982; Oussible et al., 1992; Håkansson and Reeder, 1994; Ishaq et al., 2003).

3 Materials and Methods

This chapter presents the investigation area, methodology and data used in this work. It explains the preparation of digital data sets, the field data collection, and the hydrological modelling to examine the relationship between land-use, land-management and the infiltration properties. Also the land-use change detection for the period 1950 – 2009 and the simulation scenarios are described.

3.1 Investigation area

The investigations were carried out in the catchment area of the river Schunter (3598000, 5806000, Gauß Krüger, Zone 3), a 60 km long tributary stream of the Oker, which is discharging to the river Weser. This test site is situated east of Braunschweig, Germany (Fig. 3.1). The Schunter catchment is approximately 610 km² in size and this region reflects approximately the land-use conditions in Germany with 60 % of crop- and grassland, 27 % forest, and 12 % urban area and traffic infrastructure (Statistisches Bundesamt 2010).

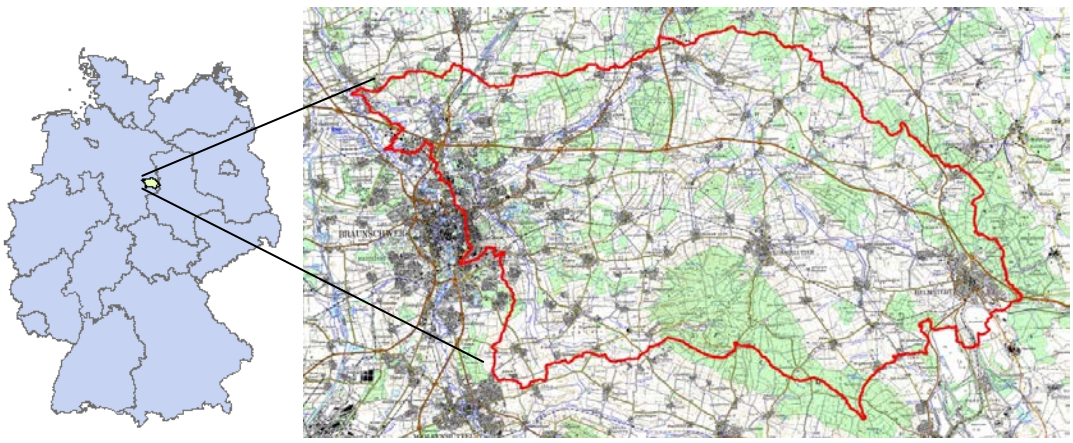

Fig. 3.1: Catchment area of the Schunter (Base map: Source BKG).

3.1.1 Geographic description

The catchment area is defined on the west by the city of Braunschweig, on the east by state border to Saxony-Anhalt in Helmstedt. To the south, the watershed of the Elm ridge is the natural boundary and in the north the city of Wolfsburg defines the study area (Fig. 3.1).

The test site covers two physical regions: The northern part is the so called "Ostbraunschweigisches Flachland"; the southern part is called "Ostbraunschweigisches Hügelland" (BfN, 2007). The Schunter stream has its source southwest of the village Räbke, in the "Ostbraunschweigischem Hügelland", a wide-open hollow landscape, from which the Elm ridge rises.
The Elm is made from lime- and sandstone and is completely forested. The whole area is covered with loess that is washed only on the slopes of the mountain ridge, resulting in excellent farmland. In the south-eastern corner of the test site is an old brown coal mining area.

The northern part the "Ostbraunschweigisches Hügelland" represents a transition zone between the more rolling hills in the South and the North German Lowland.
In contrast to the southern Loess soils many areas with older bedrock consisting of clay, marl, limestone and sandstone emerge to the surface. In the southeast rolling hills rise up to 194 m (Lappwald). The landscape then descends slowly to the northwest to an elevation of 60 meters (BfN, 2007).

The delineation of the catchment has been performed, using a digital elevation model (Chapter 3.2.5). The Schunter area can be divided into six sub catchments, according to the main tributaries (Wabe, Sandbach, and Uhrau) and the Schunter itself (Fig. 3.2).

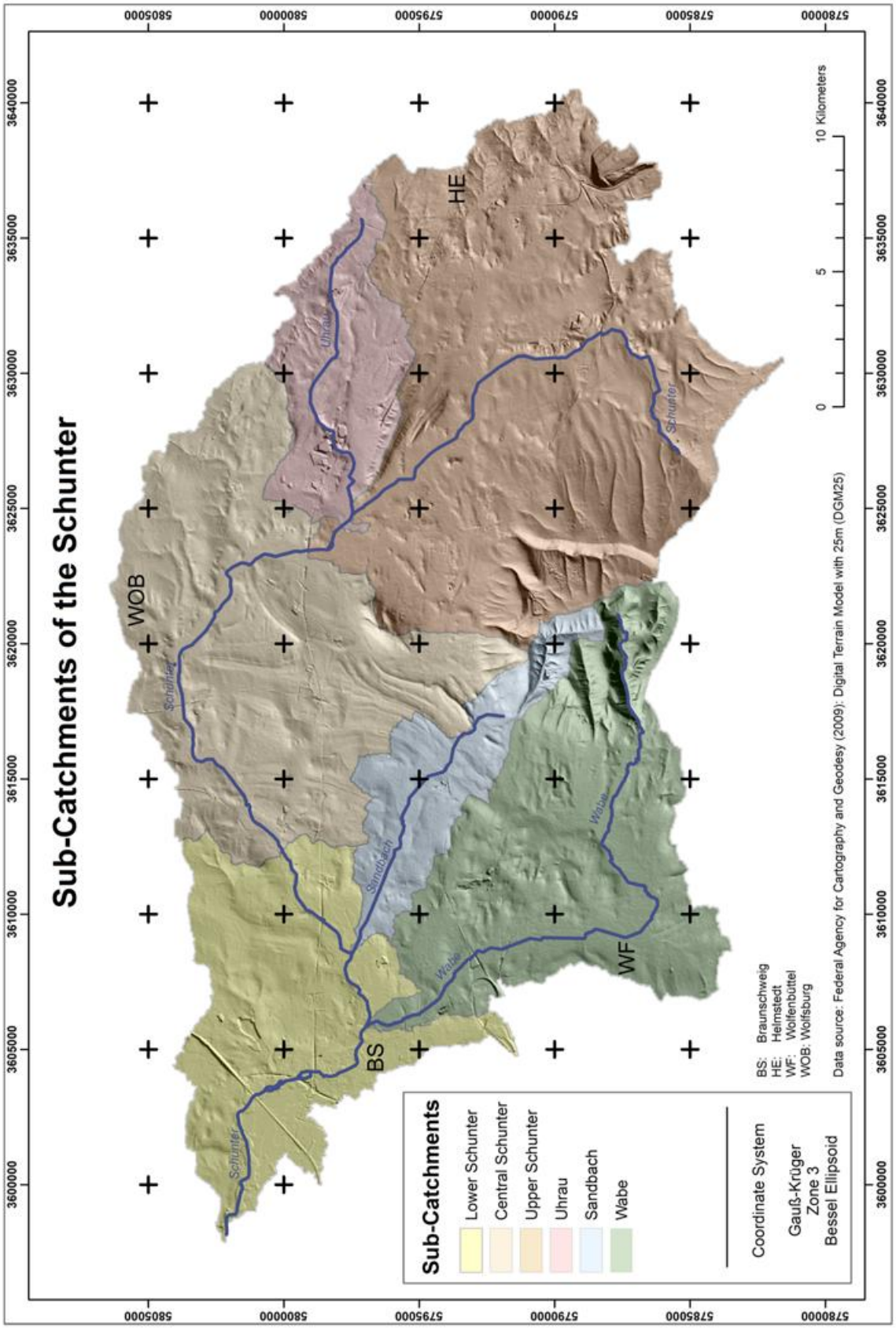

Fig. 3.2: The sub catchments of the Schunter catchment.

The sub catchments differ in their characteristic land-use distribution (Tab. 3.1). The largest sub catchment, the *Upper Schunter*, covers 33 % of the total area and has the highest proportion of forest. The third largest sub catchment, the *Wabe*, covers 18 % of the total area and has the highest proportion of cropland.

The sub catchment of the *Lower Schunter* (14 % of the total area) has the largest proportion of urban area, whereas the smallest sub catchment (*Uhrau*, 7 % of the total area) has the highest proportion of grassland of all sub catchments.

Tab. 3.1: Land-use distribution of the sub catchments of the Schunter catchment (Database: BKG, 2009).

Catchment / Land-use	Upper Schunter		Uhrau		Central Schunter		Sandbach		Wabe		Lower Schunter	
	[ha]	[%]	[ha]	[%]	[ha]	[%]	[ha]	[%]	[ha]	[%]	[ha]	[%]
Cropland	10404	51.4	1985	47.7	6837	50.1	1747	49.3	5801	53.2	3052	36.1
Grassland	1227	6.1	778	18.7	2433	17.8	502	14.1	914	8.4	1120	13.3
Forest	6545	32.3	1109	26.7	3418	25.0	1034	29.1	2752	25.3	1960	23.3
Urban area	1947	9.6	258	6.2	919	6.7	264	7.4	1353	12.4	2189	26.0
Water	122	0.6	30	0.7	51	0.4	4	0.1	78	0.7	109	1.3
Total	20245	100	4161	100	13658	100	3551	100	10898	100	8431	100

The mean elevation for the total area is 120 m above sea level (asl). The sub catchments are located in elevations between 59-322 m asl, the old mining area is the lowest depression with 37 m asl.

Tab. 3.2: Elevations and slopes of the Schunter catchment area (Database: BKG, 2009).

Catchment / Parameter	Schunter Catchment		Upper Schunter		Uhrau		Central Schunter		Sandbach		Wabe		Lower Schunter	
	Min	Max	Min	Max	Min	Max	Min	Max	Min	Max	Min	Max	Min	Max
Elevation [m]	37	322	37	314	90	181	74	280	70	314	68	322	59	113
Slope [°]	0	41	0	27	0	22	0	15	0	41	0	29	0	22

The area is generally flat with a mean slope of 2°, in the Elm region steeper slopes of 41° are reached (Tab. 3.2, Fig. 3.3).

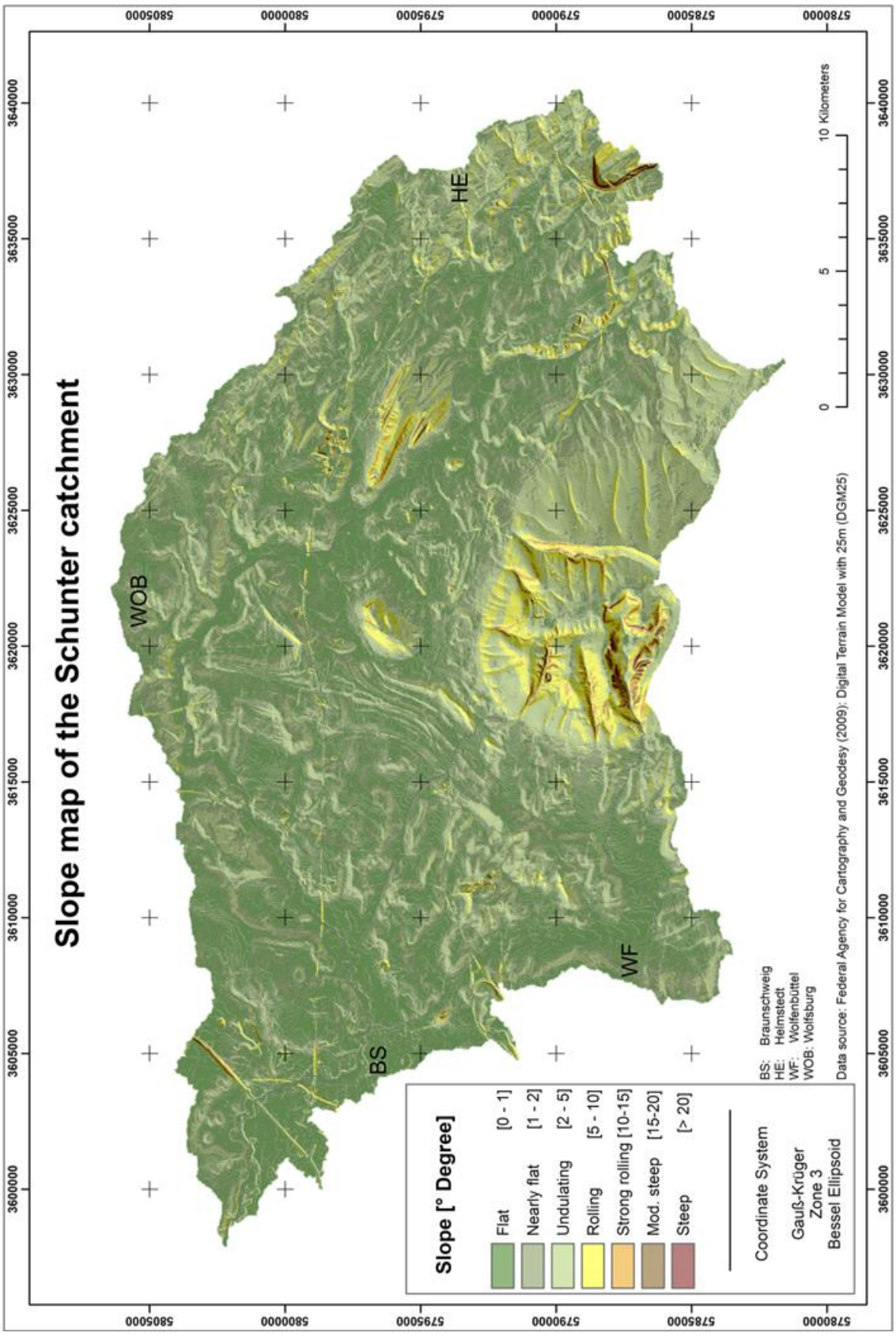

Fig. 3.3: Slope classification of the Schunter catchment (According to KA 5).

3.1.2 Climate and Hydrology of the Schunter catchment

The study area is characterized by moderate climatic temperature conditions, with an annual mean temperature of 9.2 °C, a maximum mean temperature of 17.7 °C in the warmest month and 1.2 °C in the coldest month. The 30-year climatic data of the German Meteorological Service (DWD) indicates for Braunschweig an annual rainfall of 599 mm (Fig. 3.4)

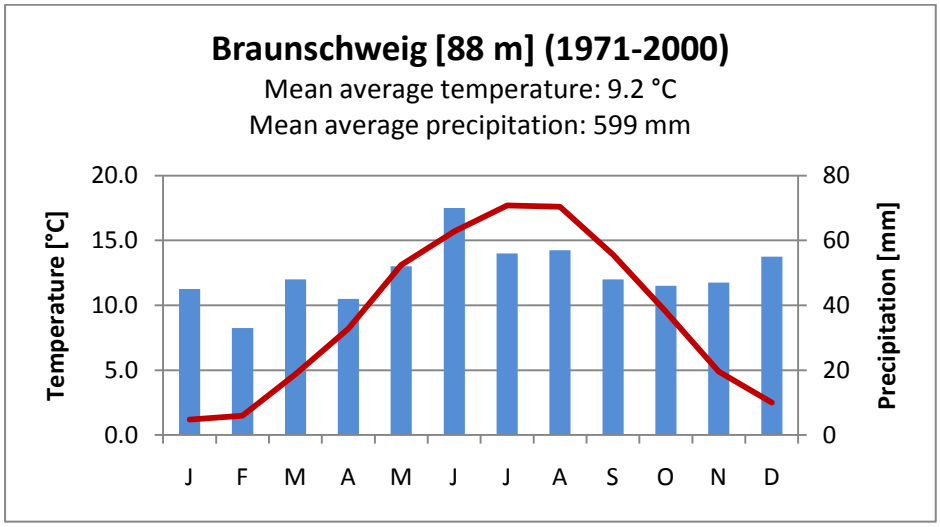

Fig. 3.4: Climate chart of Braunschweig (DWD, 2010).

Within the catchment of the Schunter, only one water gauge station at Harxbüttel, close to the outlet of the Schunter to the Oker, exists. The mean annual flood discharge is 9 to 10 times higher compared to the mean discharge, whereas the minimum discharge is around 4 times smaller than the mean discharge.

The discharge parameters are listed in Table. 3.3, detailed runoff data for 2002 and 2005 can be found in the appendix.

Tab. 3.3: Discharge parameters of Harxbüttel, Schunter (NLWKN, 2010).

	1961/2005	2005
	[$m^3 \cdot s^{-1}$]	
MHQ: Mean annual flood discharge	28.9	(HQ) 20.6
MQ: Mean discharge	3.3	2.5
MNQ: Mean annual minimum discharge	0.6	(NQ) 0.6

3.1.3 Soils in the Schunter catchment

The dominating soil types in the catchment area are Planosols in combination with Cambisols and Vertisols (Tab. 3.4). Figure 3.5 shows a map with the distribution of the soil types for the catchment area.

Tab. 3.4: Soil types in the Schunter catchment according to the World reference base (FAO, 2006).

Soil type (WRB)	Area [%]
Planosol	20.7
Planosol/Cambisol	13.8
Vertisol/Planosol	10.4
Leptosol	8.8
Podzol/Cambisol	5.5

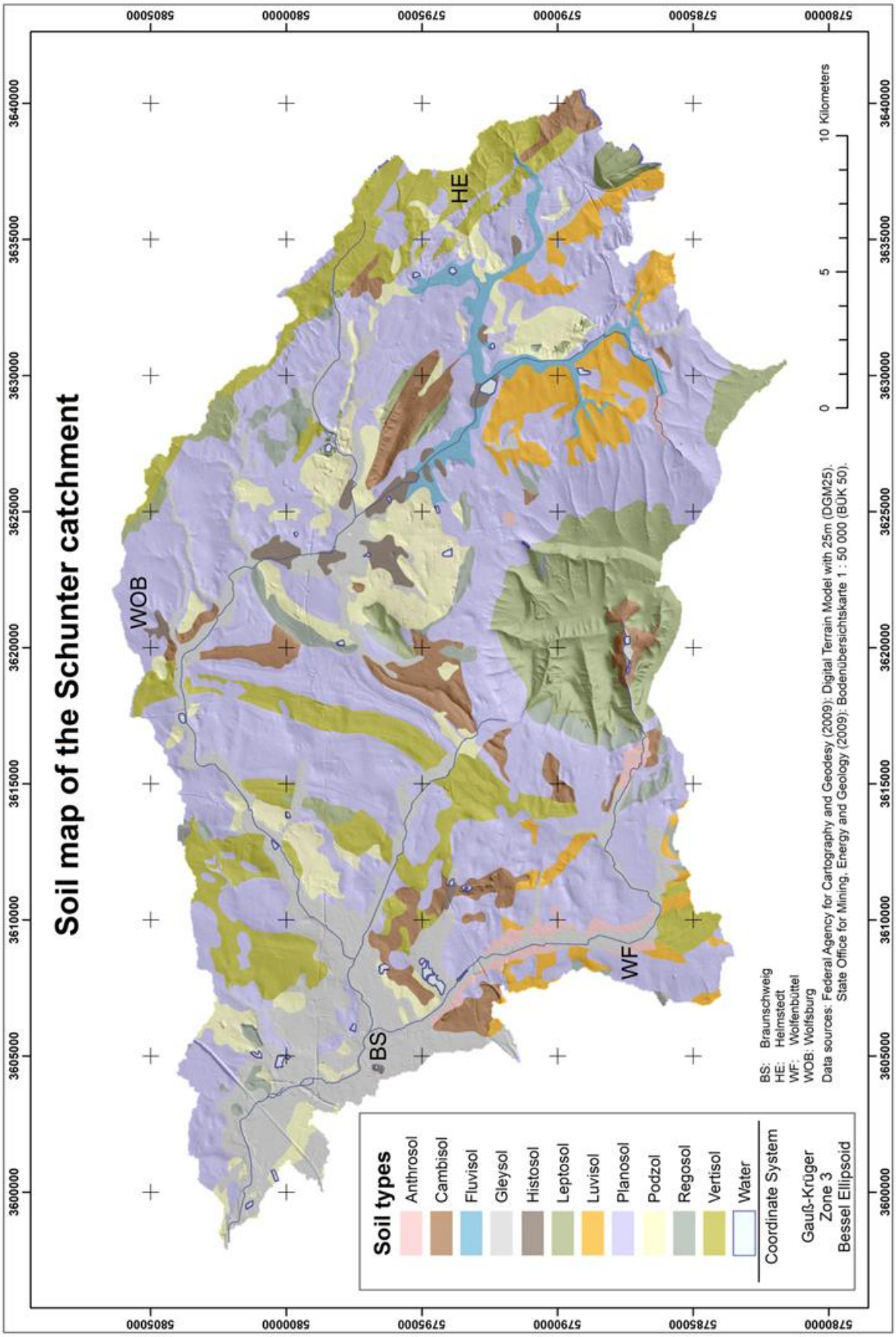

Fig. 3.5: Soil types in the Schunter catchment. (Database: BÜK 50).

For the catchment area a digital database (Bodenkundliche Übersichtskartierung 1:50.000, BÜK 50) is available.

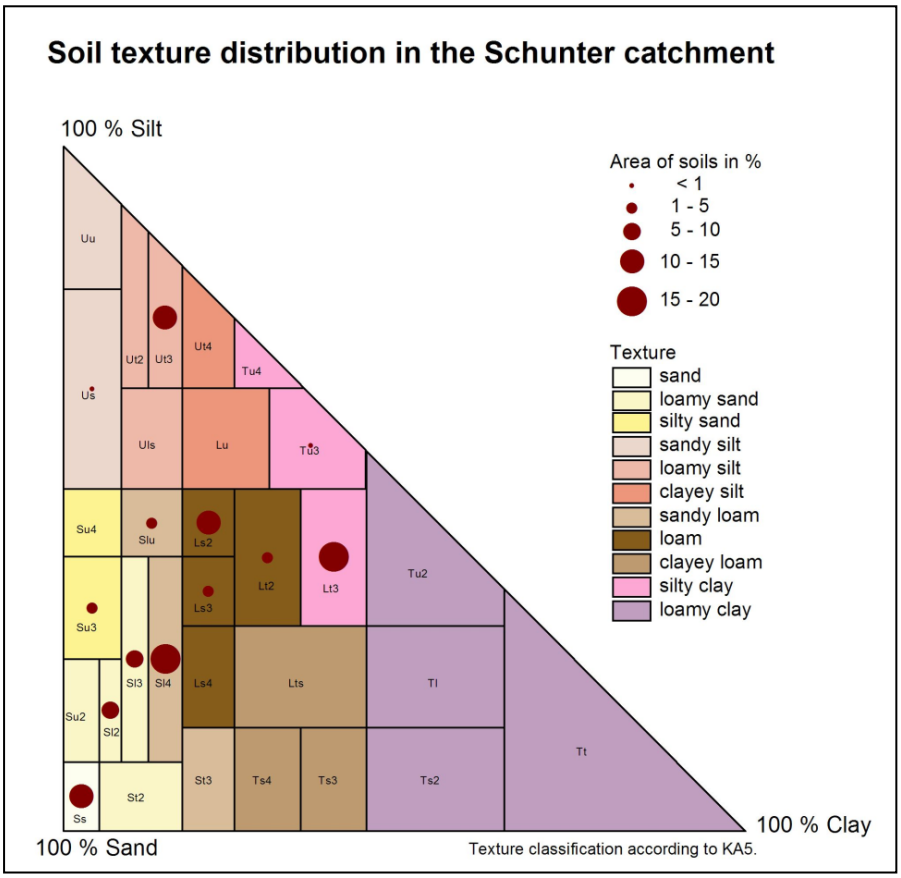

Fig. 3.6: Soil texture of the Schunter catchment (KA 5 soil classification).

The BÜK 50 database also contains detailed information on the texture of the soils in the catchment area. In order to get an impression on the variability of the soils, the existing texture combinations have been plotted into a ternary gram (Fig. 3.6). The ternarygram indicates that the catchment is dominated by sandy and loamy soils. Clay and very silty soils are missing.

3.2 Digital datasets

For the Schunter catchment area several digital datasets have been available. In order to evaluate the land-use change over time, own datasets needed to be created.

3.2.1 Digital landscape model (Land-use 2009)

The Central Basic Geodata Service for Germany (Bundesamt für Kartographie und Geodäsie, BKG) provides a digital landscape model (Amtliches Topographisch-Kartographisches Informationssystem, ATKIS) for Germany. This model contains the current land-use on a very high spatial precision (accuracy of position ± 3m), and a high level of detail (255 different objects with a variety of attributes for each object). In order to compare the recent land-use with historical information derived from maps, the digital data needs to be aggregated to a more general content. For this work five main land-use groups have been defined:

1. **Cropland**, used for crop production;
2. **Forest** and woods, with no separation between broadleaf, deciduous and mixed forest;
3. **Grassland**, containing perennial grassland, pastures and fallow land;
4. **Urban area**, containing all residential area, industrial sites and infrastructure (streets, railways);
5. **Water**, containing all larger streams, canals, lakes and ponds.

The classification of the original data to the new land-use classes can be identified in Tab. 3.5.

Tab. 3.5: Classification of ATKIS layers used.

Layer	Content	Object identifier	New class
Veg01_f	Agricultural Area	4101 (cropland)	Cropland
Veg02_f	Pasture and natural Grassland	4102 (pasture) 4103 (garden) 4104 (heath) 4105 (swamp)	Grassland
Veg03_f	Forest and Woods	4107 (forest) 4108 (wood)	Forest
Veg04_f	Cropping Land	4109 (specialized crops)	Cropland
Sie01_f	Urban area	2202 (recreation area)	Grassland
Sie02_f	Urban Area	2111 (residential area) 2112 (industrial area) 2113 (mixed utilisation) 2114 (special functionality)	Urban Area
Sie03_f	Urban area	2201 (sport facilities) 2213 (graveyard) 2227 (park) 2228 (camping site)	Grassland
Sie04_f		2301 (open cast mining)	Urban Area
Ver01_f	Traffic infrastructure	3101 (roads) 3103 (plaza) 3303 (runway) 3304 (airport) 3502 (service area)	Urban Area
Ver02_f	Railway infrastructure	3201 (railway track) 3501 (railway)	Urban Area
Ver03_f	Airport infrastructure	3301 (airport) 3302 (airport runway)	Urban Area
Gew01_f	Water	5101 (stream, river, brook) 5102 (channel) 5103 (ditch) 5112 (lake, pond)	Water
Gew03_f	Water	3402 (port)	Water

3.2.2 Historic Topographic Maps (Land-use 1950) of the Schunter catchment

In order to retrieve information about the historic land-use situation within the catchment area, 15 historical topographic maps in the scale of 1:25.000 have been scanned using an A0 large format scanner (Fig. 3.7). Since topographic maps have been updated in the past in a 5 year turnaround, the production dates of the individual maps vary between 1949 and 1952.

The individual maps have been scanned as greyscale images with a resolution of 400 dots per inch (dpi). The scanned images have been geo-referenced to the German Gauß Krüger coordinate system, using the imprinted control points of the maps. Using a polynomial correction approach the maps have been resampled to a pixel resolution on 2 m, using the ERDAS Imagine Software (Version 9.1).

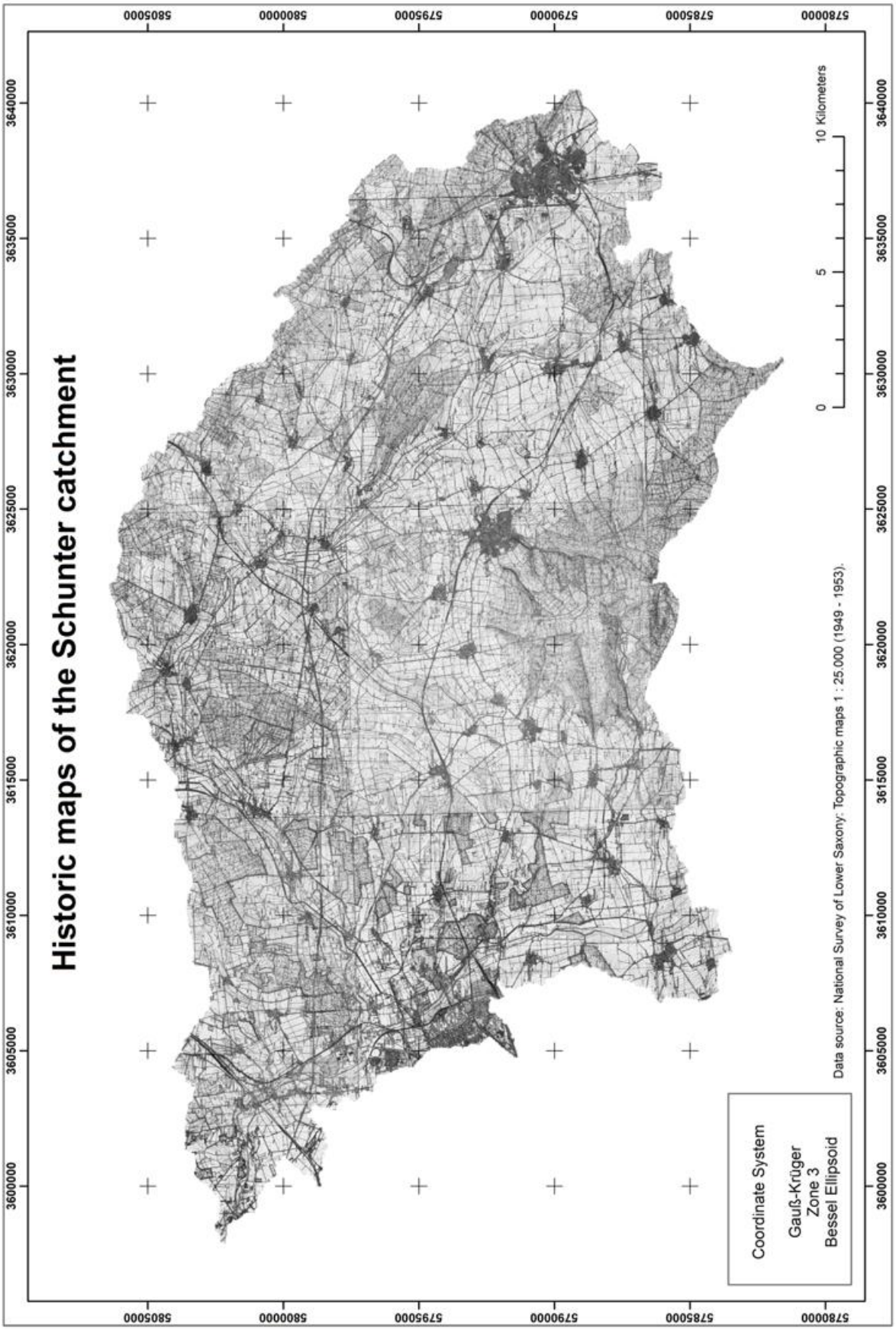

Fig. 3.7: Historic topographic maps of the Schunter catchment area.

The land-use has been manually digitized into the same five corresponding classes like the 2009 data, using a Geographic Information System (GIS) (ESRI, ArcView, and ArcGIS). The scale of the maps has been set to 1:10.000 at digitizing, in order to allow accurate digitalisation.

3.2.3 Digital soil database (BÜK 50) for the Schunter catchment

The soil survey of the state of Lower Saxony has developed a digital soil map at a scale of 1: 50.000 by a systematic analysis of pedological relevant documents. The *Bodenkundliche Übersichtskarte* 1:50.000 (BÜK 50) contains information on the soil type, texture, soil properties and information on the characteristic soil profile and horizons, which make up the profile (Boess et al., 2004). For each soil polygon of the test site a database available is available containing information on soil profiles and its properties.

3.2.4 Digital elevation model (DGM25) for the Schunter catchment

The Central Basic Geodata Service for Germany also provides digital elevation data. A high precision Digital Elevation Model (DEM) with a raster spacing of 25 m (DGM25) and accuracy in height of ± 5m is available for the test site (Fig. 3.8). The data has been computed by the Central Basic Geodata Service based on laser scanning data and photogrammetric analysis of aerial stereo photographs (BKG 2010).

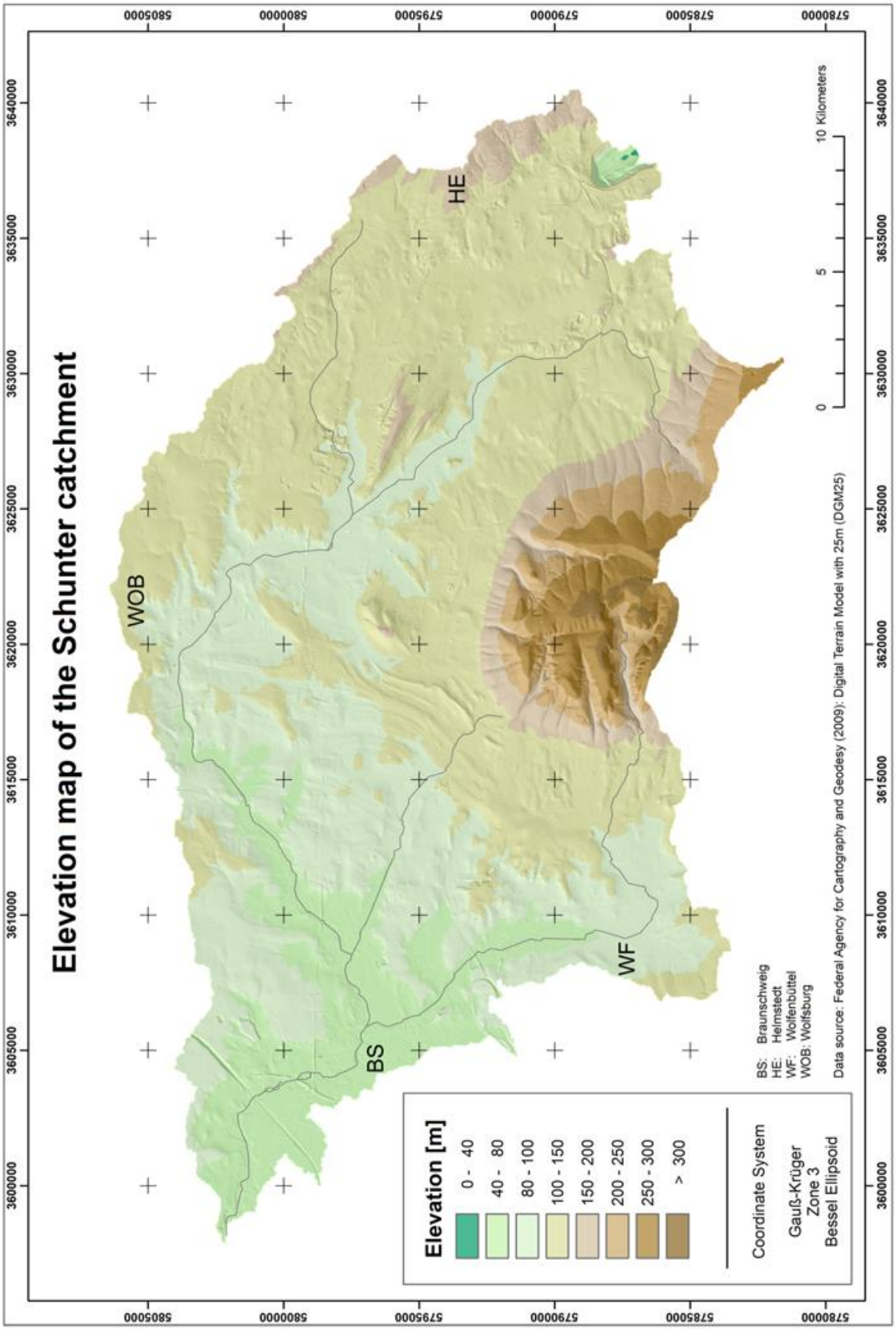

Fig. 3.8: Digital Elevation Model of the Schunter catchment.

3.2.5 Catchment delineation

The delineation of a watershed can be performed using a digital elevation model which represents the morphological properties of the site. Before carrying out hydrological computations, the hydrological correctness of the used digital elevation model needs to be ensured. This is necessary as terrain models almost always contain small errors that have arisen from their production (different input data, laser scanning digitized contour lines) which will produce artefacts, or small depressions without outlet. These errors are particularly critical in this context without outlet.
The typical catchment delineation from a DEM follows the following structure:

Filling of sinks (correction of errors of the DEM)
Computation of flow direction
Computation of flow accumulation
Stream designation
Catchment delineation

The catchment delineation is a standard routine in most Geographic Information Systems (GIS). The Watershed and the sub-catchments have been computed using the Hydro tools extension for ArcView (Schäuble, 2003), which applies some improved methods for sink filling. As a boundary condition the minimum size for a sub-catchment needs to be assigned. Since a small number produced micro catchments which are of no use, a large number just produces on big catchment. A minimum size of 100 ha for a contributing smallest unit has been selected to compute the sub-catchments.

In a final step the real stream data has been overlaid on the generated catchments in order to identify the sub-catchments which contribute to a single stream.

3.3 Soil sampling

Several soil samples were collected from the surface layer (0-30 cm) during the spring and summer seasons in the Schunter catchment area within 2008 and 2009 to carry out the reported work of this thesis.

The criterion for choosing the sample location for field measurement in this catchment was based on a stratified sample strategy. On the one hand the variety of different soil types should be covered; on the other hand the access to the fields should be given. The latter requirement was given by using mainly the area of the JKI field station at Sickte and Wendhausen.

The suitable sampling sites were identified by computing the HSG and land-use for the region and combining them to hydrologic response units (HRU) in a GIS. After the identification of the HRUs in the catchment, the combination of the hydrologic soil group and the land-use classes were plotted against the percentage of the HRUs.
According to the BÜK50 data set, only the HSG A is present in the catchment area, combining the land-use with the HSG result in 55 % of cropland, 30 % forest and 15 % grassland.
Finally, it can be identified how many samples needed to be selected from the catchment area relaying on the soil type, the dominant hydrologic soil group, and land-use. For the cropland, twenty site locations were sampled where four locations for the grassland and five locations for the forest land-use (Fig. 3.9).

As the HSG for the catchment area is only A, it was decided in include additional field data measured in other studies in order have a larger data pool for the CN estimation.

Infiltration was also measured by means of a Hood-Infiltrometer from Al-Hassoun (2009) who covering soils in Northern Germany on an organic farm (Trenthorst), in Braunschweig, but outside of the catchment area and Mariensee has been included. Also infiltration data from a comparative study of organic and conventional managed soils in Southern Germany (Tauberbischofsheim) from Hartmann et al., (2009) have been included.

With those datasets more variation in terms of soil type and land-management could be included.

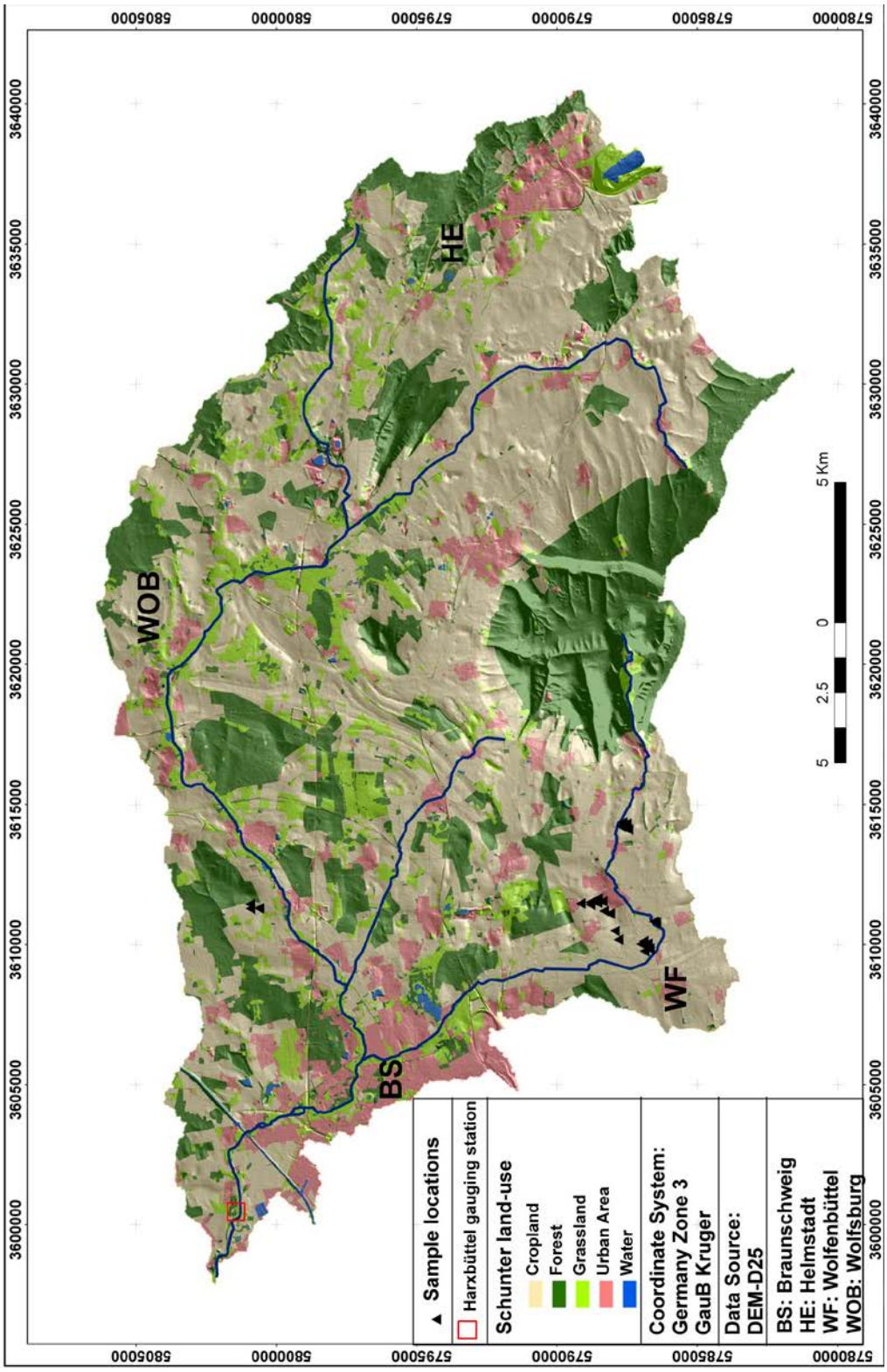

Fig. 3.9: The investigation sites in the Schunter catchment area.

3.4 Soil physical analysis of the Schunter catchment

3.4.1 Soil texture

Particle size distribution analysis for the investigated soil samples was carried out using the Hydrometer method (ISO, 1998), where the principle of the Hydrometer method is based on combination of sieving and sedimentation starting from air-dried soil.

For the soil samples, 50 g for clay soils, 100 g for sandy soils of 2-mm air-dried soil were put in a 650 ml beaker, then 30 ml of distilled water was added to the sample to get wet and 30 ml of 30 % volume fraction hydrogen peroxide solution was gently added for destruction of soil organic matter and the contents were mixed using the glass rod. The vessel was covered with a glass cover and left for 24 hours. Thereafter, the vessel was placed on the hotplate and warmed gently.

In addition, 25 ml of 1 mol/l calcium chloride solution was added for flocculation, and the content was strongly mixed with 250 ml water and washing procedure was repeated until all decomposed organic matter was destroyed. The washed residue was quantitatively transferred to a centrifuge bottle and sufficient water was added until the total volume becomes 200 ml.

For the dispersion procedure, 25 ml of (Na- Hexametaphosphate 5%) was added and the bottle was shaken for 18 hours on an end-over-end shaker, and the dispersed suspension was quantitatively transferred from the centrifuge bottle into the 0.063 mm sieve.
The soil was wet sieved using a jet of water and rubbing with a stiff brush until there is no turbidity and the water became clear. The soil residue on the sieve was washed into an evaporating dish and completely dried in an oven at 105°C and then cooled and received on the sieves <2 mm down to 0.063 mm, where the fractions retained on each sieve were weighed and the proportion of sand particles was calculated.

Afterwards the suspension, passing the 0.063 mm sieve, was quantitatively transferred into a measuring cylinder and made up to 1 litre with distilled water, then the

cylinder was strongly closed with a stopper and shaken thoroughly until all the sediment was suspended. The cylinder was placed upright in a water bath at temperature between 20°C and 30°C. Moreover, 25 ml of the dispersion agent (Na-Hexametaphosphate 5%) was put in separated cylinder and diluted with water to the volume 1litre as blank. After 1 hour, hydrometer readings were taken in time intervals of 0.5 min, 1min, 2 min, 4 min, 8 min, 30 min, 2 hours, 8 hours and 24 hours from the start of sedimentation.

3.4.2 Bulk density

The soil dry bulk density (BD) was determined by taking undisturbed soil samples from 0-10, 10-20, and 20-30 cm soil depth using metal soil cores with a volume 100 cm^3 (Carter and Ball, 1993). From every horizon, 3 replicates were taken. The samples were oven-dried at 105°C for overnight. Before and after drying, the samples were weighed. Soil dry bulk density was calculated as the ratio of the mass of oven-dried solids to the bulk or total soil volume according to the following equation:

$$\text{Dry bulk density } [g \cdot cm^{-3}] = \frac{\text{Weight of soil [g] (oven dry)}}{\text{Total volume of soil [cm}^3\text{]}} \qquad \text{[Equation 3.1]}$$

Soils with larger clay contents are affected by swelling and shrinking processes. The effective bulk density (eBD) takes these effects into account. The effective is computed according to KA5 with the following equation:

$$\text{Effective bulk density } [g \cdot cm^{-3}] = \rho_d + 0.009 \cdot \text{Cc} \qquad \text{[Equation 3.2]}$$

Where:

ρ_d : Dry bulk density or dry density

C_c: Clay content [%]

3.4.3 Soil moisture parameters

Soil water content was determined gravimetrically. Soil core samples taken by cylinders from several soil depths were used to determine soil moisture content and other soil physical properties by using the pedo-transfer functions (Arshad et al., 1996). These samples were fresh weighed and then oven-dried at 105°C for 24 hours and reweighed.

Soil moisture e.g. soil water content was calculated as the mass of water lost as a percentage of the mass of the dried soil.

$$\text{Soil water content}\left[\frac{g}{g}\right] = \frac{\text{Weight of soil (moist) - weight of soil (oven dry)}}{\text{weight of soil (oven dry)}} \qquad \text{[Equation 3.3]}$$

$$\text{Volumetric water content}\left[\frac{g}{cm^3}\right] = \text{Soil water content}\left[\frac{g}{g}\right] \cdot \text{BD}\left[\frac{g}{cm^3}\right] \qquad \text{[Equation 3.4]}$$

$$\text{Soil porosity}\left[\frac{g}{cm^3}\right] = 1 - \frac{BD}{2{,}65} \qquad \text{[Equation 3.5]}$$

$$\text{Soil water-filled pore space [\%]} = \frac{\text{Volumetric water content}}{\text{Soil porosity}} \qquad \text{[Equation 3.6]}$$

3.5 Field measurements

3.5.1 Infiltration measurement

Through this work the infiltration was measured by using a Hood-Infiltrometer (Fig. 3.10). This device allows the estimation of the steady state infiltration rate (q_s) in the field (Schwärzel and Punzel, 2007). The vertical infiltration is initially governed by capillary or sorptivity of water into the soil matrix, containing both vertical and horizontal components. After some time infiltration becomes gravity driven and linear with time as soil capillary forces are reduced, indicating that infiltration is at steady state.

Fig. 3.10: Infiltration measurement conducted by the author using a Hood-Infiltrometer.

The Hood-Infiltrometer consists of a "Mariotte"- water supply which controls the suction of water on the top of the surface, with a capacity of 5 litres, a hood with 24 cm diameter, a tension-chamber with 24 cm diameter, and graduated U-pipe manometer (Fig. 3.10).

The infiltration measurement sequence is done by placing a circular shaped hood filled with water directly onto the soil surface with a retaining ring. The gap between the retaining ring and the hood is filled with wetted sand to seal the edge and to prevent the water from leaking out of the side (Fig. 3.11).

The pressure head in the water-filled hood controlled and regulated by the "Mariotte"-water supply, and by using this device, the pressure head at the soil surface can be adjusted between zero and any negative pressure up to the bubble point of the soil. The effective pressure head (H) is equivalent to the difference between the pressure value in a U-pipe manometer (Us) and the pressure value in the standpipe of the hood (Hs). H can be calculated directly after taking the readings of both U-pipe manometer and the hood as follows:

$$H=Us-Hs \quad \text{[Equation 3.7]}$$

Where:

Hs: Hood reading

$$Us = Us\ (left) + Us\ (right) \quad \text{[Equation 3.8]}$$

By using a stopwatch, the amount of water that infiltrate into the soil per 30 seconds was recorded until the steady state of the infiltration rate was reached. The last five reading at steady state were averaged and the steady flow rate recorded. Soil infiltration measurements were conducted with 3 replicates.

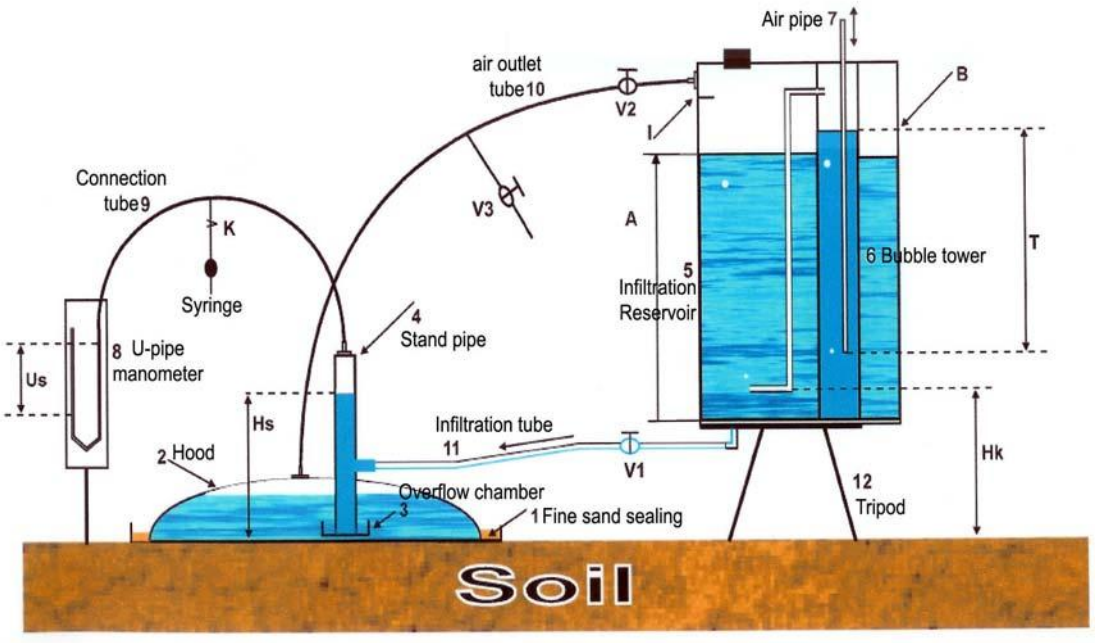

Fig. 3.11: Principle of infiltration measurement using a Hood Infiltrometer (Schwärzel and Punzel, 2007).

In comparison to other infiltration measurements (e.g. disc infiltrometer) using the Hood-Infiltrometer has some advantages:

The Hood-Infiltrometer is used for measuring saturated and near saturated soil hydraulic properties as integral information over the soil horizons. The measurements do not require any preparation of soil surface, because the hood is placed with its open side on the undisturbed soil surface. In contrast to the disc infiltrometer, no perforated plate or contact material is required on the infiltration surface. Since there is no need of any contact material, measurements with the hood infiltrometer reflect particular properties of the soil surface as compaction or silting.

The bubble tower in the Mariotte water supply has an adjustable pipe that controls the suction by allowing air entry at varying distance below the water table of the tower.

3.5.2 Saturated hydraulic conductivity

The steady state infiltration rate (q_s) which has been measured by the Hood-Infiltrometer needs to be converted into saturated hydraulic conductivity, which is the key parameter for infiltration in this work. Different approaches to determine the hydraulic conductivity by measurements or pedo-transfer functions are introduced now:

3.5.2.1 Computation according to Wooding and Gardner

The Hood-infiltrometer places a water-filled hood with its open side directly onto the soil surface, which is meant to eliminate the problems of the disk infiltrometer in establishing the hydraulic bond between the infiltration chamber and the soil surface (UGT, 2004). But the data collected in the field is just a flow rate (Q_s) which needs to be converted into saturated hydraulic conductivity.
The steady state infiltration rate was measured at pressure supply head of -1 cm for three replicates for each sample location.
According to Reynolds and Elrick (1991) the steady flow rate can be converted into the steady infiltration rate by:

$$q_s = \frac{Q_s}{\pi \cdot r^2} \quad ; \quad Q_s = q_s \cdot \pi \cdot r^2 \qquad \text{[Equation 3.9]}$$

Where:

q_s: Steady state infiltration rate $[L \cdot T^{-1}]$

Q_s: Steady flow rate $[L^3 \cdot T^{-1}]$

r: Radius of the hood $[L]$

With the knowledge of the steady flow rate (Q_s), the unsaturated hydraulic conductivity can be computed according to Wooding (1968):

$$\frac{Q_s}{\pi \cdot r^2} = K_u \cdot \left(1 + \frac{4}{\pi \cdot r \cdot \alpha}\right) \quad ; \quad K_u = \frac{q_s}{\left(1 + \frac{4}{\pi \cdot r \cdot \alpha}\right)}$$ [Equation 3.10]

Where:

K_u: Unsaturated hydraulic conductivity $[L \cdot T^{-1}]$

Q_s: Steady flow rate $[L^3 \cdot T^{-1}]$

r: Radius of the hood $[L]$

α: Soil sorptivity number $\left[\frac{1}{L}\right]$

The soil sorptivity number (α) can be estimated in the field by measuring the steady state infiltration rate under different pressure heads (UGT, 2004). This is very time consuming, since it doubles the amount of measurements. Using a neural network approach, α can be computed from texture and bulk density data with the ROSETTA model (see chapter 3.5.2.2).

With the calculation of the unsaturated hydraulic conductivity by *Wooding's* equation, and the sorptivity number (α) from the ROSETTA model, the saturated hydraulic conductivity (K_s) can be computed with the Gardner's equation (Gardner,1958).

$$K_s = \frac{K_u}{\exp(\alpha \cdot h)} \quad ; \quad K_s = \frac{\left(\frac{q_s}{\left(1 + \frac{4}{\pi \cdot r \cdot \alpha}\right)}\right)}{\exp(\alpha \cdot h)}$$ [Equation 3.11]

Where:

K_s: Saturated hydraulic conductivity $[L \cdot T^{-1}]$

K_u: Unsaturated hydraulic conductivity $[L \cdot T^{-1}]$

α: Soil sorptivity number $\left[\frac{1}{L}\right]$

h: Pressure head [L]

The obtained results of the saturated hydraulic conductivity using the Hood-Infiltrometer were ten-folds higher than the saturated hydraulic conductivity values using the other infiltrometers. This is also recognized by several other authors, when the measurements were applied in the same test site with different infiltrometers (Schwärzel and Punzel, 2007, Wahl et al., 2009). Schwärzel and Punzel (2007) stated that preparing the soil surface for disk infiltrometer measurements led to the sealing and smearing of the pores of the soil surface, and applying pressure heads near saturation might have caused mobile fine-textured particles of the contact material to clog the macropores, and this will result in a significant decrease in the saturated and near-saturated conductivity compared with the measurements without a contact layer. In addition, a drop in saturated and near saturated conductivity because of smeared pores, was also reported by Spohrer et al. (2006).

For these reasons Schwärzel and Punzel (2007) reported that smearing, sealing, and clogging of pores lead to additional flow impedances in the soil surface layer, and the saturated conditions underneath the disk infiltrometer will never be reached during the disk experiments.

In order to make the results of this work comparable to other infiltrometer measurements or K_s models the experimental results of the saturated hydraulic conductivity where divided by ten.

3.5.2.2 Pedo-transfer Functions (PTF)

Process-simulation models have become increasingly popular in both research and management problems involving flow and transport processes in the subsurface and in predicting the outcome of agricultural management on soil quality. The most difficult and expensive step towards the process of modelling is collection of data. Soil properties can be highly variable spatially and temporally and measuring these properties is time consuming and expensive (Klute, 1986; Dirksen, 1991).

Soil hydraulic parameters may be either measured directly or estimated indirectly through prediction from more easily measured data based using quasi-empirical models (Pedotransfer functions, PTF). In this work several models were used to estimate saturated hydraulic conductivity. The results were compared to the measured saturated hydraulic conductivity from the Hood-Infiltrometer.

ROSETTA pedotransfer function

The program ROSETTA (Schaap et al., 2001) allows estimating soil hydraulic properties from soil data such as soil texture data and bulk density.
ROSETTA can be used to estimate the following properties:

- Saturated hydraulic conductivity
- Unsaturated hydraulic conductivity parameters according to Van Genuchten (1980) and Mualem (1976)
- Water retention parameters according to van Genuchten (1980).

The following input data can be used:

1) Soil textural class
2) Sand, silt and clay [%]
3) Sand, silt and clay [%] and bulk density
4) Sand, silt and clay [%], bulk density and a water retention point at 330 cm (33 kPa)
5) Sand, silt and clay [%], bulk density, water retention points at 330 and 15000 cm (33 and 1500 kPa).

The first model provides class average hydraulic parameters for each soil textural class used in the US. The other four models are based on neural network analyses and provide more accurate predictions when more input variables are used.

All estimated hydraulic parameters are accompanied by uncertainty estimates that permit an assessment of the reliability of ROSETTA's predictions (Schaap and Leij 1998; Schaap et al., 1999; Schaap et al., 2001).

COSBY pedotransfer function

Cosby et al., (1984) estimated the saturated hydraulic conductivity based on a regression analysis based on the soils sand and clay content:

$$K_s = 60.96 \cdot 10^{(-0.6+0.0126 \cdot Sa - 0.0064 \cdot C_C)}$$ [Equation 3.12]

Where:

K_s: Saturated hydraulic conductivity $\left[cm \cdot d^{-1}\right]$

Sa: Sand content [%]

C_c: Clay content [%]

SAXTON pedotransfer function

Saxton et al., (1986) estimated the K_s values relaying on the sand and clay content of the soil samples by using the following equation:

$$K_s = 24 \exp\left(12.012 - 7.55 \cdot 10^{-2} \cdot Sa + \frac{-3.895 + 3.671 \cdot 10^{-2} \cdot Sa - 0.1103 \cdot C_C + 8.7546 \cdot 10^{-4} \cdot {C_C}^2}{0.332 - 7.251 \cdot 10^{-4} \cdot Sa + 0.1276 \cdot \log_{10}(C_C)}\right)$$

[Equation 3.13]

Where:

K_s: Saturated hydraulic conductivity $\left[cm \cdot d^{-1}\right]$

Sa: Sand content [%]

C_c: Clay content [%]

BRAKENSIEK pedotransfer function

Brakensiek et al., (1984) estimated the K_s values relaying on the sand and clay content, and the porosity of the soil by using the following equation:

$$K_s = 24 \exp\left(19.52348 \cdot p - 8.96847 - 0.028212 \cdot C_C + 0.00018107 \cdot Sa^2 - 0.0094125 \cdot {C_C}^2 ...\right)$$

$$... - 8.395215 \cdot p^2 + 0.077718 \cdot Sa \cdot p - 0.00298 \cdot Sa^2 \cdot p^2 - 0.019492 \cdot {C_C}^2 \cdot p^2 + 0.0000173 \cdot Sa^2 \cdot {C_C}^2 ...$$
$$... + 0.02733 \cdot {C_C}^2 \cdot p + 0.001434 \cdot Sa^2 \cdot p - 0.0000035 \cdot {C_C}^2 \cdot Sa)$$ [Equation 3.14]

Where:

Sa: Sand content [%]

C_c: Clay content [%]

p: Porosity $\left[\frac{m^3}{m^3}\right]$

VEREECKEN pedotransfer function

Vereecken et al., (1990) computed the saturated hydraulic conductivity using sand and clay content, dry density and soil organic carbon:

$$K_s = \exp(20.62 - 0.96 \cdot \ln(C_C) - 0.66 \cdot \ln(Sa) - 0.46 \cdot \ln(SOM) - 8.43 \cdot \rho_d)$$

[Equation 3.15]

Where:

K_s: Saturated hydraulic conductivity $\left[cm \cdot d^{-1}\right]$

Sa: Sand content [%]

C_c: Clay content [%]

SOM: Soil organic matter [%]

ρ_d: Dry bulk density $\left[g \cdot cm^{-3}\right]$

3.6 Simulations

3.6.1 Simulation of one-dimensional water movement

Not only is the saturated hydraulic conductivity of interest, also the behaviour over time and depth. Since this cannot be measured directly in the field with justifiable effort, the numerical model HYDRUS-1D (Šimůnek et al., 2008) was used to analyze the water flows.

HYDRUS has implemented the soil-hydraulic functions of van Genuchten (1980) who used the statistical pore-size distribution model of Mualem (1976) to obtain a predictive equation for the unsaturated hydraulic conductivity function in terms of soil water retention parameters.

HYDRUS solves numerically the Richards equation for saturated-unsaturated water flow and the water flow equation can incorporate a sink term to account for water uptake by plant roots.

$$\frac{\partial \theta}{\partial t} = \frac{\partial}{\partial x}\left[K_u \left(\frac{\partial h}{\partial x} + \cos\alpha \right) \right] - S \qquad \text{[Equation 3.16]}$$

Where:

K_u: Unsaturated hydraulic conductivity function $[L \cdot T^{-1}]$

h: Pressure head [L]

θ: Volumetric water content [L3L-3],

t: Time [T]

x: Spatial coordinate [L]

S: Sink term $[L^3 \cdot L^{-3} \cdot T^{-1}]$

α: Angle between flow direction and the vertical axis.

3.6.2 Infiltration simulation

The effects of land-use change and changes in land-management on the soil infiltration need to be evaluated on a larger scale in order to identify the magnitude that individual impacts have.

So far the hydraulic conductivity is a measure of the soils ability to transport water into deeper layers. At the moment the impact of the land-use or land-management can only be identified by field measurements, where the measured infiltration is an integrative measure of all factors affecting the infiltration. Using pedo-transfer functions only reflects the impact the input parameters (e.g. texture and bulk density) have on the infiltration, but not the land-use or management.

In order to develop scenarios of the impact of different land-use and land-management on soil infiltration an integrating measure has to be used which interlinks the different land-use to the soil type and the resulting infiltration.

The curve number method is a widely used simple approach to compute the relation between precipitation and the resulting infiltration and runoff. The basic concept needs to be modified for the later simulation.

3.6.2.1 NRCS-Curve Number

The Natural Resources Conservation Service (NRCS, formerly Soil Conservation Service or SCS) of the USDA developed a simple model for predicting direct runoff or infiltration from rainfall excess in the 1950s in the USA (Hawkins et al., 2009). Based on empirical analysis of rainfall and runoff relations of several small watersheds, the SCS came up with a set of formulas, describing these relations.

The background is the universal water balance equation:

$$P = Q + E + \Delta S \qquad \text{[Equation 3.17]}$$

Where:

P: Precipitation

Q: Runoff

E: Evapotranspiration

ΔS: Storage term

The NRSC modified the water balance to the following equation (Hawkins et al., 2009):

$$Q = P \cdot \frac{F}{S} \qquad \text{[Equation 3.18]}$$

Where:

Q: Runoff

P: Precipitation

F: Actual loss

S: Potential loss

The Evaporation of the universal water balance equation as well as the storage terms has been included into the relation of actual (F) and potential loss (S).

By substituting F (actual loss) with

$$F = P - Q \qquad \text{[Equation 3.19]}$$

the runoff can be formulated as:

$$Q = \frac{P^2}{(P + S)} \qquad \text{[Equation 3.20]}$$

Equation 3.20 explains runoff as a function of precipitation and the potential loss (S), which also can be called as retention potential, the maximum amount of water which

can be hold by the soil. Since runoff will only be produced if there some rainfall, the term initial abstraction (I_a) has been introduced (Hawkins et al., 2009), which needs to be subtracted from the total rainfall to retrieve the effective precipitation:

$$P_e = P - I_a \qquad \text{[Equation 3.21]}$$

Where:

P_e: effective Precipitation

P: Precipitation

I_a: Initial abstraction

Initial abstraction (I_a) is all losses before runoff begins. It includes water retained in surface depressions, water intercepted by vegetation, evaporation, and infiltration.

The SCS has plotted rainfall/runoff events for several watersheds in the US and introduced a dimensionless index curve number (CN) (Fig. 3.12).

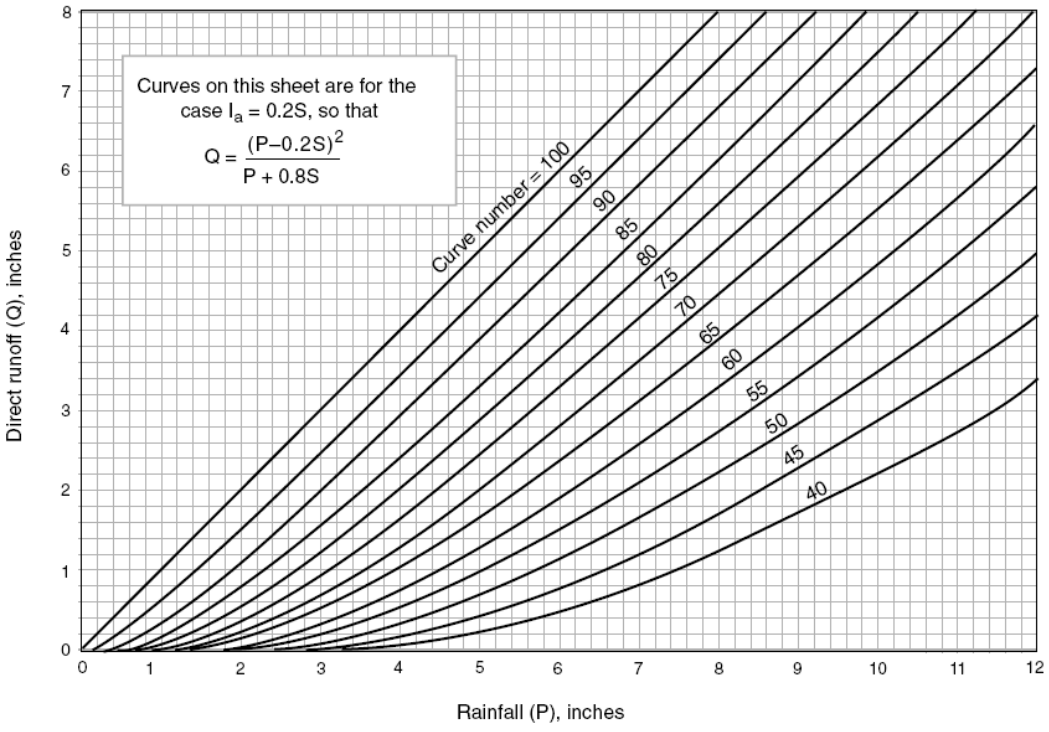

Fig. 3.12: Rainfall and direct runoff for different curve numbers (SCS, 1954).

As the runoff is not of interest in this work, the focus will be put on potential retention (S), since this value is reasonable for describing the infiltration properties on a larger scale.

The USA uses imperial units instead of metric units; the formulas have been developed in inches. The relation of the potential retention S to the curve number is shown in the following equations:

$$CN = \frac{1000}{10 + S} \quad ; \quad S = \frac{1000}{CN} - 10 \qquad \text{[Equation 3.22]}$$

Where:

S: Retention potential [inch]

$$CN = \frac{25400}{254 + S} \quad ; \quad S = \frac{25400}{CN} - 254 \qquad \text{[Equation 3.22]}$$

Where:

S: Retention potential [mm]

Conceptually, CN can vary from 0 to 100, corresponding to S = ∞ and S = 0 respectively. Using the method requires the selection of a Curve Number from tables, based on land-use, hydrologic condition, and initial moisture status.

The NRCS provided CN tables for a variety of soils and land-use conditions. In order to determine the CN, soils need to be classed by texture into four *Hydrologic Soil Group* (Tab. 3.6).

HYDROLOGIC SOIL GROUPS

The CN approach classifies soils according to their saturated hydraulic conductivity into 4 classes (A-D). The original saturated hydraulic conductivity classification is in inch (SCS 1986) and has been converted to $[cm \cdot d^{-1}]$:

HSG A:

Soils with a low runoff potential and high infiltration rates even when thoroughly wetted. They have a high rate of water transmission (> 18.29 $[cm \cdot d^{-1}]$).

HSG B:

Soils with moderate infiltration rates when thoroughly wetted and consist chiefly of moderately deep to deep, moderately well to well drained soils with moderately fine

to moderately coarse textures. These soils have a moderate rate of water transmission (9.14 – 18.24$[cm \cdot d^{-1}]$).

HSG C:

Soils with low infiltration rates when thoroughly wetted, and consist chiefly of soils with a layer that impedes downward movement of water and soils with moderately fine to fine texture. These soils have a low rate of water transmission (3.04 – 9.14 $[cm \cdot d^{-1}]$).

HSG D:

Soils with a high runoff potential. They have very low infiltration rates when thoroughly wetted and consist chiefly of clay soils with a high swelling potential, soils with a high permanent water table, soils with a clay pan or clay layer at or near the surface, and shallow soils over nearly impervious material. These soils have a very low rate of water transmission (0.00 – 3.04$[cm \cdot d^{-1}]$).

Tab. 3.6: Hydrologic Soil Groups (HSG) based on soil texture.

HSG	Soil texture
A	Sand, loamy sand, or sandy loam
B	Silt loam or loam
C	Sandy clay loam
D	Clay loam, silty clay loam, sandy clay, silty clay, or clay

The state of *Lower Saxony* has developed the BÜK50, a digital set of data containing addition soil properties like texture, bulk density, organic matter and many more.

This database allows the derivation of the hydraulic conductivity from the texture information.

In order to apply the CN, the German soil classification has to be transformed into the HSGs. The saturated hydraulic conductivity is dependent on bulk density. Based on the German manual for soil surveying (KA 5, 2005) the soil types can be classified into HSGs (Tab. 3.7):

Tab. 3.7: German soil texture classification and resulting Hydrologic Soil Groups (based on K_s and eBD) according to (KA 5, 2005).

Soil Texture	K_s Ld1+2 $[cm \cdot d^{-1}]$	HSG Ld1+2	K_s Ld3 $[cm \cdot d^{-1}]$	HSG Ld3	K_s Ld4+5 $[cm \cdot d^{-1}]$	HSG Ld4+5
Ss	372	A	270	A	121	A
Sl2	134	A	77	A	43	A
Sl3	96	A	51	A	20	A
Su2	157	A	86	A	46	A
Su3	83	A	40	A	14	B
Us	34	A	10	B	4	C
Sl4	104	A	38	A	17	B
Uls	43	A	17	B	5	C
St2	156	A	94	A	53	A
Ls4	88	A	33	A	11	B
Ls3	82	A	27	A	10	B
Ts3	68	A	15	B	8	C
Tt	24	A	3	D	2	D
Ls2	57	A	24	A	9	C
Slu	58	A	24	A	10	B
Lt3	32	A	14	B	6	C
Lts	37	A	17	B	7	C
Lt2	45	A	18	B	8	C
Tu3	23	A	14	B	5	C
Ls2	57	A	24	A	9	C
Lu	51	A	20	A	6	C
Ut2	35	A	7	C	1	D
Uu	28	A	8	C	5	C
Ut4	51	A	14	B	3	D
Ut3	38	A	10	B	4	C
Ts2	30	A	6	C	1	D
Tl	35	A	11	B	3	D
Ts4	108	A	38	A	11	B

Ld1+2: eBD < 1.6 $[g \cdot cm^{-3}]$

Ld3: eBD 1.6 < 1.8 $[g \cdot cm^{-3}]$

Ld4+5: eBD > 1.8 $[g \cdot cm^{-3}]$

With the knowledge of the HSG and the land-use, the CN can be determined by using tabulated values (Tab. 3.8) from several study sites in Germany:

Tab. 3.8: Selected curve number values based on studies in Germany (DWVK 1984, Voges 1999 Halbfaß 2005, Hartmann et al., 2009).

Land-use Land-management	Curve number according to Soil group			
	HSG A	HSG B	HSG C	HSG D
Fallow land (bare soil)	77	86	91	94
Cropland (root crops)	70	80	87	90
Cropland (cereals)	64	76	84	88
Cropland (conventional tillage)	67	78	85	89
Cropland (conservation tillage)	62	73	79	80
Cropland (organic farming, conventional tillage)	55	64	70	73
Grassland (permanent)	30	58	71	78
Grassland (pasture)	49	69	79	84
Forest/Woods	36	60	73	83
Forest (dense)	25	55	70	77
Sealed area	100	100	100	100
Water	100	100	100	100

By knowing the HSG, the problem to identify the correct CN for the specific land-management situation in the field arises. Since the documentation of the SCS curve number approach does not explain the way, the CN have been generated in the past (Hawkins et al., 2009), very likely the CN have only been retrieved graphically by plotting the relation between runoff and precipitation (Fig. 3.12).

In this work a new approach to identify the CN by measurements is introduced:

Sum up, equation 3.23 allows the computation of the curve number:

$$CN = \frac{25400}{254 + S} \qquad \text{[Equation 3.23]}$$

The value *S* is the retention potential, which describes the maximum amount of water which can infiltrate the soil before producing runoff. In fact this is equal to the saturated hydraulic conductivity. By replacing S with K_s the curve number can be computed for each land-use, land-management situation, when the hydraulic conductivity has been measured in the field. This leads to equation 3.24:

$$CN_m = \frac{25400}{254 + K_s}$$ [Equation 3.24]

Where:

CN_m: Measured CN $\left[\frac{1}{L \cdot T^{-1}}\right]$

K_s: Saturated hydraulic conductivity $\left[L \cdot T^{-1}\right]$

The CN_m is equal to the CN, but has the unit $\left[\frac{1}{L \cdot T^{-1}}\right]$ for mathematical reasons.

On a catchment scale the CN is of minor interest, but is needed in order to get a measure for the impact of land-use and land-management on the infiltration properties.

The retention potential *S*, can be computed with existing soil data, land-use and management information and the CN_m. By using the saturated hydraulic conductivity (K_s), S becomes S_{max} and this value becomes a direct measure of the impact of land-use and land-management on the infiltration properties of a catchment.

3.6.3 Scenarios

To identify the impact of the land-use and land-management on the infiltration capacity on a catchment scale, 11 scenarios for the Schunter catchment have been developed (Tab. 3.9).

Tab. 3.9: Infiltration capacity scenarios for the Schunter catchment.

Sce-nario	Land-use	Management	Tillage	Impact	Assumption
I	1950	100 % organic farming	conventional	no technology	historic situation
II	1950	100 % conventional farming	conventional	technology	historical land-use, introduction of technology
III	1950	no agriculture	-	best retention potential	no land-management
IV	2009	97 % conventional 3 % organic farming	72 % conventional 25 % conservation	technology and urban growth	status quo
V	2009	97 % conventional 3 % organic farming	72 % conventional 25 % conservation	forcing of bio-energy, loss of grassland	reduction of grassland area by 10 %
VI	2009	87 % conventional 13 % organic farming	62 % conventional 25 % conservation	Forcing of organic farming	Increase of organic faming area by 10 %
VII	2009	87% conventional 3 % organic farming	62 % conventional 35 % conservation	Forcing of conservation tillage	Increase of conservation agriculture area by 10 %
VIII	2009	72 % conventional farming 5 % organic farming 17 % Grassland	34 % conventional 38 % conservation	optimised retention potential	optimised land-management
IX	2009	no agriculture	-	best retention potential	no land-management
X	2070	97 % conventional 3 % organic farming	72 % conventional 25 % conservation	urban growth	future with growth rate of 1950 -2009
XI	2070	no agriculture	-	best retention potential	no land-management

In order to evaluate the historic situation, *scenario I* tried to model this situation 60 years ago, with low fertiliser inputs and little technology use. The second scenario tries to evaluate the impact of technology on the land-use of 1950. Scenario III computes the total possible retention, if there would be no agriculture. This scenario is used to relate other scenarios to the maximum possible retention in the area.

Scenario IV defines the current status in the region with around 3 % of organic farms (Biowelt, 2010) and 25 % of conservation tillage applied (Soco, 2009).
Scenario V projects the impact of grassland turnover due to increased bio-energy production. *Scenario VI* and *VII* evaluate the impact of increased organic farming and conservation tillage respectively.
Scenario VIII tries to predict to best land-management on the recent land-use, by optimising the retention potential.
Scenario IX computes the total possible retention for 2009, if there would be no agriculture.
Scenario X uses the land-use change in the last 60 years and tries to project the same growth rates to the future 2070.
Finally the last scenario predicts the retention potential if no agriculture is performed and all areas expect urban areas and water are covered with forest for 2070. This scenario shows like scenarios *III* and *IX* the maximum retention potential which could theoretically be reached.

3.7 Land-use change

Land-use information was derived from ATIKS data (Chapter 3.2.1) for 2009 and from digitized topographic maps (Chapter 3.2.2) 1950 respectively. Combining this data in a Geographic information system (GIS) allows the computation and mapping of the areas which had changed. Based on the land-use change in the past 60 years and assuming the same growth rates for the different land-use types allows the projection of the land-use for the Schunter catchment in the year 2070. The land-use data for the years 1950, 2009 and 2070 were used to model the different infiltration capacity scenarios (Chapter 3.6.3).

3.8 Statistical analysis

Correlation and multiple regression analyses have been performed in order to predict the saturated hydraulic conductivity from field soil data. The statistical analyses were accomplished employing the statistical software-package SPSS Version 12 (2003).

4 Results

4.1 Land-use

The results of the aggregated land-use classes for 1950 and 2009 are given in Tab. 4.1.

Tab. 4.1: The land-use classification for the Schunter catchment for 2009 (based on ATKIS data) and for 1950 (based on topographic maps).

Land-use class	Land-use 1950		Land-use 2009	
	[ha]	[%]	[ha]	[%]
Cropping area	34480	56.6	29779	48.9
Forest	15913	26.1	16779	27.5
Grassland	7134	11.7	6924	11.4
Urban area	3188	5.1	6980	11.5
Water	231	0.4	484	0.8
Total catchment area	60946	100.0	60946	100.0

Land-use changes occur as an abrupt change, with severe changes in the soil properties (e.g. conversion of grassland to cropland). Observed over a longer period of time, a state of equilibrium according to the environmental conditions will be reached. If we consider a very long period of 60 years, certain land- use already reached again a state of equilibrium, while other changes (e.g. conversion of cropland to grassland) are still in the approach to a new equilibrium. With only two observation times of land-use, only statements for the observed situations (snapshots) can be made. For a more detailed description of processes, the analysis of land-use changes in a higher temporal resolution (e.g. every 2 years) is necessary, but within the framework of this work this could not be done.

4.1.1 Land-use 2009

The land-use of the Schunter catchment was dominated by agricultural and forestry-use (Tab. 4.1). More than sixty percent of the total area is used by agriculture (cropping + grassland) while the forest covers 27.5%. The urban area covers 11.5%, whereas water including filled mining sites covers 0.7%, respectively.

The Schunter watershed was distinguished into six sub-basins as shown in Table 4.2. The Upper Schunter sub-basin revealed the biggest area (33.2%) in the watershed, while the other sub-basins Wabe, Lower Schunter, Central Schunter, Uhrau, and Sandbach revealed 17.9 %, 13.8 %, 22.4 %, 6.8 %, and 5.8 % from the whole Schunter area.

Tab. 4.2: The Schunter sub catchments land-use classification 2009.

Land-use 2009	Wabe		Lower Schunter		Central Schunter		Upper Schunter		Uhrau		Sandbach	
	[ha]	%	[ha]	%	[ha]	%	[ha]	%	[ha]	%	[ha]	%
Cropland	5794	53.2	3047	36.1	6834	50.0	10384	51.3	1981	47.6	1741	49.0
Forest	2740	25.1	1954	23.2	3414	25.0	6533	32.3	1107	26.6	1031	29.0
Grassland	905	8.3	1108	13.1	2420	17.7	1219	6.0	773	18.6	499	14.1
Urban area	1360	12.5	2196	26.1	927	6.8	1969	9.7	259	6.2	268	7.5
Water	100	0.9	127	1.5	65	0.5	139	0.7	41	1.0	13	0.4
Total	10899	100	8432	100	13660	100	20244	100	4161	100	3552	100

The land-use characteristics of the catchment however change towards the Lower Schunter region in which the urban area covers 26.1% from the whole area compared to the other sub catchment in which the urban area revealed 12.5%, 6.8%, 9.7%, 7.5, and 6.2% from the total area of Wabe, Central Schunter, Upper Schunter, Sandbach,

and Uhrau, respectively (Table 4.2). This can be traced back to the adherent of the city of Braunschweig to the Lower Schunter catchment.

The percentage of forest differs within the sub-basins. In the Upper Schunter region, forest is the predominant land-use (32.3%).

In addition, cropland was distinguished through the sub-basins, where the Wabe region revealed 53.2% from the total area is covered by cropping land. While the Lower Schunter region revealed the smallest area, with 36.1 % cropland (Table 4.2).

In the Uhrau catchment, the fraction of grassland is 18.6 % from the sub catchment area showing the biggest region covered with the grassland class, while in the Upper Schunter region revealed the smallest area covered with 6.0% of grassland fraction, and the other sub-basins showed 8.3%, 13.1%, 17.7% and 14.1% in Wabe, Lower Schunter, Central Schunter, and Sandbach, respectively (Fig. 4.1).

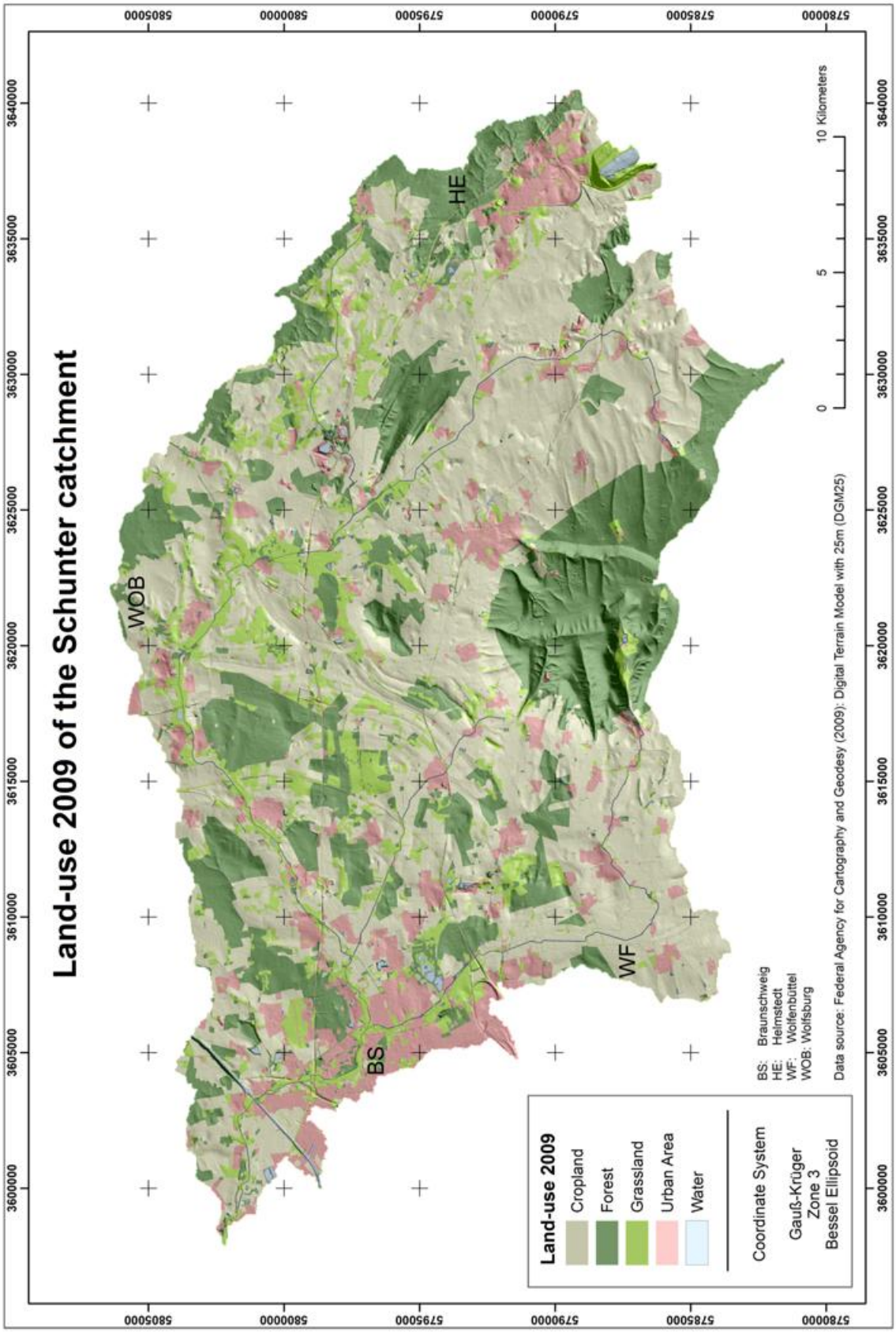

Fig.4.1: Land-use in the Schunter catchment 2009.

4.1.2 Land-use 1950

The results of the digitalisation of the topographic maps from 1950 revealed the following results.

The Schunter catchment is dominated by agricultural and forestry use. Table 4.1 demonstrates that 68 percent of the total area is covered by agriculture (cropland and grassland) while forest covers 26%. Urban area only covers 5% of the total catchment area in 1950 and the water classes cover only 0.4% from the total area respectively.

The land-use characteristics of the sub catchment revealed that the Lower Schunter region had the largest urban area for all catchments with 9.4 % of the total area compared to the other sub catchment in which the urban area revealed 4.6 %, 3.0 %, 6.0 %, 2.8 %, and 2.7 % from the total area of Wabe, Central Schunter, Upper Schunter, Uhrau, and Sandbach respectively (Tab. 4.3).

The percentage of the land-use class forest differs within the sub-basins as shown in Table 4.3. In the Upper Schunter region, forest is the predominant land-use (31.5%). While the other sub catchments such as Wabe, Lower Schunter, Central Schunter, Uhrau, and Sandbach revealed 23.9 %, 21.6 %, 22.4 %, 26.0 %, and 27.4 % forest from the whole area respectively.

Tab. 4.3: The Schunter sub catchments land-use classification 1950.

Land-use 1950	Wabe		Lower Schunter		Central Schunter		Upper Schunter		Uhrau		Sandbach	
	[ha]	%	[ha]	%	[ha]	%	[ha]	%	[ha]	%	[ha]	%
Cropland	6652	61.0	4243	50.3	8109	59.4	11109	54.9	2366	56.9	2001	56.3
Forest	2603	23.9	1822	21.6	3061	22.4	6373	31.5	1080	26.0	974	27.4
Grassland	1046	9.6	1500	17.8	2069	15.2	1464	7.2	579	13.9	476	13.4
Urban area	501	4.6	790	9.4	411	3.0	1274	6.0	118	2.8	94	2.7
Water	96	0.9	75	0.9	9	0.0	24	0.8	18	0.4	7	0.2
Total	10898	100	8430	100	13659	100	20244	100	4161	100	3552	100

In addition, the cropland class was distinguished through the sub-basins, where the Wabe region revealed 61.0 % from the whole total. While the Lower Schunter region revealed the smallest area, in which the cropland land-use class covered 50.3 % from the sub catchment area and for the Central Schunter, Upper Schunter, Uhrau, and Sandbach were 59.4 %, 54.9 %, 56.9 %, and 56.3 % respectively.

In Lower Schunter region, the fraction of grassland has been 17.8 % in 1950 from the sub catchment area showing the largest area covered with the grassland, while in the Upper Schunter region revealed the smallest area covered with 7.2 % of grassland fraction. The other sub-basins showed 9.6 %, 15.2 %, 13.9 %, 13.4 % grassland fraction in Wabe, Central Schunter, Uhrau, and Sandbach respectively.

The spatial distribution of the land-use classes for the Schunter catchment area is shown in Fig. 4.2.

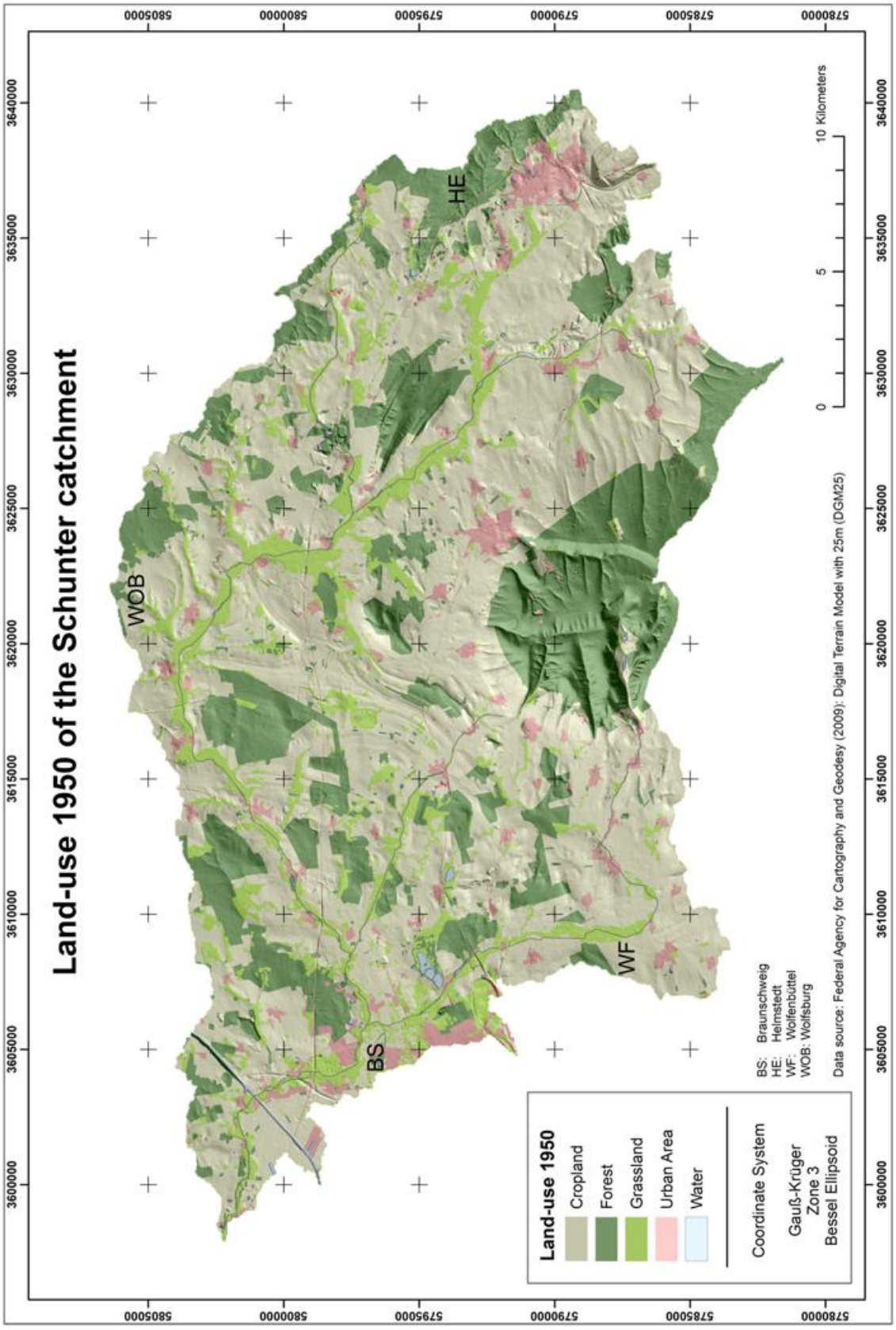

Fig.4.2: Digitized land-use map of the Schunter catchment area (1:50.000) in 1950.

4.2 Soil physical properties of the Schunter catchment

This chapter presents the results of the soil sample analysis, from the field data.

4.2.1 Soil texture

The texture of the investigated soil samples is given in (Table 4.4). The results indicate that there are two main texture classes under the cropland-use; loamy and silty loam (Wabe sub-basin, Sickte region), where the clay content varied from 12.2% to 36.2% with an average of 22.9 ± 6.64 %.

In order to enlarge the variability of the soil texture samples for the following infiltration computation, experimental results of other studies (Al-Hassoun, 2009 and Hartmann et al., 2008), for several sites in Germany, were added to this work. The texture data for the additional data can be found in the annex.

The texture distribution of all soil samples has been plotted into a soil texture triangle (Fig. 4.3).

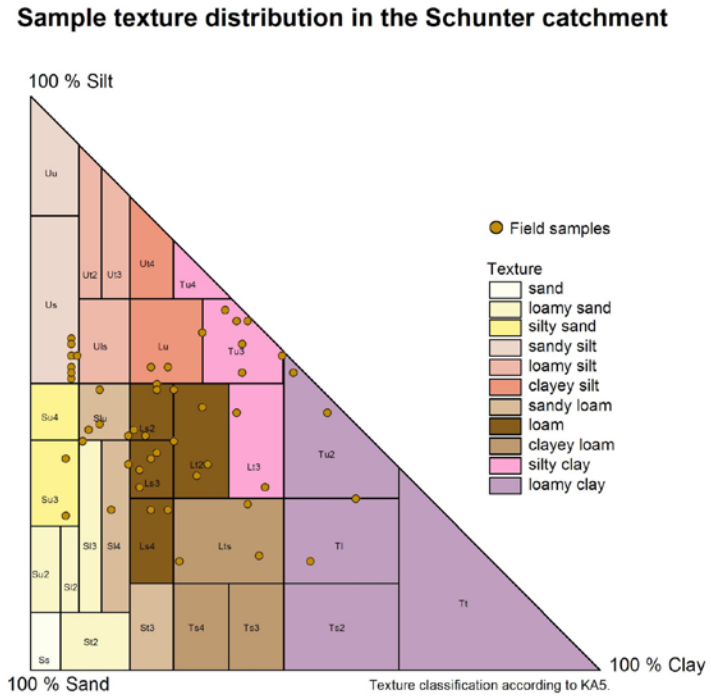

Fig.4.3: Texture distribution of all soil samples used in this work.

Tab. 4.4: Soil texture of the samples from the Schunter catchment area.

Field ID	Sample date	Sand [%]	Silt [%]	Clay [%]	Soil texture	Soil class (KA 5)
W-F1	19.08.09	32.8	18.5	48.6	Clay	Tl
S-F1	20.08.09	33.2	35.9	30.9	Clay Loam	Lt2
S-F2	11.08.09	48.2	28.4	23.5	Loam	Ls4
W-G1	06.08.09	13.6	29.9	56.5	Clay	Tl
W-G2	06.08.09	55.5	18.9	25.6	Sandy Clay Loam	Lts
W-G3	18.08.09	27.1	31.7	41.2	Clay	Lt3
W-G4	18.08.09	39.9	20.3	39.8	Clay Loam	Lts
W-C1	15.07.09	32.4	29.3	38.3	Clay Loam	Lts
S-C4	11.06.09	18.5	45.3	36.2	Silty Clay Loam	Lt3
S-C5	23.06.09	24.7	45.6	29.7	Clay Loam	Lt2
S-C6	24.06.09	41.7	41.4	16.9	Loam	Slu
S-C7	29.06.09	26.0	53.4	20.6	Silt Loam	Lu
S-C8	10.09.08	35.9	39.6	24.5	Loam	Ls3
S-C9	10.06.09	39.3	48.5	12.2	Loam	Slu
S-C11	17.09.08	42.2	36.9	20.9	Loam	Ls3
S-C12	17.09.08	46.6	34.6	18.8	Loam	Ls3
S-C13	11.09.08	57.9	27.9	14.2	Sandy Loam	Sl4
S-C14	07.07.09	25.7	49.0	25.3	Loam	Lt2
S-C15	06.07.09	23.6	52.6	23.8	Silt Loam	Lu
S-C16	30.06.09	37.0	33.7	29.3	Clay Loam	Lt2
S-C17	30.06.09	38.3	41.3	20.4	Loam	Ls2
S-C18	11.09.08	48.9	32.3	18.9	Loam	Ls3
S-C18a	11.09.08	40.4	37.7	21.9	Loam	Ls3
S-C19	30.06.09	50.9	28.3	20.8	Loam	Ls4
S-C22	30.06.09	28.1	50.2	21.7	Silt Loam	Lu
S-C23	10.09.08	28.4	50.2	21.4	Silt Loam	Lu

Land-use: C: Cropland, F: Forest, G: Grassland

Location: S: Sickte, W: Wendhausen

4.2.2 Bulk density

Soils with larger clay contents are affected by swelling and shrinking processes. The effective bulk density (eBD) takes these effects into account. The effective bulk density varied under different land-use and different land-management within the catchment as shown in Table 4.5.

Under agricultural land-use, the results revealed that the effective bulk density varied with an average of 1.57 ± 0.08 $g \cdot cm^{-3}$ (Wabe sub-basin, Sickte region).
The grassland class revealed the lowest values of the effective bulk density, where the values of the effective bulk density varied from 0.99 to 1.29 $g \cdot cm^{-3}$ with an average 1.18 ± 0.13 $g \cdot cm^{-3}$ (Central Schunter, Wendhausen region).

Moreover, the values of the effective bulk density under the forest land-use varied from 1.04 to 1.35 $g \cdot cm^{-3}$ with an average 1.20 ± 0.15 $g \cdot cm^{-3}$ in Sickte and Wendhausen, respectively.

4.2.3 Soil moisture parameters

The soil water contents of the soil samples under different land-uses are given in Table 4.5. The soil water contents varied with an average from 15.1 %, 32.3 %, and 40.8 % under cropland, forest, and grassland, respectively.
In order to make the different land-uses comparable the results in (Table 4.5) reflect the soil physical parameters for the upper mineral soil horizons under the investigated sites. The upper mineral soil horizons also reflect the impact of different land-use and land-management changes on the direct surface runoff.

Tab. 4.5: Soil physical characteristics for the field samples from the Schunter catchment

Field ID	eBD	C_{org}	Water content	Soil porosity	Water filled pore space	Volumetric water content	Water field capacity
	[g cm^{-3}]	[%]	[%]	[%]	[%]	[g cm^{-3}]	[cm^3 cm^{-3}]
W-F1	1.35	6.92	49.8	65.6	69.2	0.45	0.39
S-F1	1.22	5.94	20.6	64.4	30.2	0.19	0.31
S-F2	1.04	4.59	26.4	68.6	31.9	0.22	0.26
W-G1	1.23	10.25	58.6	72.7	58.2	0.42	0.48
W-G2	0.99	5.29	35.6	71.4	37.7	0.27	0.26
W-G3	1.29	4.99	36.7	65.5	51.3	0.34	0.37
W-G4	1.22	4.30	32.3	67.5	41.2	0.28	0.34
W-C1	1.58	2.13	25.2	53.4	58.3	0.31	0.35
S-C4	1.50	1.43	17.2	55.5	36.5	0.20	0.36
S-C5	1.64	1.53	12.1	48.1	34.6	0.17	0.32
S-C6	1.65	1.32	7.4	43.5	25.4	0.11	0.25
S-C7	1.48	1.08	10.8	51.3	27.2	0.14	0.29
S-C8	1.63	1.06	18.3	46.7	55.1	0.26	0.28
S-C9	1.42	1.01	14.7	50.6	38.1	0.19	0.25
S-C11	1.60	1.85	20.6	46.8	62.1	0.29	0.26
S-C12	1.44	1.62	21.4	52.1	52.0	0.27	0.25
S-C13	1.53	1.33	14.4	46.9	43.1	0.20	0.22
S-C14	1.50	4.07	12.4	52.0	30.3	0.16	0.30
S-C15	1.63	1.30	12.3	46.7	37.3	0.17	0.30
S-C16	1.61	1.53	11.6	49.0	32.0	0.16	0.30
S-C17	1.59	2.44	18.2	46.9	54.6	0.26	0.27
S-C18	1.72	1.46	14.4	41.6	53.4	0.22	0.24
S-C18a	1.59	1.54	16.1	47.4	47.4	0.22	0.27
S-C19	1.59	1.18	7.3	47.2	21.8	0.10	0.25
S-C22	1.47	6.01	15.0	52.1	36.7	0.19	0.29
S-C23	1.57	1.21	18.1	47.9	52.3	0.25	0.29

4.2.4 Infiltration measurements for the Schunter catchment

With the Hood-Infiltrometer, the steady flow rate was measured in the field. The data was converted to the steady state infiltration rate by using the equation 3.13 of Reynolds and Elrick, (1991). The results are presented in Tab. 4.6.

Tab. 4.6: Steady state infiltration rate (q_s) and saturated hydraulic conductivity of the field samples for the Schunter catchment.

Field ID	Date	q_s [mm h^{-1}]	Alpha [1/cm]	K_s [cm d^{-1}]	K_s /10 [cm d^{-1}]
W-F1	19.08.09	1458	0.0196	571	57.17
S-F1	20.08.09	1428	0.0108	329	32.96
S-F2	11.08.09	1614	0.0124	422	42.24
W-G1	06.08.09	948	0.0189	360	36.03
W-G2	06.08.09	960	0.0184	356	35.65
W-G3	18.08.09	1158	0.0145	348	34.88
W-G4	18.08.09	1332	0.0184	494	49.46
W-C1	15.07.09	1230	0.0156	395	39.53
S-C4	11.06.09	1032	0.0103	228	22.80
S-C5	23.06.09	1248	0.0104	278	27.82
S-C6	24.06.09	654	0.0147	199	19.94
S-C7	29.06.09	690	0.0066	100	10.06
S-C8	10.09.08	2088	0.0124	546	54.65
S-C9	10.06.09	1434	0.0082	256	25.65
S-C11	17.09.08	468	0.0138	134	13.49
S-C12	17.09.08	420	0.0126	111	11.15
S-C13	11.09.08	450	0.0231	202	20.29
S-C14	07.07.09	648	0.0078	110	11.06
S-C15	06.07.09	828	0.0082	148	14.81
S-C16	30.06.09	861	0.0142	255	25.54
S-C17	30.06.09	418	0.0116	103	10.35
S-C18	11.09.08	343	0.0234	155	15.59
S-C18a	11.09.08	264	0.0129	71	7.16
S-C19	30.06.09	384	0.0190	146	14.66
S-C22	30.06.09	540	0.0071	84	8.44
S-C23	10.09.08	2028	0.0081	358	35.86

The obtained results of the saturated hydraulic conductivity using the Hood-Infiltrometer were ten-folds higher compared to values using a disc-infiltrometer, when applied at the same test site (Schwärzel and Punzel, 2007, Wahl et al. 2009).

Schwärzel and Punzel (2007) stated that preparing the soil surface for disk infiltrometer measurements led to the sealing and smearing of the pores of the soil surface, and applying pressure heads near saturation might have caused mobile fine-textured particles of the contact material to clog the macropores, and this will result in a significant decrease in the saturated and near-saturated conductivity compared with the measurements without a contact layer. In addition, a drop in saturated and near saturated conductivity because of smeared pores, was also reported by Spohrer et al. (2006). For these reasons Schwärzel and Punzel (2007) reported that smearing, sealing, and clogging of pores lead to additional flow impedances in the soil surface layer, and the saturated conditions underneath the disk infiltrometer will never be reached during the disk experiments. Thus, the experimental results of the saturated hydraulic conductivity by using the Hood-Infiltrometer were divided by ten (as reported by Schwärzel and Punzel 2007) to get a reliable K_s data comparable to other K_s models.

The soil infiltration rate was strongly related to the different land-use classes as shown in Figure 4.4. Steady state infiltration rate was found to be significantly greater in forest, due to the large organic carbon with the consequence of high retention effect, followed by the grassland, and the cropland land.

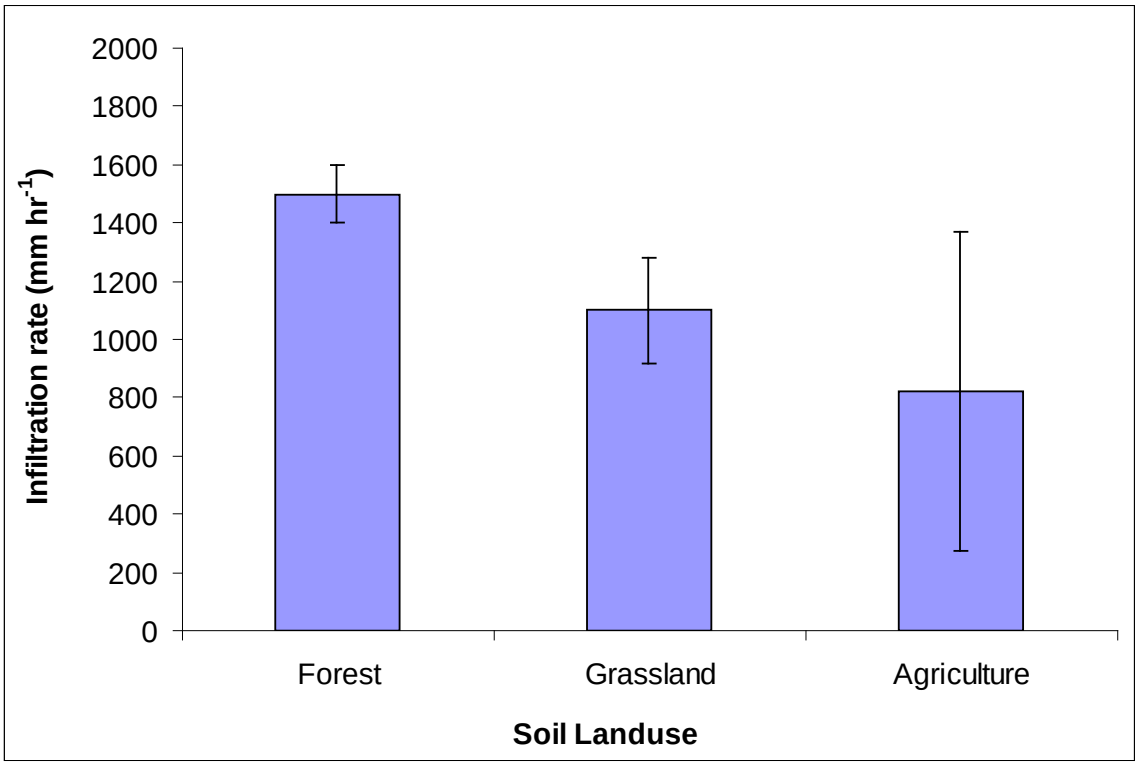

Fig.4.4: Steady infiltration rate for different land-use classes at 0.05 level LSD.

4.3 Saturated hydraulic conductivity

4.3.1 Computation according to Wooding and Gardner

Considering the experimental conditions for the steady infiltration field data, the unsaturated hydraulic conductivity results were calculated based on Wooding (equation 3.10) and for the final saturated hydraulic conductivity by the exponential function of Gardner (Equation 3.11) (Tab. 4.6).

The results of Table 4.6 show that the saturated hydraulic conductivity is related to the land-use. Saturated hydraulic conductivity was found to be significantly greater in forest with an average 441.2 ± 122.2 cm d^{-1}, followed by grassland with an average 390.0 ± 69.9 cm d^{-1}, and cropland land with an average 204.7 ± 123.1 cm d^{-1} (Fig. 4.5).

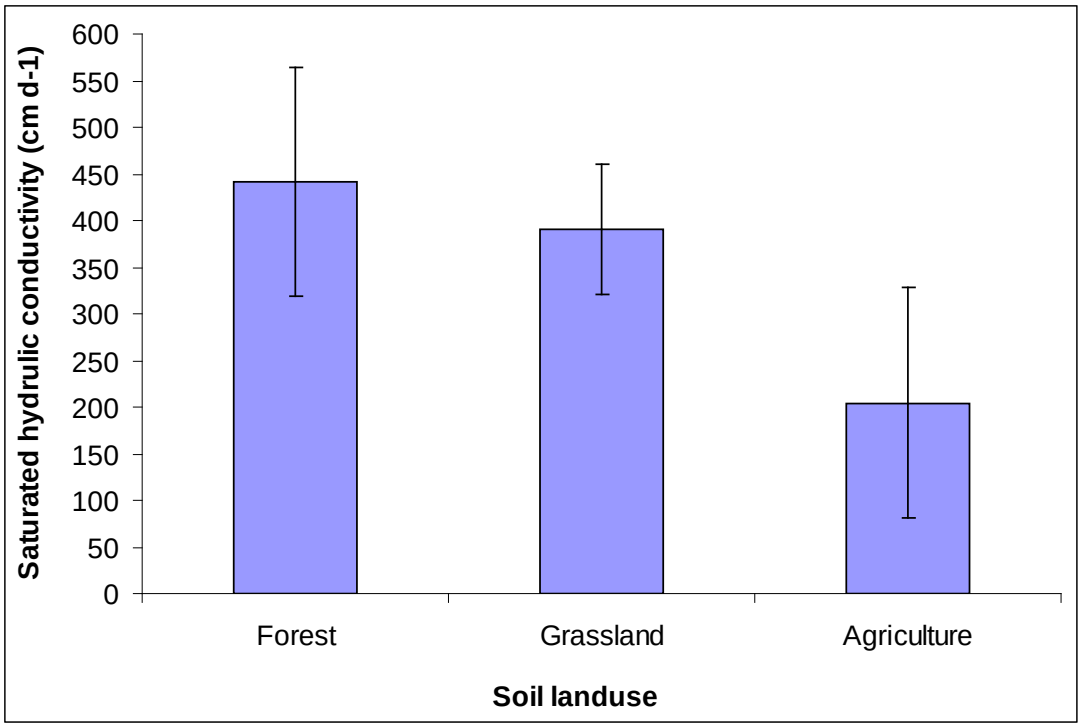

Fig.4.5: Average saturated hydraulic conductivity for different land-use at LSD 0.05 level**.**

4.3.2 Computation according to Pedotransfer functions

Infiltration measurements are time consuming. In order to retrieve soil hydraulic conductivity the use of pedo-transfer functions has been tested and compared to measured results. In addition, experimental results of other hood infiltration measurements (Al-Hassoun, 2009 and Hartmann et al. 2009), for different sites in Germany, were implemented in this work to get more variation impacts of different land-use, soil type, and land-management on the saturated hydraulic conductivity.

The five different PTFs, the Rosetta model (Schaap et al., 2001), Cosby et al. (1984), Saxton et al. (1986), Brakensiek et al. (1984), Vereecken et al. (1990) were used to compute the saturated hydraulic conductivity. The PTFs results were compared to the measured results in the field (Tab. 4.7).

Tab. 4.7: Predicted saturated hydraulic conductivity (K_s [cm d^{-1}]) from PTFs compared to measured results for the Schunter catchment.

ID	Measured	Rosetta	Cosby	Saxton	Brakensiek	Vereecken
W-F1	57.17	18.15	19.38	3.60	7.97	7.11
S-F1	32.96	26.15	25.45	8.54	38.45	91.54
S-F2	42.24	75.13	43.85	13.20	200.85	187.10
W-G1	36.03	22.18	9.88	5.16	27.92	0.64
W-G2	35.65	107.98	52.54	9.85	249.29	138.33
W-G3	34.88	20.57	18.32	5.21	20.95	19.47
W-G4	49.46	33.61	27.11	4.33	31.76	33.92
W-C1	39.53	4.14	22.29	5.39	2.49	35.24
S-C4	22.80	5.14	15.36	8.00	8.60	28.60
S-C5	27.82	2.89	20.24	10.86	2.63	84.37
S-C6	19.94	6.79	40.02	28.90	3.21	312.77
S-C7	10.06	9.93	24.03	23.52	17.21	218.94
S-C8	54.65	3.92	30.24	14.04	3.17	181.88
S-C9	25.65	22.30	40.01	50.77	35.63	407.90
S-C11	13.49	6.45	38.28	18.52	3.44	241.97
S-C12	11.15	15.66	44.86	22.26	14.47	259.11
S-C13	20.29	22.27	66.64	36.24	8.04	205.72
S-C14	11.06	6.71	22.23	15.28	6.28	140.28
S-C15	14.81	4.07	21.38	18.06	4.06	153.09
S-C16	25.54	3.67	29.09	9.09	2.55	115.50
S-C17	10.35	6.06	34.44	20.42	3.50	255.54
S-C18	15.59	5.86	47.89	21.55	1.39	244.57
S-C18a	7.16	5.89	35.80	17.05	3.92	227.57
S-C19	14.66	9.69	49.35	17.09	4.07	209.48
S-C22	8.44	9.45	25.13	20.50	7.64	208.61
S-C23	35.86	5.93	25.46	21.02	6.45	215.39

4.3.3 Simulation of one-dimensional water movement for selected soils of the Schunter catchment.

The numerical model Hydrus-1D was used to evaluate the impact of different land-use and land-management on the water movement. Texture and bulk density data from three soil samples taken on the same soil type (clay loam, Lt2) were used to model hydrological characteristics.

Implementing the results of texture analysis, the effective bulk density, and the measured saturated hydraulic conductivity for the three land-uses in the Hydrus-1D model, the hydrological parameters (Q_r, Q_s, α, n) can be optimized (Tab. 4.8).

Tab. 4.8: Hydraulic properties of sampled soils under different land-use in the Schunter catchment.

Field ID	Soil type	eBD	θ_r [$cm^3\ cm^{-3}$]	θ_s [$cm^3\ cm^{-3}$]	α [1/cm]	n	K_s [$cm\ d^{-1}$]
S-F1	Clay Loam	1.22	0.085	0.481	0.0108	1.480	32.96
W-G4	Clay Loam	1.22	0.094	0.504	0.0184	1.361	49.46
S-C16	Clay Loam	1.61	0.068	0.376	0.0142	1.351	25.54

θ_r: Residual water content

θ_s: Saturated water content

α: Sorptivity number

n: pore size distribution index

K_s: Saturated hydraulic conductivity

The results are summarized in Figure 4.6 illustrating differences in the soil water retention curves under the three land-uses.

For the forest and grassland an increase of the field capacity compared to the cropland. Under cropland, the water content at the field capacity was 0.2461 [$cm^3\ cm^{-3}$], while under the forest and grassland the water content at the field moisture capacity was 0.297 and 0.309 [$cm^3\ cm^{-3}$], respectively.

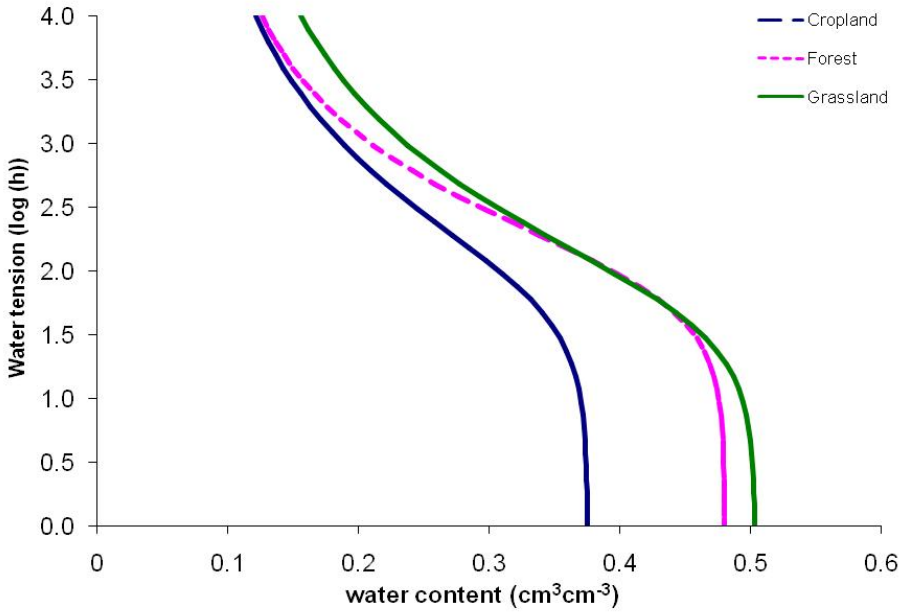

Fig.4.6: Water retention curves on a clay loam under different land-uses in the Schunter catchment.

With using the numerical model, the impact of the land-use on the infiltration rate was studied through investigate the cumulative infiltration curve under the different land-uses.

The cumulative infiltration curve under the different land-use impacts is shown in (Fig. 4.7). As seen on the graph, the infiltration under the grassland is much larger than forest and cropland; these results correspond with the effects of water retention.

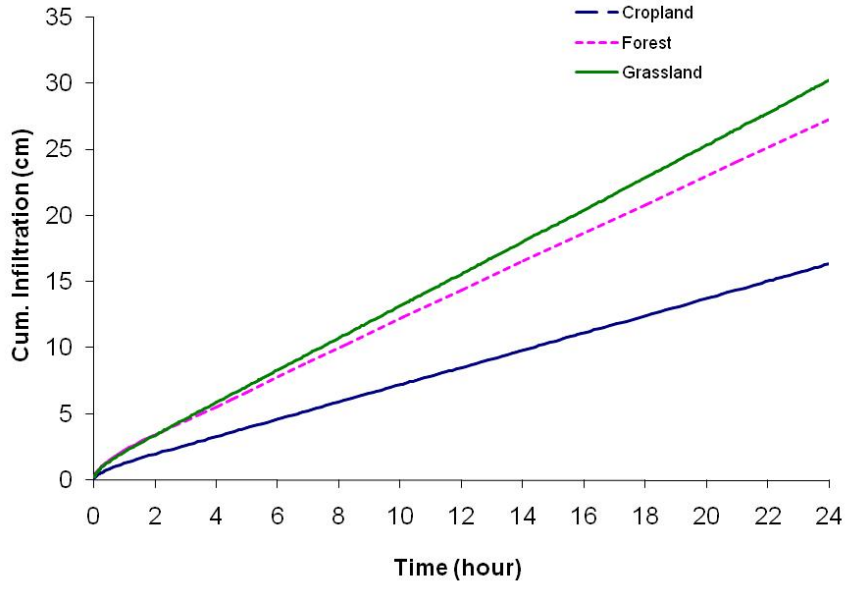

Fig.4.7: Cumulative infiltration of different land-uses in the Schunter catchment.

The volumetric water content was significantly higher under grassland and forest compared to cropland in the top soil surface (0-30 cm). Figure 4.8 shows the water content distribution in the top soil surface at 10 cm by using the numerical model of the Hydrus-1D. The volumetric water content after one hour of infiltration was constant under the different land-uses with a value of 0.371, 0.478, and 0.498 [cm^3 cm^{-3}], under cropland, forest, and grassland, respectively.

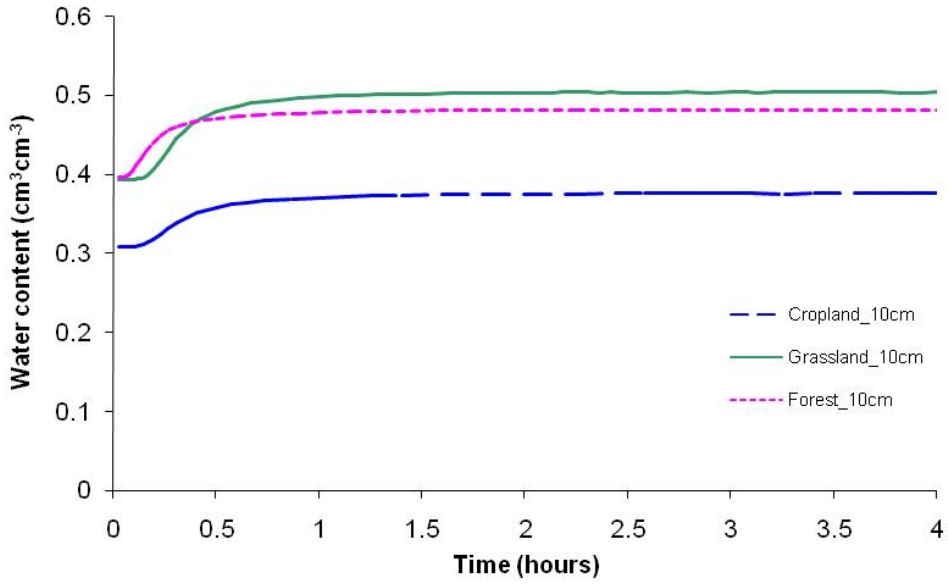

Fig.4.8: Volumetric water content for different land-uses 10 cm under the soil surface.

As a consequence of the land the soil water storage under grassland and forest was higher compared to cropland. In addition, these results correspond with the field moisture capacity results as shown in (Table 4.5).

In a second modelling step the impact of land-management on the water movement has been investigated: Texture and bulk density data from two soil samples taken on the same soil type (loamy clay, Tu2) but with different land-management (organic farming and conventional tillage) were used to model hydrological characteristics (Tab. 4.9).

Tab. 4.9: Hydraulic properties of sampled soils under different land-management in Brehmen catchment area.

Field ID	Soil type	Land management	eBD	θ_r [$cm^3\ cm^{-3}$]	θ_s [$cm^3\ cm^{-3}$]	α [1/cm]	n	K_s [$cm\ d^{-1}$]
B-C01	Loamy clay	organic	1.65	0.089	0.411	0.0121	1.330	28.26
B-C02	Loamy clay	conventional	1.73	0.085	0.388	0.0127	1.296	17.81

θ_r: Residual water content

θ_s: Saturated water content

α: Sorptivity number

n: pore size distribution index

K_s: Saturated hydraulic conductivity

Water retention curves under the impact of different land-management are shown in Fig. 4.9.

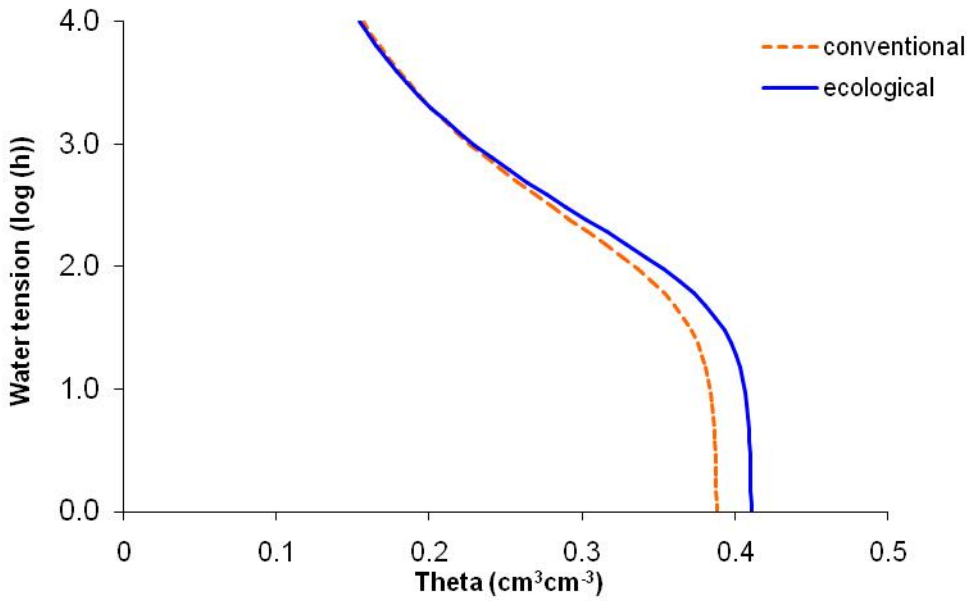

Fig.4.9: Water retention curves for a soil under organic and conventional management in Brehmen catchment.

Organic management revealed an increase of the field capacity compared to conventional tillage. Under conventional tillage the water content at the field capacity is relatively equal, 0.281, compared to 0.289 [cm^3 cm^{-3}] under organic management. With decreasing water tension organically managed soils show larger water content.

The cumulative infiltration curve for different land-management is shown in Fig. 4.10. As seen on the graph, the infiltration under the organic management is larger than the conventional tillage.

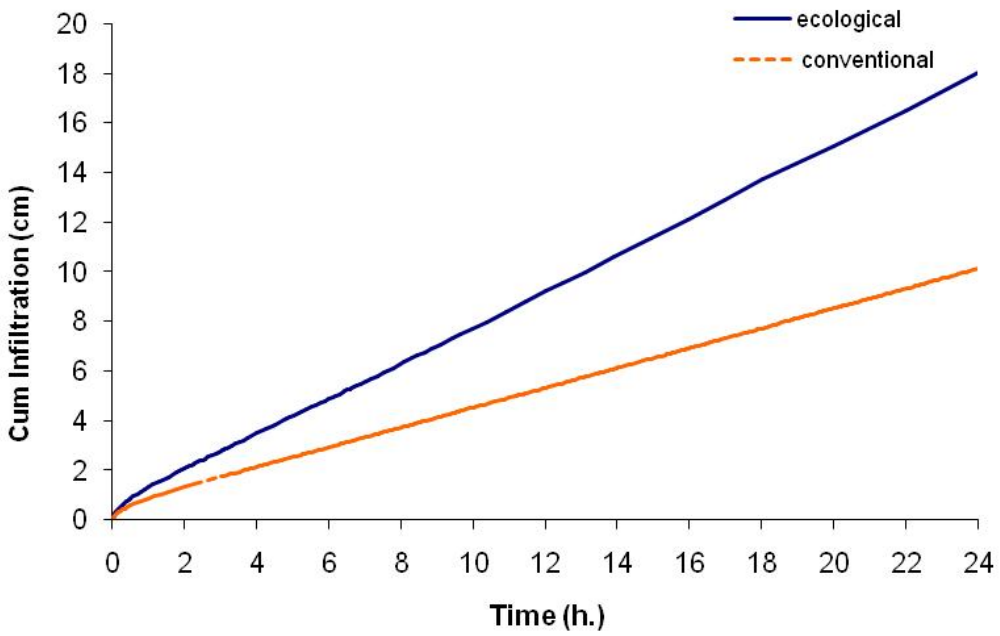

Fig.4.10: Cumulative infiltration under different land-management in Brehmen catchment.

The saturated hydraulic conductivity has been simulated over time at different depths. At a depth of 10 cm the K_s values under conventional tillage was 0.119 [cm h^{-1}] while under organic management was nearly three times higher with 0.349 [cm h^{-1}], as show in (Figure 4.11)

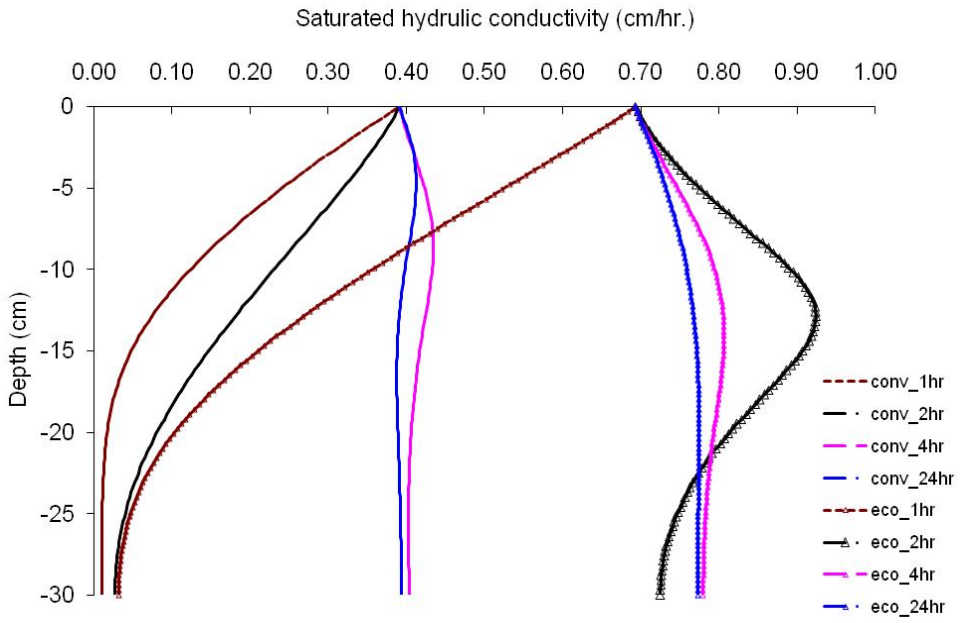

Fig.4.11: Change of saturated hydraulic conductivity under organic and conventional management in Brehmen catchment.

In addition, it requires two hours for the entire top soil surface (0-30 cm) to be saturated under the organic management and the K_s values be close to the maximum saturated hydraulic conductivity (0.7 [cm h^{-1}]), while it requires four hours under conventional tillage to be close to the saturation with a maximum K_s value be of 0.4 [cm h^{-1}].

4.4 Land-use change for the Schunter catchment.

The results of the land-use mapping of the Schunter catchment for 1950 and 2009 and the projection of the developments in the future are shown in Table 4.10 and Fig. 4.12. This Scenario uses the land-use change in the last 59 years (1950-2009) and assumes the same growth rates (urbanisation) to the future in 2070. This is just a theoretical consideration, since there has been a strong reconstruction and urbanisation in the post World War II years. On the other hand this assumption is not too unrealistic since there is a strong trend of urban sprawl by building industrial and business areas.

Tab. 4.10: Land-use of the Schunter catchment area in 1950, 2009 and projected for 2070.

Land-use [%]	1950	2009	2070
Cropland	56.6	48.9	41.2
Forest	26.1	27.5	28.9
Grassland	11.7	11.4	11.0
Urban Area	5.2	11.5	17.7
Water	0.4	0.7	1.2
Sum	100.0	100.0	100.0

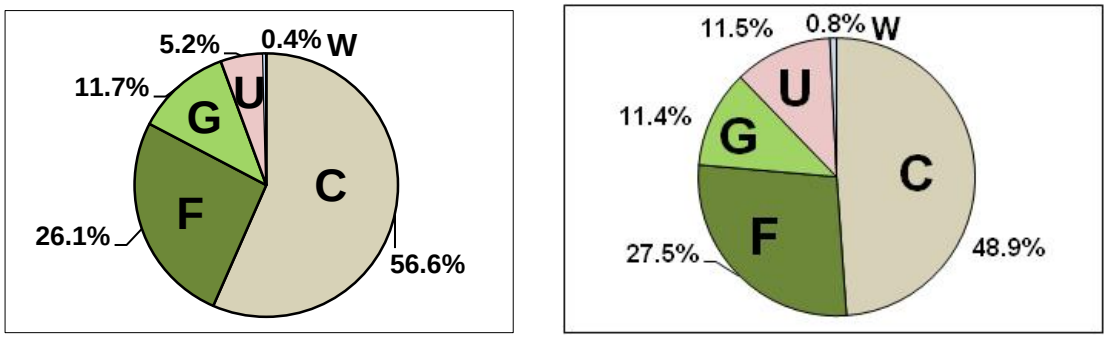

Fig.4.12: Land-use distribution in 1950 (left) and 2009 (right) for the Schunter catchment. (C: Cropland, F: Forest, G: Grassland, U: Urban area, W: Water).

Between 1950 and 2009 Cropland shows the biggest loss, whereas urban area shows the largest increase (Tab. 4.11). Also Grassland has been decreased but only on a small amount. The area covered with forest has slightly increased, probably due to forestation, since directly after World War II wood was used for firing and heating. There is also an increase in water area. This can be explained by the close down of mining activities. The remaining open casts are recently filled with water.

Tab. 4.11: Land-use change between 1950 and 2009 in the Schunter catchment.

Land-use	1950 – 2009 [%]	1950 – 2009 [ha]
Cropland	- 7.7	- 4700
Forest	+ 1.4	+ 866
Grassland	- 0.3	- 210
Urban Area	+ 6.2	+ 3791
Water	+ 0.4	+ 253

To show the dynamics of the land-use change, the land-use in 2009 was traced back to its use in 1950. The results are displayed in Table 4.12. The diagonal of the table shows the stable land-uses which stayed the same over the past 60 years.

Tab. 4.12: The distribution in percent of each land-use class in 1950 to the current status 2009 in the Schunter catchment.

1950/2009	Cropland	Forest	Grassland	Urban Area	Water
Cropland	**78.0**	2.5	9.5	9.6	0.5
Forest	1.5	**95.6**	1.3	1.4	0.2
Grassland	35.5	7.92	**45.2**	10.0	1.3
Urban Area	3.6	4.2	5.9	**85.9**	0.4
Water	2.7	2.9	10.4	1.6	**82.4**

These results reveal that 78 % of the cropland-use in 1950 is still used as cropland in 2009. Moreover the impact of cultivation of grassland in the Schunter catchment area was pronounced, where 35.5 % of the grassland in 1950 has been converted to cropland in 2009.

It is interesting to compare the absolute change of grassland between 1950 and 2009 (Table 4.11) and the land-use distribution. The total change has only been a reduction of 0.3 %. But in the last 60 years only 45.2 % of the grassland was kept stable (Tab. 4.12). The conversion of grassland to cropland (35.5 %) resulted in a loss, but and the straightening of the river Schunter delivered new grassland (10.4%). The reduction of agricultural production and the conversion of cropland to grassland lead also to in increase in grassland by nearly 10%. The conversion of urban area to grassland arises from the fact, that in this classification scheme, industrial and mining sites are grouped to urban area. The closed mining sites have been renaturated to grassland.
The very complex structures of land-use change distribution have been mapped in Figure 4.13.

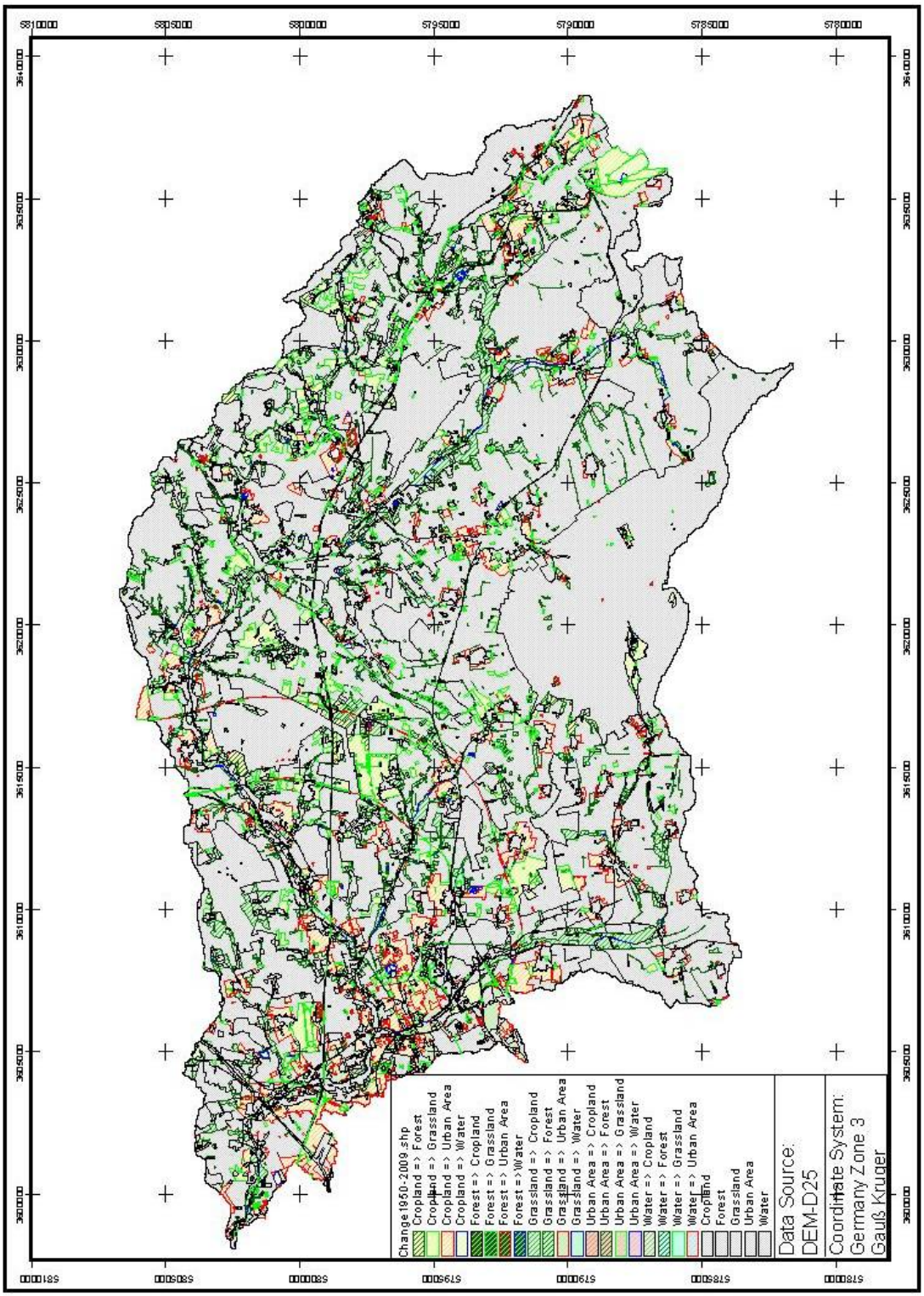

Fig.4.13: Land-use change between 1950 and 2009 in the Schunter catchment.

The land-use change is also presented on a sub catchment scale:

Wabe

The Wabe catchment is close to the city of Braunschweig, the urban growth is the dominating process, which results in a decrease of cropland (Fig. 4.14) and Table 4.13.

Tab. 4.13: Land-use of the Wabe catchment area in 1950 and 2009 and projected for 2070.

Land-use [%]	**1950**	**2009**	**2070**
Cropland	61.0	53.2	45.3
Forest	23.9	25.1	26.4
Grassland	9.6	8.3	7.0
Urban Area	4.6	12.5	20.4
Water	0.9	0.9	0.9
Sum	100.0	100.0	100.0

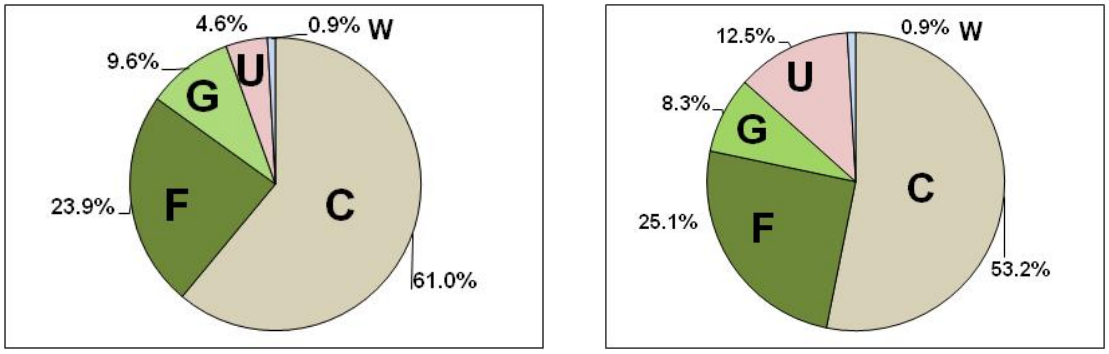

Fig.4.14: Land-use distribution in 1950 (left) and 2009 (right) for the Wabe catchment.
(C: Cropland, F: Forest, G: Grassland, U: Urban area, W: Water).

Tab. 4.14: Land-use change between 1950 and 2009 for Wabe catchment.

Land-use	**1950 – 2009 [%]**	**1950 – 2009 [ha]**
Cropland	- 7.9	- 858
Forest	+ 1.2	+ 137
Grassland	- 1.3	- 141
Urban Area	+ 7.9	+ 859
Water	+ 0.0	+ 4

The contribution of each land-use in 1950 to the current status in 2009 is listed in Table 4.15. These results reveal that 80 % of the cropland-use in 1950 contributed to the total area which forms the cropland-use today, while 2.0 %, 7.6 %, and 10.5 % of the initial cropland in 1950 converted to forest, grassland, and urban area in 2009, respectively.

Moreover, the Wabe sub-catchment reveals a pronounced impact of cultivation the grassland, where 41.3 % of the grassland in 1950 converted to cropland in 2009, while 6.1 %, 32.4 %, and 19.6 % of the initial grassland converted to forest, grassland and urban area in 2009, respectively (Table 4.15).

Tab. 4.15: The distribution in percent of each land-use class in 1950 to the current status 2009 for the Wabe catchment.

1950/2009	Cropland	Forest	Grassland	Urban Area	Water
Cropland	**79.8**	2.0	7.6	10.5	0.2
Forest	1.1	**97.2**	0.7	0.9	0.1
Grassland	41.3	6.1	**32.4**	19.6	0.7
Urban Area	5.6	2.7	5.5	**86.1**	0.1
Water	0.5	1.7	14.4	1.1	**82.2**

Lower Schunter

The Lower Schunter catchment is also close to the city of Braunschweig. Here the largest increase of urban area has taken place in the past 60 years as shown in Table 4.16 and Fig. 4.15.

Tab. 4.16: Land-use of the Lower Schunter catchment area in 1950 and 2009 and projected for 2070.

Land-use [%]	**1950**	**2009**	**2070**
Cropland	50.3	36.2	21.9
Forest	21.6	23.2	24.8
Grassland	17.8	13.1	8.5
Urban Area	9.4	26.0	42.7
Water	0.9	1.5	2.1
Sum	100.0	100.0	100.0

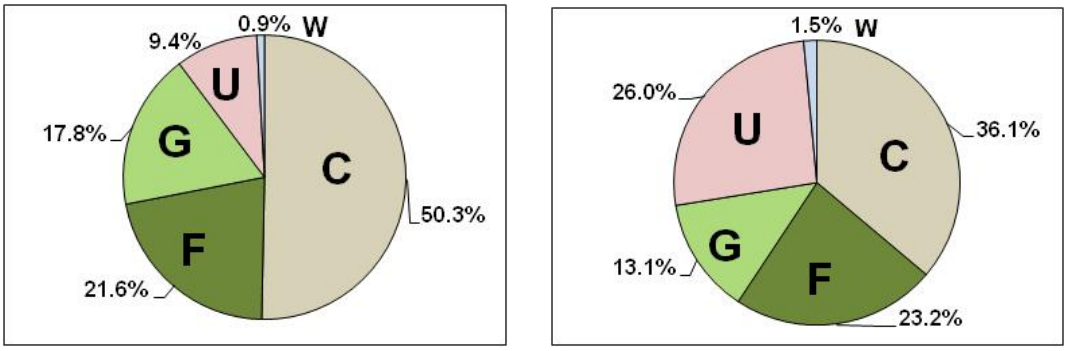

Fig.4.15: Land-use distribution in 1950 (left) and 2009 (right) for the Lower Schunter catchment. (C: Cropland, F: Forest, G: Grassland, U: Urban area, W: Water).

Table 4.17 reveals the results of the land-use change in the Lower Schunter sub catchment from 1950 to 2009. The results reveals that the urban growth in the Lower Schunter compared to the other sub catchments in the Schunter area is a pronounced process in the sub catchment compared to the other land-use change, where urban area land-use increased by 16.7 % compared to a loss of the cropland and the grassland by 14.2 % and 4.7 % respectively.

Tab. 4.17: Land-use change between 1950 and 2009 Lower Schunter catchment.

Land-use	**1950 – 2009 [%]**	**1950 – 2009 [ha]**
Cropland	- 14.2	- 1197
Forest	+ 1.6	+ 132
Grassland	- 4.7	- 392
Urban Area	+ 16.7	+ 1405
Water	+ 0.6	+ 52

The land-use distribution between 1950 and 2009 is demonstrated in Table 4.18. These results reveal that 61 % of the crop land-use in 1950 contributed to the total area which forms the crop land-use in current status quo in 2009, while 2.6 %, 9.7 %, and 25.31 % of the initial cropland in 1950 converted to forest, grassland, and urban area in 2009, respectively. In addition, Lower Schunter sub catchment reveals a pronounced impact of cultivation the grassland, and converting the grassland to urban area where 27.6 % of the grassland in 1950 converted to cropland in 2009, while 21.9

% of the initial grassland converted to urban area in 2009 (Table 4.18). Otherwise there is no pronounced change in the forest land-use through 1950 to 2009 where 95 % of the initial forest land-use in 1950 contributes to the forest land-use in 2009 (Table 4.18).

Tab. 4.18: The distribution in percent of each land-use class in 1950 to the current status 2009 for the Lower Schunter catchment.

1950/2009	Cropland	Forest	Grassland	Urban Area	Water
Cropland	**61.6**	2.6	9.7	25.3	0.8
Forest	0.6	**95.3**	1.0	3.0	0.1
Grassland	27.6	5.0	**44.3**	21.9	1.2
Urban Area	0.8	4.1	1.8	**93.3**	0.1
Water	2.0	0.1	2.2	1.6	**94.0**

Central Schunter

The Central Schunter catchment is characterised by a strong loss of cropland and a small increase of grassland (Tab. 4.19).

Tab. 4.19: Land-use of the Central Schunter catchment area in 1950 and 2009 and projected for 2070.

Land-use [%]	**1950**	**2009**	**2070**
Cropland	59.4	50.0	40.7
Forest	22.4	25.0	27.6
Grassland	15.1	17.7	20.3
Urban Area	3.0	6.8	10.6
Water	0.1	0.5	0.8
Sum	100.0	100.0	100.0

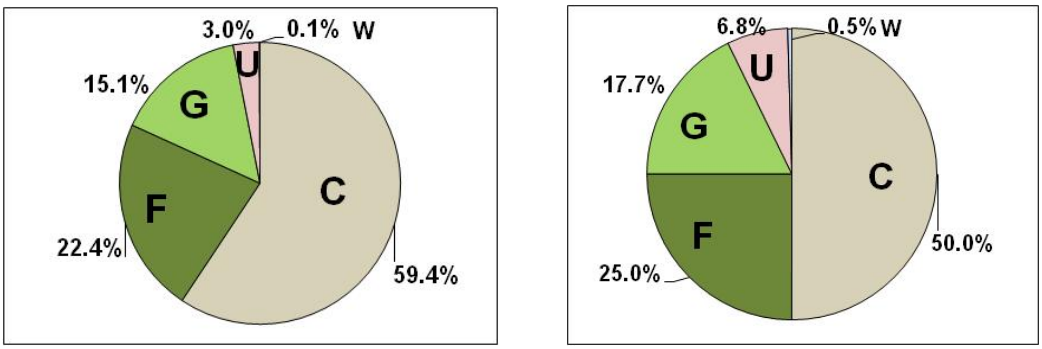

Fig.4.16: Land-use distribution in 1950 (left) and 2009 (right) for the Central Schunter catchment. (C: Cropland, F: Forest, G: Grassland, U: Urban area, W: Water).

The results of the land-use classification of the Central Schunter sub catchment for 1950 and 2009 are shown in Figure 4.16. Cropland shows the biggest loss by 9.3 %, whereas urban area, forest and grassland show an increase by 3.8 %, 2.6 %, and 2.6 % respectively Tab. 4.20.

Tab. 4.20: Land-use change between 1950 and 2009 in the Central Schunter catchment.

Land-use	**1950 – 2009 [%]**	**1950 – 2009 [ha]**
Cropland	- 9.3	- 1276
Forest	+ 2.6	+ 353
Grassland	+ 2.6	+ 352
Urban Area	+ 3.8	+ 516
Water	+ 0.4	+ 55

The land-use distribution between 1950 and 2009 is demonstrated in Table 4.22. These results reveal that 77 % of the crop land-use in 1950 contributed to the total area which forms the cropland-use in 2009, while 3.4 %, 13.2%, and 6.1 % of the initial cropland in 1950 converted to forest, grassland, and urban area in 2009, respectively. In addition, the Central Schunter sub catchment reveals a pronounced impact of cultivation the grassland, and converting the grassland to forest where 23.4 % of the grassland in 1950 converted to cropland in 2009, while 10.7 % of the initial grassland converted to forest in 2009, and 61.2 % of the initial grassland contributed to the current area of the grassland in 2009 (Table 4.21).

Tab. 4.21: The distribution in percent of each land-use class in 1950 to the current status 2009 for the Central Schunter catchment.

1950/2009	Cropland	Forest	Grassland	Urban Area	Water
Cropland	**77.1**	3.4	13.2	6.1	0.2
Forest	2.4	**94.8**	2.1	0.6	0.1
Grassland	23.4	10.7	**61.2**	3.2	1.6
Urban Area	5.6	3.3	4.3	**86.1**	0.8
Water	4.9	11.8	14.5	3.3	**65.5**

Upper Schunter

The Upper Schunter catchment is characterised by a medium loss of cropland and grassland (Tab. 4.22).

Tab. 4.22: Land-use of the Upper Schunter catchment area in 1950 and 2009 and projected for 2070.

Land-use [%]	**1950**	**2009**	**2070**
Cropland	54.9	51.3	47.7
Forest	31.5	32.3	33.1
Grassland	7.2	6.0	4.8
Urban Area	6.3	9.7	13.2
Water	0.1	0.7	1.2
Sum	100.0	100.0	100.0

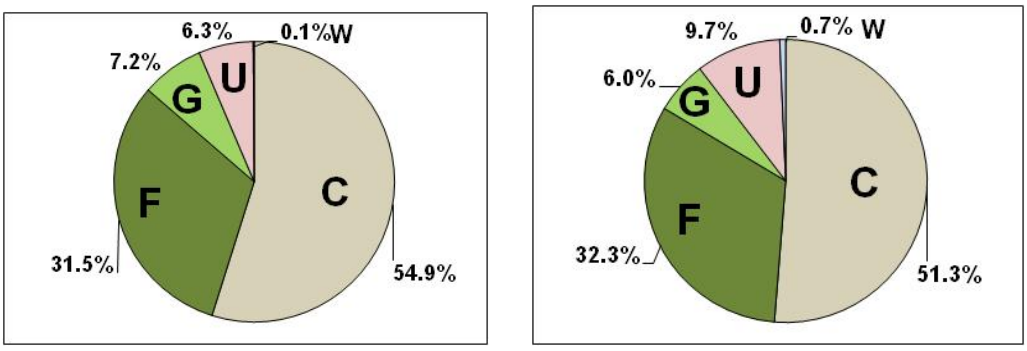

Fig.4.17: Land-use distribution in 1950 (left) and 2009 (right) for the Upper Schunter catchment. (C: Cropland, F: Forest, G: Grassland, U: Urban area, W: Water).

The change in the land-use for the Upper Schunter was not pronounced (Fig.4.17). Cropland shows the biggest loss by 3.6 %, whereas urban area shows an increase by 3.4% with a decreasing in grassland by 1.2 % (Tab. 4.23).

Tab. 4.23: Land-use change between 1950 and 2009 in Upper Schunter catchment.

Land-use	**1950 – 2009 [%]**	**1950 – 2009 [ha]**
Cropland	- 3.6	- 725
Forest	+ 0.8	+ 160
Grassland	- 1.2	+ 245
Urban Area	+ 3.4	+ 695
Water	+ 0.6	+ 114

The catchment of the Upper Schunter shows a stable cropland-use with 85 % of the cropland in 1950 contributed to current area, while 1.7 %, 5.0 %, and 6.9 % of the initial cropland in 1950 have been converted to forest, grassland, and urban area in 2009, respectively (Table 4.24).

However, Upper Schunter sub catchment reveals a pronounced impact of cultivation the grassland, and converting the grassland to forest where 51.5 % of the grassland in 1950 converted to cropland in 2009, while 9.3 % of the initial grassland converted to forest in 2009, and only 32.7 % of the initial grassland contributed to the current status area of the grassland in 2009 (Table 4.24).

Tab. 4.24: The distribution in percent of each land-use class in 1950 to the current status 2009 for the Upper Schunter catchment.

1950/2009	Cropland	Forest	Grassland	Urban Area	Water
Cropland	**85.5**	1.7	5.0	6.9	0.8
Forest	1.3	**96.5**	1.0	1.2	0.1
Grassland	51.5	9.0	**32.7**	5.3	1.6
Urban Area	3.7	4.3	9.3	**82.2**	0.5
Water	10.6	11.4	14.7	3.4	**59.8**

Uhrau

The Uhrau catchment is characterised by a strong loss of cropland and a big increase in grassland (Tab. 4.25).

Tab. 4.25: Land-use of the Uhrau catchment area in 1950 and 2009 and projected for 2070.

Land-use [%]	**1950**	**2009**	**2070**
Cropland	56.9	47.6	38.4
Forest	26.0	26.6	27.3
Grassland	13.9	18.6	23.2
Urban Area	2.8	6.2	9.6
Water	0.4	1.0	1.5
Sum	100.0	100.0	100.0

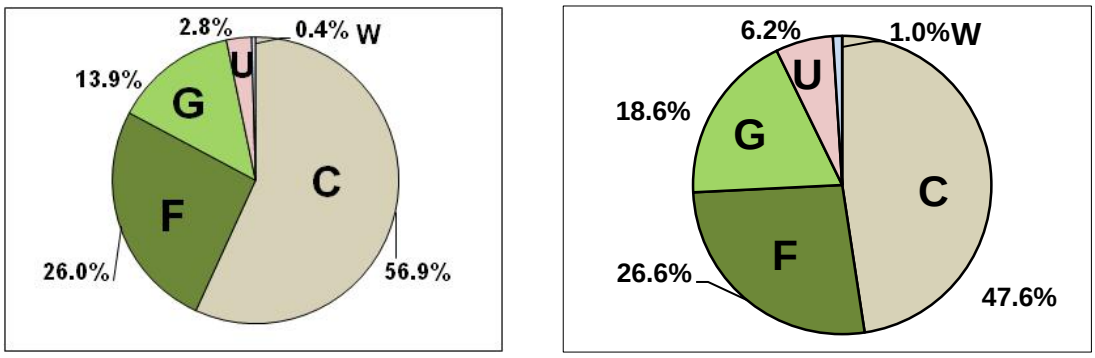

Fig.4.18: Land-use distribution in 1950 (left) and 2009 (right) for the Uhrau catchment. (C: Cropland, F: Forest, G: Grassland, U: Urban area, W: Water).

For the Uhrau sub catchment, the cropland shows the biggest loss by 9.3 %, whereas the grassland shows the largest increase in this sub-basin by 4.7 % (Tab. 4.26). Also the urban area has been increased but only on a small amount by 3.4 %. The area covered with forest has slightly increased, probably due to forestation, by 0.7 %.

Tab. 4.26: Land-use change between 1950 and 2009 in Uhrau catchment.

Land-use	**1950 – 2009 [%]**	**1950 – 2009 [ha]**
Cropland	- 9.3	- 385
Forest	+ 0.7	+ 28
Grassland	+ 4.7	+ 193
Urban Area	+ 3.4	+ 141
Water	+ 0.6	+ 23

These results show that 73 % of the cropland in 1950 contributed to the cropland in 2009, while 3.4 % and 4.9 % of the initial cropland in 1950 converted to forest and urban area in 2009, respectively. Furthermore, the Uhrau sub catchment reveals a pronounced impact of converting the cropland to grassland, where 18 % of the total area cultivated in 1950 converted to grassland in 2009. In addition, the sub catchment reveals the impact of cultivation the grassland, and converting the grassland to cropland where 35.5 % of the grassland in 1950 converted to cropland in 2009, while 52.5 % of the initial grassland in 1950 contributed to the current status quo of the grassland in 2009, and 4 % of the initial grassland converted to urban area in 2009 (Table 4.27).

Tab. 4.27: The distribution in percent of each land-use class in 1950 to the current status 2009 for the Uhrau catchment.

1950/2009	Cropland	Forest	Grassland	Urban Area	Water
Cropland	**73.6**	3.4	17.9	4.9	0.2
Forest	2.3	**89.8**	2.9	3.6	1.4
Grassland	35.5	7.0	**52.5**	3.7	1.3
Urban Area	6.3	14.4	8.7	**69.5**	1.1
Water	5.8	2.1	16.5	1.3	**74.3**

Sandbach

The Sandbach catchment is characterised by a strong increase of urban area and a strong loss of cropland as shown in Fig. 4.19 and Table 4.28.

Tab. 4.28: Land-use of the Sandbach catchment area in 1950 and 2009 and projected for 2070.

Land-use [%]	**1950**	**2009**	**2070**
Cropland	56.3	49.0	41.7
Forest	27.4	29.0	30.6
Grassland	13.4	14.0	14.7
Urban Area	2.7	7.6	12.5
Water	0.2	0.4	0.5
Sum	100.0	100.0	100.0

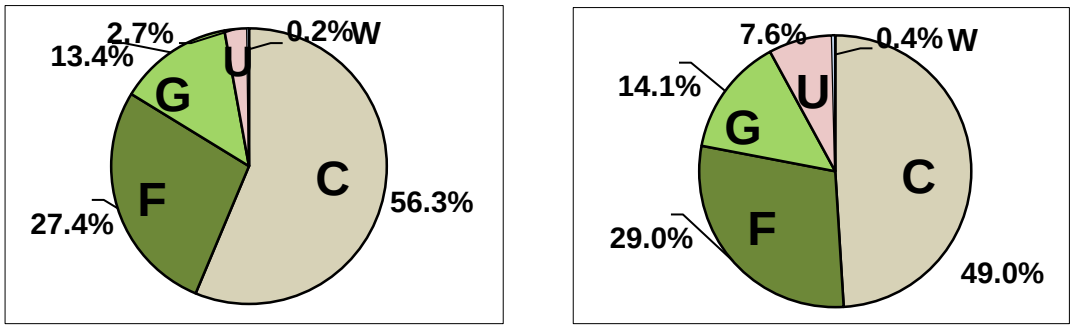

Fig.4.19: Land-use distribution in 1950 (left) and 2009 (right) for the Sandbach catchment. (C: Cropland, F: Forest, G: Grassland, U: Urban area, W: Water).

For the Sandbach sub catchment, the land-use change display the same phenomenon such as the change in Uhrau sub catchment, where the cropland also shows the biggest loss by 7.3 %, whereas the urban area shows the largest increase in this sub-basin by 4.9 % (Tab. 4.29).

Tab. 4.29: Land-use change between 1950 and 2009 in the Sandbach catchment.

Land-use	**1950 – 2009 [%]**	**1950 – 2009 [ha]**
Cropland	- 7.3	- 260
Forest	+ 1.6	+ 57
Grassland	+ 0.7	+ 23
Urban Area	+ 4.9	+ 174
Water	+ 0.2	+ 6

These results for the Sandbach catchment show that 74 % of the cropland still is cropland in 2009, while 3.3 % and 7.7 % of the initial cropland in 1950 converted to forest and urban area in 2009, respectively. Furthermore, Sandbach sub catchment reveals the same pronounced impact like the Uhrau sub catchment for converting the cropland to grassland, where 15 % of the cultivated total area in 1950 converted to grassland in 2009.

In addition, the sub catchment reveals the impact of cultivation the grassland, and converting the grassland to cropland where 52 % of the grassland in 1950 converted to cropland in 2009, while 37 % of the initial grassland in 1950 contributed to the current status quo of the grassland in 2009, and 3 % of the initial grassland converted to urban area in 2009 (Table 4.30).

Tab. 4.30: The distribution in percent of each land-use class in 1950 to the current status 2009 for the Sandbach catchment.

1950/2009	Cropland	Forest	Grassland	Urban Area	Water
Cropland	**73.6**	3.3	15.3	7.7	0.1
Forest	1.9	**95.3**	1.6	1.2	0.0
Grassland	51.6	7.0	**37.1**	3.3	0.9
Urban Area	2.6	2.3	1.1	**93.7**	0.5
Water	0.0	9.0	7.3	1.2	**82.5**

4.5 Infiltration simulation for the selected soil samples

4.5.1 Curve number computation for the selected soils

The measured curve numbers (CN_m) have been computed for all field measurements, PTFs and compared to previous published CN values from the literature (NEH, 2004; Voges, 1999; Hartmann et al., 2008) which basically relayed on the curve number values from the SCS (1986).

The CN_m for each soil type and corresponding land-use classes for all field data are presented in Table 4.31.

Tab. 4.31: Computed CN_m based on the applied saturated hydraulic conductivity and the pedotransfer functions for the selected sites.

Field ID	Land-use	Crop	HSG	CN_m meas.	CN NEH	CN_m Rosetta	CN_m Cosby	CN_m Saxton	CN_m Vereecken	CN Brakensiek
S-F1	Forest	-	A	44	36	49	50	75	40	22
S-F2	Forest	-	A	38	36	25	37	66	11	12
W-F1	Forest	-	A	31	36	58	57	88	76	78
M-G2	Grass.	-	A	53	49	36	25	19	19	10
T-G1	Grass.	-	A	60	49	72	35	48	89	8
T-G2	Grass.	-	A	67	49	59	34	33	64	7
T-G3	Grass.	-	A	57	49	72	35	48	89	8
W-G1	Grass.	-	A	41	49	53	72	83	48	98
W-G2	Grass.	-	A	42	49	19	33	72	9	16
W-G3	Grass.	-	A	42	49	55	58	83	55	57
W-G4	Grass.	-	A	34	49	43	48	85	44	43
M-G1	Grass.	-	B	77	69	92	65	65	93	37
B-C3	Crop. (cv.)	WW	A	88	67	83	65	65	73	37
B-C6	Crop. (cv.)	WR	A	86	67	75	72	69	28	68
B-C10	Crop. (cv.)	MS	A	84	67	91	75	75	68	88
FV4_132	Crop. (cv.)	WW	A	72	67	55	40	22	56	5
FV4-232	Crop. (cv.)	FB	A	89	67	45	40	22	36	5
FV36-4	Crop. (cv.)	WR	A	81	67	47	39	22	43	5
FV36-10	Crop. (cv.)	WR	A	79	67	39	39	23	28	5
FV36-10	Crop. (cv.)	WW	A	88	67	48	39	23	46	5
FV36-12	Crop. (cv.)	WR	A	79	67	43	38	23	35	5
M-C3	Crop. (cv.)	WB	A	66	67	60	30	26	87	7
M-C4	Crop. (cv.)	WB	A	63	67	35	21	18	63	20
S-C4	Crop. (cv.)	MS	A	53	67	83	62	76	75	47

Field ID	Land-use	Crop	HSG	CN_m meas.	CN NEH	CN_m Rosetta	CN_m Cosby	CN_m Saxton	CN_m Vereecken	CN Brakensiek
S-C6	Crop. (cv.)	WW	A	56	67	79	39	47	89	8
S-C7	Crop. (cv.)	WW	A	72	67	72	51	52	60	10
S-C8	Crop. (cv.)	OT	A	32	67	87	46	64	89	12
S-C9	Crop. (cv.)	WR	A	50	67	53	39	33	42	6
S-C11	Crop. (cv.)	WW	A	65	67	80	40	58	88	9
S-C12	Crop. (cv.)	WB	A	69	67	62	36	53	64	9
S-C13	Crop. (cv.)	WW	A	56	67	53	28	41	76	11
S-C14	Crop. (cv.)	MS	A	70	67	79	53	62	80	15
S-C15	Crop. (cv.)	MS	A	63	67	86	54	58	86	14
S-C17	Crop. (cv.)	MS	A	71	67	81	42	55	88	9
S-C18	Crop. (cv.)	SB	A	62	67	81	35	54	95	9
S-C19	Crop. (cv.)	MS	A	63	67	72	34	60	86	11
S-C18a	Crop. (cv.)	SB	A	78	67	81	42	60	87	10
S-C22	Crop. (cv.)	MS	A	75	67	73	50	55	77	11
S-C23	Crop. (cv.)	OT	A	41	67	81	50	55	80	11
W-C1	Crop. (cv.)	RW	A	39	67	86	53	82	91	42
B-C8	Crop. (cv.)	SP	B	87	78	93	71	72	88	68
FV7-1	Crop. (cv.)	WW	B	97	78	66	38	23	73	5
FV7-30	Crop. (cv.)	WW	B	97	78	59	37	22	64	5
FV7-32	Crop. (cv.)	WW	B	94	78	58	36	22	64	5
S-C5	Crop. (cv.)	WW	B	48	78	90	56	70	91	23
S-C16	Crop. (cv.)	MS	B	50	78	87	47	74	91	18
B-C2	Crop. (cv.)	WW	C	59	85	96	75	77	87	92
B-C5	Crop. (og.)	TR	A	57	55	85	76	79	59	97
B-C7	Crop. (og.)	OT	A	83	55	84	71	66	52	60
T-K-C1	Crop. (og.)	WW	A	40	55	77	41	50	83	8
T-K-C2	Crop. (og.)	TC	A	60	55	59	34	33	64	7
T-K-C4	Crop. (og.)	FB	A	63	55	77	41	50	83	8
B-C4	Crop. (og.)	SP	B	73	64	94	67	73	93	57
B-C9	Crop. (og.)	FL	B	75	64	96	74	70	82	76
B-C1	Crop. (og.)	SP	C	47	70	94	75	76	78	91
FV4-132	Crop. (cs.)	FB	A	63	62	55	40	22	56	5
T-e-C3	Crop. (cs.)	WW	A	53	62	81	41	53	87	9
T-e-C5	Crop. (cs.)	WB	A	51	62	81	41	53	87	9

Crops: FB-Faba bean; FL-Flax; MS-Maize; OT-Oats; RW-Winter Rye; SB-Summer barley; SP-Spelt; TC-Triticale; TR-Turnip rape; WB-Winter barley; WR-Winter rape; WW-Winter wheat.

Management: cv-conventional management; og-organic farming; cs-conservation tillage.

Table 4.32 shows the average CN_m for each Soil group and land-use class. The results of the measured curve number values are very close to the curve number values

published in the literature, whereas the computed CNs based on pedo-transfer functions show much bigger differences compared to the literature values.

Tab. 4.32: Mean CN_m for measured and computed K_s values for the selected sites.

Land-use	HSG	CN publ.	CN_m measured	CN_m Rosetta	CN_m Cosby	CN_m Saxton	CN_m Vereecken	CN_m Brakensiek	No. of Samples
Forest	A	36	37.7 (6.5)	44.0 (17.1)	48.0 (10.1)	76.3 (11.1)	42.3 (32.6)	37.3 (35.6)	3
Grassland	A	49	49.5 (11.4)	51.1 (18.0)	42.5 (15.7)	58.9 (25.4)	52.1 (29.1)	30.9 (33.0)	8
Grassland	B	69	77.0	92.0	65.0	65.0	93.0	37.0	1
Cropland (cv.)	A	67	67.5 (14.6)	68.2 (17.0)	44.7 (9.2)	48.3 (18.9)	68.4 (20.9)	17.6 (10.5)	28
Cropland (cv.)	B	78	78.8 (23.4)	75.5 (16.2)	47.5 (13.8)	47.2 (27.2)	78.5 (13.1)	20.7 (24.5)	6
Cropland (cv.)	C	85	59.0	96.0	75.0	77.0	87.0	92.0	1
Cropland (og.)	A	55	60.6 (15.4)	76.4 (10.4)	52.6 (19.4)	55.6 (17.5)	68.2 (14.2)	36.0 (40.9)	5
Cropland (og.)	B	64	74.0 (1.4)	95.0 (1.4)	70.5 (4.9)	71.5 (2.1)	87.5 (7.8)	66.5 (13.4)	2
Cropland (og.)	C	70	47.0	94.0	75.0	76.0	78.0	91	1
Cropland (cs.)	A	62	55.6 (6.4)	72.3 (15.0)	40.7 (0.6)	42.7 (17.9)	76.7 (17.9)	7.7 (2.3)	3

Numbers in brackets identify the standard deviation

For forest, grassland and cropland the measured CN_m in HSG A are almost identical to the literature values, although the variation of the single values is relatively high (Tab. 4.32). Compared to the CN_m derived from the pedo-transfer functions, the measured values perform better in terms of the mean value and the standard deviation. For the soil groups B and C no statements can be made since the number of samples is to low.

Table 4.33 shows the CN_m for different crops under conventional management, for crops with more than 2 samples. Compared to the published value of 67 for cropland under HSG A, the measured results show slightly higher values for winter wheat,

Oilseed rape and summer barley. Winter barley and maize fit very well to the published values. The measured value for oats differs very much, but since only two samples were available this value is for information only.

Tab. 4.33: Mean CN_m for different crops under conventional management for the selected sites.

Crop	HSG	CN_m measured	No. of Samples
Winter wheat	A	71 (13.3)	7
Winter wheat	B	84 (24.0)	4
Oilseed rape	A	75 (14.3)	5
Maize	A	68 (9.9)	5
Winter barley	A	66 (3.0)	3
Summer barley	A	70 (11.3)	2
Oats	A	37 (6.4)	2

Due to the wider crop rotations in organic farming, a table like Tab. 4.33 could not be produced from the measured data.

From the results of the CN_m measurements can be concluded that the use of the K_s value to compute the measured CN_m is suitable for the determination of the water retention potential.
There are hints that the CN_m varies also with the crop, but further research in the future is needed.
In order to compute the different scenarios for the Schunter catchment, the following curve number table has been used:

Tab. 4.34: Curve number table used for the simulation on a catchment scale.

Land-use/Management	HSG A	HSG B	HSG C	HSG D
Cropland (conventional tillage)	67	78	85	89
Cropland (conservation tillage)	62	73	79	80
Cropland (organic faming)	55	64	70	73
Grassland	49	69	79	84
Forest	36	60	73	83
Urban Area	100	100	100	100
Water	100	100	100	100

4.5.2 Direct runoff computation using the curve number approach

The target parameter of the original "curve number" model is the calculation of direct runoff (q) based on rainfall data and the combined parameters for the hydrologic response units (CN in relation the hydrologic soil groups). One problem of the old concept has been the regionalization of the hydrologic response units, since detailed soil information was not available. With the advent of soil information systems, like the BÜK 50, a regionalization by using pedo-cells is now possible.

During the hydrological year, a catchment area is subject to major changes in phenology. These changes (development and maturity of plants, harvest of crops etc.) have an enormous effect on the effective rainfall (change of interception and evapotranspiration), which controls the amount of infiltrating water. With the knowledge of all of these limitations an exemplary calibration of the runoff computation for one year has been computed. This result is just a snapshot, in order to see the performance of the original curve number model. In order to evaluate the impact of land-use/land-management changes on runoff detailed calibration procedures have to be perform, which is theoretically possible, but beyond the scope of this work.

As it has to be mentioned it was not intended to improve the concept of runoff computation by this work, but in order to evaluate the usefulness of the measured curve numbers, the direct runoff has been computed for the Schunter catchment.

Measured runoff data from the Harxbüttel gauge for the year 2002 (NLWKN, 2005) a very wet year with severe flooding, have been used to compare them with computed direct runoff from the curve number model. The areal rainfall has been computed using four meteorological stations (Braunschweig, Königslutter, Helmstedt, Wolfsburg–Sülfeld; DWD 2009) using the Thiessen polygon method (de Lange, 2006).

The data has been computed for the hydrological year 2002 (Nov. 2001- Oct. 2002) based on daily areal rainfall data. For the NRCS-CN runoff computations, the runoff was computed based on the measured curve number (CN_m) method described in section 4.5.1 and according to equation 4.1.

$$Q = \frac{(P - 0.2S)^2}{(P + 0.8S)} \qquad P \geq 0.2S,\ Q = 0 \text{ otherwise} \qquad \text{[Equation 4.1]}$$

Where:

Q: surface runoff [mm]
P: precipitation [mm]
S: potential water retention [mm]

The computed daily direct runoff was monthly summarized, taking into account that the precipitation is equal or higher than 0.2S (Hawkins et al. 2009). Otherwise the runoff was set to zero.

In Fig 4.20 the measured runoff values have been plotted against the computed direct runoff, total rainfall and average temperature for each month.

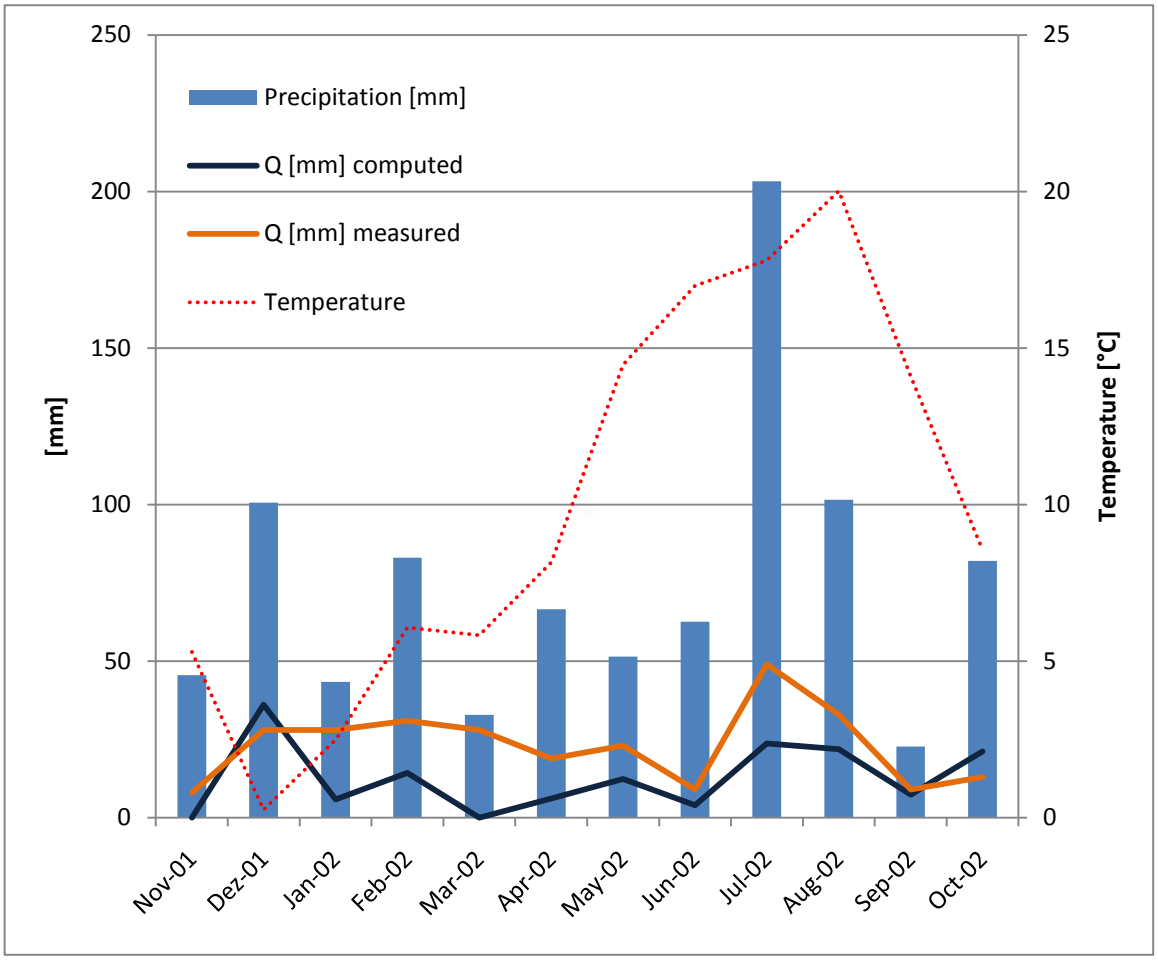

Fig.4.20: Comparison of the measured and computed surface runoff for the Schunter catchment for the hydrologic year 2002.

The results show that direct runoff computed by the CN method is systematically underestimated compared to the measured runoff. Conceptually the CN approach only takes into account the direct runoff from precipitation. The hydrologic base flow cannot be computed with that approach (NRCS, 1982).

In December 2001 the runoff is overestimated and in January underestimated. As it can be seen by the temperature line, most of the precipitation in December has been fallen as snow and lead to the time lack in runoff. It is known that the CN approach does not work properly for snow (Hawkins et al., 2009).

4.5.3 Scenarios

For the computation of the different infiltration scenarios the HOT model from the Julius Kühn-Institut has been used. This model is a simple Microsoft Excel based

implementation of the Curve Number approach for different land-use and land-management scenarios (Fig. 4.21).

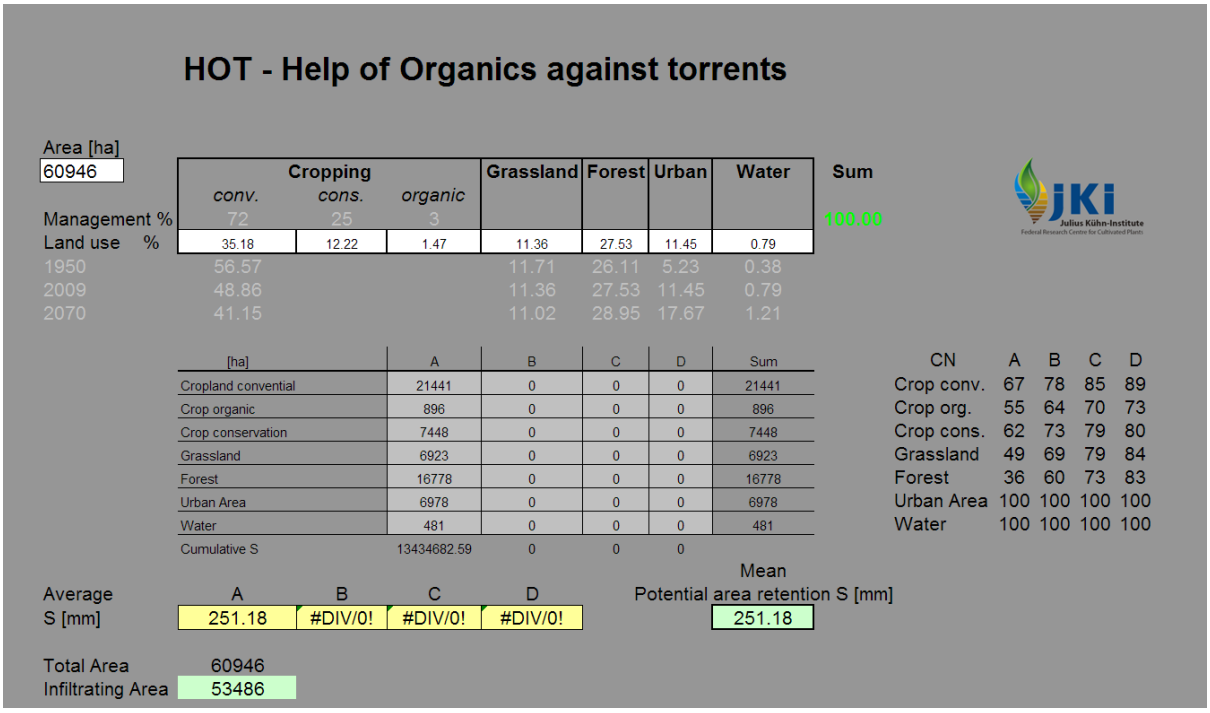

Fig.4.21: Screenshot of the User interface of the Hot-Model (Lilienthal et al., 2009).

According to the input information the mean maximum potential storage value S_{max} for the total area will be computed. This S_{max} value can be interpreted in analogy to precipitation in [mm] or [l·m²]. As the land-use in the catchment is given in hectares, a retention value of 1 [mm] is equal to 10 [$m^3 \cdot ha^{-1}$]. Since urban and water area are not usable for infiltration, the term of "infiltrating area" will be introduced.

This is the area which allows infiltration. Due to urbanisation, this area is getting smaller by time. For all of the following results, the retention potential is related according to the "infiltrating area" (Tab. 4.35). The maximum potential storage in relation to the infiltrating area will be defined as *infiltration capacity*.

Tab. 4.35: Results of the infiltration capacity scenarios for the Schunter catchment.

Scenario (year)	**Management**	**Assumption**	**Infiltrating Area [ha]**	**Mean S_{max} [mm·ha^{-1}]**	**Cumulative S_{max} [10^2·mm·ha^{-1}]**	**Potential Storage [%]**	**Loss of storage 1950 = 100 %**
I (1950)	100 % organic farming	historic situation	57527	282	162373	63	0
II (1950)	100 % conventional farming	urbanisation & technology	57527	233	133856	52	-17.6
III (1950)	no agriculture	agriculture changes to forest	57527	452	259766	100	+60.0
IV (2009)	97 % conventional 3 % organic farming	status quo	53486	251	134347	56	-17.3
V (2009)	97 % conventional 3 % organic farming	grassland - 10 %	53486	249	133379	55	-17.9
VI (2009)	87 % conventional 13 % organic farming	organic faming + 10 %	53486	256	136807	57	-15.7
VII (2009)	87% conventional 3 % organic farming	conservation tillage + 10 %	53486	253	135256	56	-16.7
VIII (2009)	72 % conventional 5 % organic farming 17 % Grassland	optimized land-management	53486	263	140679	58	-13.4
IX (2009)	no agriculture	agriculture changes to forest	53486	452	241520	100	+48.7
X (2070)	97 % conventional 3 % organic farming	future	49439	266	131340	59	-19.1
XI (2070)	no agriculture	agriculture changes to forest	49439	452	223246	100	+37.5

For more information on the tillage practice, please refer to tab. 3.9.

The mean S_{max} value is the average retention for the infiltrating area in the whole catchment. Since this value does not take into account the loss of area due to urbanisation, the cumulative S_{max} is a measure for the total amount of water which can be hold back in the catchment area (infiltration capacity). The potential maximum storage capacity is the relation of the theoretically possible maximum water capacity (Scenarios III, IX and XI), were no agriculture is performed and the current maximum

water storage capacity. And finally the loss of storage is the relation of the cumulative S_{max} (infiltration capacity) for the current scenario in relation to the land-use in 1950 (Scenario I). The loss of infiltration capacity has not be computed for scenarios III, IX and XI since this scenarios just compute the S_{max} value with no agricultural use at all.

Table 4.35 shows the results of the different scenarios. Scenario VIII is optimised using the solver function in Excel, with two constrains:

1. Forest, urban and water area can not be changed
2. All other uses can only be changed by ± 50% of their existing acreage (Reference land-use 2009).

The optimized land-use would need a strong conversion of cropland to grassland (+ 6%) and more conservation tillage practice (+3%) and organic farms (+2%).

In the following sections the impact of land-use change and the impact of land-management will be demonstrated.

4.5.4 Impact of land-uses changes on the water storage capacity

With the change of the land-use and increasing urbanization activity within the Schunter area between 1950 to 2009, the total water storage capacity decreased from 282 mm (scenario I) to 251 mm (scenario IV), respectively. Also the infiltrating area decreased by 4041 ha. As the reduction of the storage capacity of 1 mm equals a loss of 10 m³ of water per hectare, between 1950 and 2009, 310 m³ less water per hectare can be stored. To gain a better look inside, the contribution of each land-use class on the total water storage capacity is shown in table 4.36.

Tab. 4.36: Results of the maximum water storage capacity scenarios for the Schunter catchment.

Scenario	Land-use	S_{max} [mm]	Fraction of S_{max} [%]	Fraction of S_{max} [% ·100 ha^{-1}]	Area [ha]
1950 (I)	Cropland conventional tillage	0	0.0	0.00	0
Only organic faming	Cropland organic farming	125	44.1	0.13	34477
Infiltr. area: 57527 ha	Cropland conservation tillage	0	0.0	0.00	0
Total S: 282 mm	Grassland	32	11.6	0.16	7137
Potential S_{max} used: 63 %	Forest	125	44.3	0.28	15913
2009 (IV)	Cropland conventional tillage	50	20.0	0.09	21441
Current land-use	Cropland organic farming	3	1.4	0.15	896
Infiltr. area: 53480 ha	Cropland conservation tillage	22	8.6	0.12	7448
Total S_{max}: 251 mm	Grassland	34	13.6	0.20	6924
Potential S used: 56 %	Forest	142	56.4	0.34	16778
2070 (X)	Cropland conventional tillage	46	17.2	0.10	18058
Projected land-use	Cropland organic farming	3	1.2	0.16	750
Infiltr. area: 49440 ha	Cropland conservation tillage	20	7.4	0.12	6271
Total S_{max}: 266 mm	Grassland	36	13.5	0.20	6716
Potential S used: 59 %	Forest	161	60.7	0.34	17644

The effect of the land-use change can be seen in table 4.36. The value total S_{max} is not a suitable parameter to compare the effect of land-use change over different years, because this value does not take into account the decrease of the infiltrating area decreased due to urbanisation. Better measures are the fractions of S_{max} which relates the S_{max} value of a certain land-use to the S_{max}-value of the catchment. Using the fraction of S_{max} shows that the impact of forest on the total storage capacity of the catchment increases since 1950, although the absolute area of forest has not changed very much (increase of 865 ha between 1950 and 2009).

Another interesting parameter is the fraction of S_{max} related to 100 ha, this can be interpreted as the impact of a change of 100 ha of a specific land-use in percent on the total storage capacity. For example in 2009 a change of 100 ha conventional tillage cropland will result in a change of 0.09% on the total storage capacity of the

catchment, whereas a change of 100 ha organic farm land has nearly the double impact (0.15% change of the storage capacity).
Also for the future projection the impact of organic farmland increases, due to the loss of infiltrating area.

The land-use in 1950 was dominated by agriculture, which is considered to be organic at that time. Forest and agricultural land-use contribute nearly equal with 44 % to the total water storage capacity. Because the infiltrating area is getting smaller by time due to urbanisation, these impact factors also change by time.
In addition, the results of the infiltration capacity from 1950 to 2009 for the whole catchment reveal that, the amount of the potential infiltration capacity used is reduced from 63% in 1950 to 56% in 2009 with reducing the infiltrating area and increasing the urbanization impact.

The impact of the land-use change in the Schunter catchment reveals another phenomenon, whereas with increasing the urbanization activity from 1950 to 2009 by 6% and decreasing the cropland by 8%, the infiltrating area decreased from 57527 hectare in 1950 to 53480 hectare in 2009, and the contribution of the grassland and the forest to the infiltration capacity increased compared to the cropland impact.
It is also interesting to look at the impact of land-use change on a sub-catchment level.

Tab. 4.37: Results of the water storage capacity scenarios for the Lower Schunter sub catchment.

Scenario	Land-use	S_{max} [mm]	Fraction of S_{max} [%]	Fraction of S_{max} [% ·100 ha^{-1}]	Area [ha]
1950 (I) Only organic faming Infiltr. area: 7564 ha Total S_{max}: 278 mm Potential S used: 62%	Cropland conventional tillage	0	0.0	0.00	0
	Cropland organic farming	117	42.0	0.99	4241
	Cropland conservation tillage	0	0.0	0.00	0
	Grassland	52	18.9	1.26	1501
	Forest	109	39.2	2.15	1821
2009 (IV) Current land-use Infiltr. area: 6113 ha Total S_{max}: 260 mm Potential S used: 58 %	Cropland conventional tillage	45	17.3	0.79	2197
	Cropland organic farming	3	1.2	1.31	92
	Cropland conservation tillage	19	7.5	0.98	763
	Grassland	48	18.4	1.66	1105
	Forest	145	55.6	2.84	1956
2070 (X) Projected land-use Infiltr. area: 4654 ha Total S_{max}: 297 mm Potential S used: 66 %	Cropland conventional tillage	36	12.2	0.90	1330
	Cropland organic farming	3	0.8	1.50	55
	Cropland conservation tillage	16	5.2	1.13	462
	Grassland	41	13.7	1.91	717
	Forest	203	68.2	3.26	2091

The Lower Schunter sub-catchment as mentioned in the previous chapter is close to the city of Braunschweig, and the urbanization activity reveals the largest increase during the past 60 years. The total maximum water storage capacity shows a pronounced decreasing from 278 mm (62%) in 1950 to 160 mm (58 %) in 2009 (Table 4.37).

The total area of the Lower Schunter catchment is 8432 but the total infiltrating area decreased from 7564 hectare in 1950 to a projected infiltration area of 4654 hectares in 2070. Because this catchment is strongly influenced by urbanization, a small change of other land-uses has a larger impact on the total storage capacity. For

instance a change of 100 ha grassland would result in a change of 1.67% of the total storage in the sub catchment.

To have a view also to a more agriculturally influenced sub-catchment, the results for the Central Schunter sub-catchment will be presented in more detail here (Tab.4.38). The results of the other sub-catchments can be found in the appendix.

Tab. 4.38: Results of the water storage capacity scenarios for the Central Schunter sub catchment.

Scenario	Land-use	S_{max} [mm]	Fraction of S_{max} [%]	Fraction of S_{max} [% ·100 ha^{-1}]	Area [ha]
1950 (I) Only organic faming Infiltr. area: 12946 ha Total S_{max}: 273 mm Potential S used: 60 %	Cropland conventional tillage	0	0.0	0.00	0
	Cropland organic farming	127	46.7	0.59	7936
	Cropland conservation tillage	0	0.0	0.00	0
	Grassland	41	15.1	0.75	2017
	Forest	104	38.2	1.28	2993
2009 (IV) Current land-use Infiltr. area: 12385 ha Total S_{max}: 245 mm Potential S used: 54 %	Cropland conventional tillage	49	19.8	0.41	4810
	Cropland organic farming	3	1.4	0.68	200
	Cropland conservation tillage	21	8.6	0.51	1670
	Grassland	51	20.6	0.87	2365
	Forest	122	49.7	1.49	3340
2070 (X) Projected land-use Infiltr. area: 11837 ha Total S_{max}: 263 mm Potential S used: 58 %	Cropland conventional tillage	41	15.7	0.40	1330
	Cropland organic farming	3	1.1	0.67	55
	Cropland conservation tillage	18	6.8	0.50	462
	Grassland	61	23.0	0.85	717
	Forest	141	53.4	1.45	2091

In the Central Schunter catchment, cropland is the dominating land-use; grassland and forest have increase during the last 60 years, so this sub-catchment can expect an

increase in the total storage capacity in the future. Also the impact of organic farming is very high in the sub-catchment. A change of 100 ha land to organic farming would change the total storage capacity by 0.68%. So this sub-catchment would be suitable for a change in the management of cropland.

4.5.5 Impact of management changes on the water storage capacity

The impact of management changes have been investigated using the scenarios II, V, VI, VII, VIII. The results are presented in table 4.39. The spatial distribution of the maximum storage capacity can be found as a map in the appendix.

Tab. 4.39: Results of selected water storage capacity scenarios for the Schunter catchment.

Scenario	Land-use	S_{max} [mm]	Fraction of S_{max} [%]	Fraction of S_{max} [% ·100 ha^{-1}]	Area [ha]
1950 (I) Only organic faming Infiltr. area: 57527 ha Total S_{max}: 282 mm Potential S used: 52 %	Cropland organic farming	125	44.1	0.13	34477
	Grassland	33	11.6	0.16	1737
	Forest	125	44.3	0.28	15913
1950 (II) Only conventional faming Infiltr. area: 57527 ha Total S_{max}: 233 mm Potential S used: 52 %	Cropland conventional tillage	75	32.2	0.09	34477
	Grassland	33	14.1	0.20	7137
	Forest	125	53.7	0.34	15913
2009 (IV) Current land-use Infiltr. area: 53486 ha Total S_{max}: 251 mm Potential S used: 56 %	Cropland conventional tillage	50	20.0	0.09	21441
	Cropland organic farming	4	1.4	0.15	896
	Cropland conservation tillage	22	8.6	0.12	7448
	Grassland	34	13.6	0.20	6924
	Forest	142	56.4	0.34	16778
2009 (V) - 10% Grassland Infiltr. area: 53486 ha Total S_{max}: 249 mm Potential S used: 55 %	Cropland conventional tillage	52	20.8	0.09	22136
	Cropland organic farming	4	1.4	0.16	896
	Cropland conservation tillage	22	8.7	0.12	7478
	Grassland	30	12.4	0.20	6229
	Forest	142	56.8	0.34	16778
2009 (VI) + 10% organic farming Infiltr. area: 53486 ha Total S_{max}: 256 mm Potential S used: 57 %	Cropland conventional tillage	43	16.9	0.09	18463
	Cropland organic farming	15	5.9	0.15	3871
	Cropland conservation tillage	22	8.5	0.11	7445
	Grassland	34	13.4	0.19	6924
	Forest	142	55.4	0.33	16778

Scenario	Land-use	S_{max} [mm]	Fraction of S_{max} [%]	Fraction of S_{max} [% ·100 ha^{-1}]	Area [ha]
2009 (VII)	Cropland conventional tillage	43	17.1	0.09	18467
+ 10% conservation tillage	Cropland organic farming	4	1.4	0.15	896
Infiltr. area: 53486 ha	Cropland conservation tillage	30	12.0	0.12	10422
Total S_{max}: 253 mm	Grassland	34	13.5	0.20	6924
Potential S used: 56 %	Forest	142	56.0	0.33	16778
2009 (VIII)	Cropland conventional tillage	32	12.3	0.09	13804
Optimised land-use	Cropland organic farming	5	2.0	0.15	1347
Infiltr. area: 53486 ha	Cropland conservation tillage	33	12.4	0.11	11171
Total S_{max}: 263 mm	Grassland	51	19.5	0.19	10385
Potential S used: 58 %	Forest	142	53.9	0.32	16778

The impact of technology (use of bigger and heavier machinery, use of agrochemicals) is represented by the scenarios I and II. For the Schunter catchment, the total water storage capacity shows a decrease of 49 mm from 282 mm to 233 mm (Tab. 4.39) just by using a different management practice.

The effect of increased bio-fuel production is simulated with scenario V. The decrease of grassland by 10% results in a decrease of 2 mm total storage capacity, or 1% total storage compared to the status quo (scenario IV). In absolute figures it is just a change of around 700 ha which have a very strong impact.

The increase of organic farmland by 10 % of the total area is simulated in scenario VI and results in an increase of 5 mm total storage capacity. This can be reached by converting around 3000 ha.

Scenario VII simulates an increase of conservation tillage by 10 % of the total area. This results in an increase of 2 mm total storage capacity. The area needed for conversion is around 3500 ha. Compared to the change of organic farmland, more land is needed to reach only half of the effect.

Finally, optimizing land-use with more grassland (scenario VIII) resulted in an increase of 12 mm storage capacity. But to reach this, around 7600 ha of conventional land have to be converted. Organic farmland has to be increased by 450 ha, conservation cropland by around 3700 ha and grassland by around 3500 ha. To reach this optimal land-use 12.5% of the total land in the catchment needs to be converted. This is a very high effort, but just by changing small amounts of cropland to organic farming is much more effective.

4.6 Statistical Analysis of the selected soil samples

The determination of the Curve Number is the key parameter for modelling the infiltration potential in the Schunter catchment. In order to evaluate the measured CN_m and the CN_m derived from pedo-transfer functions, some basic statistical analysis have been performed.

Descriptive Statistics

The statistics for all field parameters are listed in table 4.40. The field data shows a wide variety of measurements for different textured soils, as well a different bulk densities and carbon contents.

Tab. 4.40: Descriptive statistics for all measured field parameters (n=58) for the selected sites.

	Min	Max	Mean	STD
Sand [%]	1.2	66.9	32.5	16.4
Silt [%]	18.5	63.0	44.1	11.6
Clay [%]	5.7	56.5	23.4	13.4
eBD []	0.99	1.77	1.52	0.16
C_{org} [%]	0.6	10.3	2.3	1.8
K_s [$cm \cdot d^{-1}$]	0.78	57.2	18.2	13.7
q_s [$mm \cdot h^{-1}$]	23	2088	675	490

The standard deviation of the hydraulic conductivity and the steady state infiltration is very high, due to the reason that all different land-uses were included in the analysis.

Correlation Analysis

In the past the Curve Numbers have been computed from precipitation runoff relations of small catchments. The curve numbers were published in the literature as coarse land-use groups. But now by computing the curve numbers from K_s measurements more detailed descriptions of land-use and land-management become possible. Measuring the K_s in the field is not always possible, so the determination of the K_s values by pedo-transfer functions might be an option. At first in influence of

the measured field parameters on the K_s values have to be investigated. Table 4.41 shows the results of a correlation analysis.

Tab. 4.41: Correlation analysis for the measured field parameters and the saturated hydraulic conductivity for the selected sites.

	Sand	Silt	Clay	eBD	C_{org}	K_s	q_s
Sand	1	-0.585**	-0.712**	-0.202	-0.149	0.163	0.018
Silt		1	-0.153	0.428**	-0.422**	-0.687**	-0.410**
Clay			1	-0.125	0.547**	0.397**	0.333*
eBD				1	-0.590**	-0.413**	-0.329*
C_{org}					1	0.431**	0.274*
K_s						1	0.901**
q_s							1

** Correlation is significant at the 0.01 level (2-tailed).
* Correlation is significant at the 0.05 level (2-tailed).
eBD: Effective bulk density
C_{org}: org. Carbon
K_s: saturated hydraulic conductivity
q_s: steady Infiltration rate

The saturated hydraulic conductivity is strongly negatively correlated to the silt content, followed by a moderate positive correlation to carbon content, a moderate negative correlation to the effective bulk density and finally a moderate positive correlation to the clay content. All these correlations are highly significant. The clay and sand content are strongly intercorrelated, also carbon content and effective bulk density are strongly correlated.

The strongest correlation between the steady state infiltration rate and the saturated hydraulic conductivity can be explained due to the fact, that the K_s value is computed by the steady state infiltration rate.

To evaluate the potential of the pedo-transfer function, a multiple regression analysis has been performed in order to see, if the saturated hydraulic conductivity simply can be predicted from soil parameters.

Multiple Regression Analysis

For the multiple regression analysis only those variable have been selected, which showed a significant correlation to the K_s value. These have been the silt and clay content, the effective bulk density and the carbon content. Al Hassoun (2009) has shown that also the amount of earthworms play an important role for the saturated hydraulic conductivity. Earthworms were not investigated since a modelling on a larger scale based on existing information is the subject of this work.
The multiple regression analysis was performed in a stepwise backward linear approach, were different methods have been tested. Table 4.42 shows the results of the different models.

Tab. 4.42: Regression models for the estimation of the saturated hydraulic conductivity based on selected soil parameters.

Model	**Predictors**	**R^2**	**Adjusted R^2**	**Standard error**	**Formula**
I	eBD, clay, silt, carbon	0.578	0.546	9.25	$Y=68.425-0.717\cdot(silt\%)+0.357\cdot(clay\%)-0.948\cdot(C_{org}\%)-16.21\cdot(eBD)$
II	eBD, clay, silt,	0.572	0.548	9.24	$Y=58.805-0.698\cdot(silt\%)+0.298\cdot(clay\%)-11.068\cdot(eBD)$
III	Silt, clay	0.559	0.543	9.29	$Y=44.493-0.757\cdot(silt\%)+0.306\cdot(clay\%)$

All three regression models only explained around 55% of the variance with a relative high standard error of 9. This shows that a prediction of the K_s value simply using pedo-transfer function will not work properly.

In a final step a correlation analysis of different K_s values derived from several pedo-transfer function will be presented.

Tab. 4.43: Correlation analysis between measured K_s and modelled values from the pedo transfer functions for the selected sites.

	K_s – M	K_s – R	K_s – C	K_s – S	K_s – V	K_s – B
K_s – M	1					
K_s – R	0.157	1				
K_s – C	-0.108	0.513**	1			
K_s – S	-0.507**	0.364**	-0.119	1		
K_s – V	0.186	0.875**	0.571**	0.660**	1	
K_s – B	-0.455**	0.262*	0.468**	0.162	0.055	1

** Correlation is significant at the 0.01 level (2-tailed).
* Correlation is significant at the 0.05 level (2-tailed).
K_s – M: measured saturated hydraulic conductivity
K_s – R: saturated hydraulic conductivity calculated by the ROSETTA model
K_s – C: saturated hydraulic conductivity calculated by the COSBY model
K_s – S: saturated hydraulic conductivity calculated by the SAXTON model
K_s – V: saturated hydraulic conductivity calculated by the VEREECKEN model
K_s – B: saturated hydraulic conductivity calculated by the BRAKENSIEK model

The highest correlation of -0.507 could be detected between the model of Saxton and the measured saturated hydraulic conductivity, followed by the model of Brakensiek (Tab. 4.43). The results show that the estimation of the saturated hydraulic conductivity for the computation of the CN should be done only based on real field measurements, since the pedo-transfer function do not perform well, also other effects (e.g. earthworms and macropores) are not taken into account.

5 Discussion

The infiltration capacity concept

Understanding how land-use influences the water storage capacity of soils in a river catchment will enable planners to formulate policies to reduce undesirable effects of land-use and land-management change. Land-use changes (e.g. urbanization) enhance impervious ground surfaces, decrease the infiltration rate and increase the runoff rate, causing low base flow and increase the rate of flood events.

Two processes lead to a reduction of infiltration: 1. the loss of infiltrating area by land-use change (e.g. increasing sealing due to urbanization), and 2. the loss of infiltration by changes of the land-management (silent sealing).
The effects of land-use changes can be identified by land-use classifications, based on historic maps or cadastral data. Land-use changes occur as an abrupt change, with severe changes in the soil properties (e.g. conversion of grassland to cropland). Observed over a longer period of time, a state of equilibrium according to the environmental conditions will be reached. If we consider a very long period of 60 years, certain land- use already reached again a state of equilibrium, while other changes (e.g. conversion of cropland to grassland) are still in the approach to a new equilibrium. In this work only two observation times of land-use were available, so only statements for the observed situations (snapshots) can be made. For a more detailed description of processes, the analysis of land-use changes in a higher temporal resolution (e.g. every 2 years) is necessary. On a catchment scale remote sensing data from satellites can offer valuable information for the derivation of land-use information (National Institute of Hydrology (1997).
With the loss of infiltratable area due to urbanization, the concept of *infiltration capacity* needs to be introduced, when working on a catchment scale. In this context, the infiltration capacity can not be understood in the sense of Horton (1940) as the maximum infiltration rate, but as the maximum water storage capacity of a soil in relation to the available infiltration area.
The infiltration properties of different infiltratable land-use classes (e.g. forest, cropland and grassland) can be described using the concept of maximum water storage capacity.

Based on field measurements of infiltration under several land-use and land-management situations, a modelling approach has been developed, to determine the maximum potential water storage capacity (S_{max}). This maximum water storage capacity is closely related to the saturated hydraulic conductivity (K_s), and also a suitable indicator, which can be used to compare different land-use/land-management scenarios. S_{max} is a theoretical value describing the maximum potential of a given soil/land-use unit. Although, in reality the water storage is highly variable due to different soils and land-uses in a catchment scale, S_{max} allows the direct comparison of different soil/land-use units.

Since the required input parameters for detailed process models are often not available at a regional scale, general assumptions and simplifications have to be applied, in order to perform meaningful statements. In this special case an integrated measure is needed, which takes into account the soil properties in combination to the land-use and the land-management. Such an integrated measure can be found as a part in the Curve Number (CN) from the “Curve Number Model" of the National Resource Conservation Service (1972). The CN is a dimensionless value which has been identified experimentally for a variety of different soil, land-use and of land-management situations for small scale catchments in the US. The CN is related to the water retention potential (S), and S is originally used to compute the direct runoff from a precipitation event. Since this work addresses only the agricultural viewpoint of impacts of land-use and land-management, the main focus has been put to the relation of CN to the water retention potential and the computation of S_{max}.

The CN-Model has often been criticized for its obscure determination of the CN from precipitation/runoff relations, which have not been properly published, even not in the official handbooks (Hawkins et al. 2009). In this work new ways for the determination of the CN have been developed. Based on field infiltration measurements, now the CN can be directly measured (CN_m)! Using the saturated hydraulic conductivity allows the computation of the maximum water storage capacity (S_{max}) for a given soil, land-use and land-management combination. Since the maximum storage capacity is used, also the prevailing wetting status of the soil can be neglected.

The original Curve number model became one of the most popular techniques among the engineers and the practitioners, mainly for small catchment hydrology (Mishra and Singh, 2006), because of its simplicity. Nevertheless, (Hawkins, 1993; Ponce and Hawkins, 1996; Michel et al., 2005) revealed that the original CN's main weak points are that it does not reveal the impact of rainfall intensity and its temporal distribution, it does not consider the effects of spatial scale, it is highly sensitive to changes in values of its sole parameter; and it does not address clearly the effect of adjacent moisture condition.

While CN values were obtained experimentally from rainfall and runoff measurements over a wide range of geographic, soil, and land-management conditions, its applicability was investigated in various regions and for various land-uses and climate conditions, (Romero et al., 2007; King and Balogh, 2008). In spite of the widespread use of this method, there is so far not an agreed procedure to estimate CN from measurements. Many methods were proposed using rainfall runoff relation but they were leading to different CN values. The main difficulty is the large variability observed in the CN values evaluated for the same watershed for various rainfall depths. This variability was attributed to variations in the antecedent moisture conditions to the temporal and spatial variability of rainfall, to scale effects, and many other reasons. Therefore, many studies aimed at improving the method and finding a better way to incorporate the Antecedent Moisture Conditions (AMC) (e.g. Simanton et al., 1996; Mishra et al., 2005b; Jain et al., 2006; Sahu et al., 2007; Brocca et al., 2008; Kannan et al., 2008; Mishra et al., 2008).

Thus, the method had to be modified to produce accurate results attributed to the land-use change, soil properties, and the land-management, and to overcome the defect points of the conventional CN method. Insofar as the curve number can be taken as a measure of watershed retention potential (Hawkins et al., 2009), it is naturally compared with the infiltration capacities measure (saturated hydraulic conductivity or K_s) as an alternative measure of retention ability closely linked to soil properties, profile, and land-use. The value S_{max} is the potential maximum retention, which describes the maximum amount of water that can infiltrate into the soil before producing runoff (the main sole of the curve number model). In fact this is equal to the saturated hydraulic conductivity.

An innovative approach of this work is the replacement of S_{max} with K_s from field measurements under several land-use and land-management situations. With this approach the CN_m can be determined in the field by real measurements. This allows the consideration of special land-use/land-management situation which are not covered by the standard handbook. Compared to published CN values for German environmental conditions (DWVK 1984, Voges 1999 Halbfaß 2005, Hartmann et al., 2009) the measured CN_m performed very well.

Finally, it can be concluded that the S_{max} value becomes a direct measure of the impact of land-use and land-management on the infiltration properties of a catchment. In addition, the measured curve number model (CN_m) can be directly determined instead of the conventional CN (SCS, 1972) in which the gauged runoff values at the outlet of the watershed were plotted against the precipitation values to compute the conventional CN.

In addition, in respect to the results of this work, with using the measured curve number (CN_m), the variation of the conventional CN values evaluated for the same watershed for various rainfall depths were minimized, while this variation was attributed to variations in the antecedent moisture conditions (Kannan et al., 2008; Mishra et al., 2008; Hawkins et al., 2009). Whereas, the conventional curve number depends on land-use, soil characteristics, and antecedent moisture condition (USDA-SCS, 1986), and the SCS-method adjusted the curve number value to a lower value under dry conditions and a higher value under wet conditions through using different tables. Furthermore, Hawkins et al., 1985; Chow et al., 1988, Arnold et al., 1990; Mishra et al., 2008; Hawkins et al., 2009 provided different equations and relationships for the curve number and different values corresponding to the differences in the antecedent moisture condition.

However, with using the CN_m, the arguments of converting the antecedent moisture conditions (AMC) between different literatures to convert the conventional CN values from one level to another according to the AMC in which depending on the previous five days become obsolete, where the new CN_m depended on its computation based on the (measured) saturated hydraulic conductivity.

Measuring the hydraulic conductivity through this work was relayed on the tension infiltrometer (Hood-Infiltrometer, UGT-2004) which has become a standard approach for in *situ* measurements of infiltration, hydraulic conductivity, and assessments of water movement through macropores and the soil matrix (Reynolds et al., 2000). The advantage of this approach is that only steady state infiltration measurements are needed to compute the saturated hydraulic conductivity and no knowledge of the antecedent moisture conditions is required (Gardner, 1958; Wooding, 1968; Reynolds and Elrick, 1991; Siriri et al., 2006; Schwärzel and Punzel, 2007; Wahl et al., 2009; Wahren et al., 2009).

Thus, the CN_m provides a direct measurement in *situ* for the impact of land-use and land-management on the soil characteristics without additional equations to convert the curve number from one value to another, and hence reduce the experimental error to reflect that only the change in the CN attributed to the change in land-use and land-management and their impact on the infiltration capacity. Moreover, it can be concluded that the CN results of the DVWK (1984) reflect the closest value to the measured curve number CN_m compared to the other pedo-transfer based models, whereas the DVWK consider in their approach the impact of field measurements on the land-use, and land-management on the CN values.

The suitability of the original CN method for assessing the infiltration capacity has been criticized for 3 reasons (Hawkins et al. 2009):

1. The absence of a time dimension
2. Lack of a non-zero equilibrium infiltration velocity
3. Sensitivity of rainfall intensity

With the concept of the maximum water storage capacity based on measured CN_m this criticism becomes obsolete: 1. the CN_m has a time dimension, the unit is $\left[\frac{1}{L \cdot T^{-1}}\right]$ for mathematical reasons, coming from the connection of the infiltration measurement.
2. All physically-based infiltration equations feature a fixed steady-state rate or capacity. For example, with the popular Green and Ampt (1911) equation, the steady-state rate is K_s. However, with the original CN equation the stable ultimate loss rate is zero while with the CN equation it is limited to I_a+S, which is approached

asymptotically as P increases. Using the CN_m approach introduced the limit, since this is the steady-state K_s.

3. The originally CN-modelled infiltration rate is rainfall intensity sensitive; a curious feature, which is neither intuitive nor seen in other current infiltration models (Hawkins et al. 2009). As the CN_m approach relies on the saturated hydraulic conductivity in order to simulate the maximum water storage capacity. This is not critical in this work, because it was not intended to compute the direct runoff.

The application of the curve number model in hydrology is different. In an earlier paper from Fennessey and Hawkins (2001) they criticize that the original CN is a hydrologic parameter that relies implicitly on the assumptions of extreme runoff events, and during non-extreme runoff events in humid regions, the underlying assumptions are almost never valid. This is true since the CN in the original concept need to be modified according to the antecedent moisture condition. This is a very error-prone process. With the new CN_m approach, saturated conditions are evaluated, providing the maximum potential of a land-use/soil unit. For hydrological models based on the CN_m approach, specific calibration procedures can be applied, but this is beyond the framework of this work. Using this concept in hydrology, it has to be kept in mind that the CN method is only a quasi-empirical design tool and does not represent a true physical process.

Since the CN_m allows taking into account every land-use/land-management situation by measurement, several other models, using the CN (e.g. EPIC, SWAT or soil erosion models), can be improved by updating the CN by measurements.

A useful future work is the set-up of a database of additional CN_m based on field data for different land-management as well as for different agricultural cultivars.

Evaluation of the land-use development impact in the Schunter catchment

The land-use change contributes to an increased frequency and severity of flood generation. For forest land-use, it has been stated that the promotion of sustainable forest management will considerably increase the water retention in landscapes (FAO, 2003).

The results confirm the well-known fact that the topsoil conditions in forests are more favourable for infiltration than under arable use (Fig 4.4, chapter 4.2.4). These results correspond well to the findings by Hartge (1988) who stated that land-use controls soil infiltration and the variation of the infiltration capacity was produced due to the effect of land-use systems on soil properties. The highest infiltration capacity noted in the forest soil was due to a higher content of soil organic matter and an improved soil structure as well as a high fraction of macro-pores produced by the root activity (Wahren et al., 2009; Mapa, 1995).

The biggest impact on the infiltration capacity of the Schunter catchment is the loss of infiltrating area. During the 59 years between 1950 and 2009, 3800 ha land have been lost to urban area. This equals 6 % of the total area of the Schunter catchment. The process of urbanization is irreversible, so densification of existing settlements should be the most urgent action of the city planner, instead of designation of new housing and industrial sites.

The contribution of the land-uses to the water storage capacity

Land-use change is an important characteristic in the runoff process that affects the infiltration capacity. Due to the development and the urbanization activity, land-use is subjected to changes causing soils to be impervious surfaces, which leads to decrease in soil infiltration capacity and consequently increase the amount of runoff. With respect to the experimental data in the Schunter area, soil saturated hydraulic conductivity is clearly related to land-use (Fig. 4.5, chapter 4.3). Not only the macropores and the pre-event soil moisture are influenced by the land-use, but also the water retention characteristics due to a changed pore distribution (Wahren et al., 2007a). Thus, the change in land-use will have distinct effects on infiltration capacity and the water retention.

Fig.5.1: The impact of urbanization on the surface runoff in the Schunter catchment.

With changing land-use and increasing urbanization activity within the Schunter area from 1950 to 2009, the total water storage capacity was decreased by 17.3 % (Table 4.35, chapter 4.5.4), and these results consistent with several authors (Hartge, 1988; Wahren et al., 2009) who deduced that deforestation, grazing, urbanization, and other land-use activities can significantly postpone the seasonal and annual distribution of surface flow and decrease the infiltration capacity. In addition, the contribution of each land-use to the total water storage capacity was changed through 1950 to 2009.

Thus, it can be concluded that decreasing cropland by 9 % from 1950 to 2009 with increasing the urbanization activity in the Schunter catchment results in decreasing the infiltrating area by 17.3% and increasing the contribution of the forest and the grassland to the total water storage capacity by 15% in 2009 compared to their contribution in 1950 (Table 4.36, chapter 4.5.4). These results consistent with Wood and Blackburn (1981), Schukla et al., (2003) and Fu et al., (2006) who stated that change in land-use affect physical, chemical, and biological characteristics of the soil and the infiltration capacity influenced by the soil structure, and land-use. In addition

Gifford and Hawkins (1978) mentioned that increases in ground cover often result in increase of the soil infiltration rate, and these concept was consistent with experimental results where with increasing the forest land-use by 1.4 % in 2009 compared to 1950, the contribution of the forest to infiltration capacity increased by 12 % (Table 4.36, chapter 4.5.4). This result corresponds with Wood (1971) and Wahl et al., (2003) who demonstrated that most soils under forest have the ability to absorb water at rapid rates. The scenario for 2070, assuming increasing urbanization activity and changing the land-use with the same rate like between 1950 and 2009, showed that the total infiltrating area decreased by 8 % (Table 4.36, chapter 4.5.4).

The Lower Schunter sub-catchment reflects the highest increase of urbanization activity compared to the other sub catchment of the Schunter area, and hence the total water storage capacity shows a pronounced decreasing by 4 % from 1950 to 2009 (Table 4.37, chapter 4.5.4). In addition, the Lower Schunter sub-catchment reflects another phenomenon with change the spatial distribution of the land-use between 1950 and 2009, where with decreasing of infiltrating area by 19 %, the impact of the forest land-use on the infiltration capacity increased by 16.5 %. A number of researchers have studied the effect of the spatial variability of the watershed data used in models on simulated flows (Cotter et al., 2003; Kalin et al., 2003; Chen and Mackay, 2004).

Grassland has a higher infiltration capacity compared to the arable land. The results correspond well with the research by Ernest and Tollner (2002) and Al-Hassoun (2009) who deduced that the infiltration rate is higher under grass compared to field crops. This could be attributed to the higher soil compaction in arable lands due to a high stress induced by field machinery leading to higher soil dry bulk density and decreased infiltration rates (Table 4.6, chapter 4.2.4).
On the other hand, the perennial grass produces a greater amount of plant biomass in the soil, leading to a higher accumulation of the surface organic matter (Table. 5.1), which in turn contributes to enhanced infiltration rates, compared to the annual vegetation (Wienhold and Tanaka, 2000).

In addition, with respect to the results of the Schunter sub-catchment spatial distribution, it could be concluded that the contribution of the forest and grassland to the total water storage capacity in Upper Schunter are smaller than their contribution in the Lower Schunter in 2009. This phenomenon could be interpreted in one hand to the loss of the cropland and grassland in the Lower Schunter three times higher than the loss in the Upper Schunter and on the other hand increasing the urbanization activity by five times higher in the Lower Schunter compared to the Upper Schunter which results in decreasing the total infiltrating area.

This ability of the forest and the grassland to increase the water storage capacity in the watershed relay on their saturated hydraulic conductivity potential. The hydraulic conductivities at saturation of the forest sites are between two and four times higher than the corresponding saturated hydraulic conductivities of the cropland sites, whereby the absolute variation for replicates under the arable sites (204.65 ± 123.1 cm d^{-1}) and for the forest sites was (441.23 ± 122.2 cm d^{-1}). This finding is proved by the work of Wahren et al., (2009), who pronounced that the higher small-scale heterogeneity under forest is mainly due to the presence of decayed root channels leading to spots with high infiltration rates. Obviously, the ploughed arable land has a destroyed macropores structure. After infiltration, water cannot further percolate into the subsoil because the macropores are cut at the lower boundary of the plough horizon. Thus, the infiltration capacity at the arable plot is lower than at the forest plots and less variable.

In the present work, the influence of the land-use on the saturated hydraulic conductivities is in agreement with the organic matter content and the effective bulk density under the different land-use (Table 5.1).

Tab. 5.1: Factors affecting the saturated hydraulic conductivity with the different land-use for the Schunter catchment.

Land-use	Effective bulk Density [g·cm³]	Organic matter [%]	Sat Conductivity [cm d^{-1}]
Forest	1.27 ± 0.2	8.35 ± 3.7	441 ± 122
Grassland	1.41 ± 0.2	6.65 ± 4.6	390 ± 69.9
Cropland	1.57 ± 0.1	2.82 ± 1.6	204.7 ± 123

The higher soil infiltration capacity and so the saturated hydraulic conductivity was associated with the higher content of the soil organic matter under the forest land-use and grassland compared to the agriculture land-use. This interpretation goes along with Le Bissonnais and Arrouays, (1997) who revealed the high soil aggregate stability established in the forest and grassland was due to a high content of soil organic carbon.

Finally, with respect to the experimental data for the whole catchment and the sub catchments, the results indicated that the impact of one hundred hectare of organic farming is similar as the impact of one hundred hectare of grassland on the potential storage. These results meant that to maintain the potential water maximum retention within the watershed in case loss of the grassland due to bio- energy production, a convenient strategy can be the conversion of grassland to organic cropland, where our results reveal that decreasing the grassland by 10 % compared to the status quo in 2009 increase the loss of the storage capacity for the catchment by 17.9 %, while increasing the organic management by 10 % compared to the status quo in 2009 reduce the loss of the storage capacity for the catchment by 15.7 % (Table 4.35, chapter 4.5.3) .

Evaluation of land-management change impact

The rate of water infiltration into the soil, its consequence movement in the soil matrix and surface runoff are important consideration in developing land-management practices which increase the efficiency of rainfall use and maintain a favourable soil water condition that is crucial for plant and soil health.

Soil sealing is considered one of the main threats to soil as organic matter decline, flooding, erosion, soil biodiversity loss, contamination and landslides (Campbell, 2008). The problem of soil sealing intensified by inappropriate agronomic managements is qualified as “silent sealing”. It can also be expressed as a loss of the soil infiltration capacity induced by the soil surface sealing or the subsoil sealing (soil compaction).

The results of Al-Hassoun (2009) revealed that the higher soil aggregate stability was related to a greater content of soil organic matter under conservation tillage in comparison to conventional tillage, and the higher infiltration rate was generated not only by larger numbers of soil macropores and biopores but also by a higher soil resistance to the surface sealing.

The high soil aggregate stability can be achieved under tillage treatments, which guarantee no or minimum soil disturbance and contribute to higher inputs of surface crop residues as a resource of organic management. The organic management, due to the improved soil structure and the higher biological activity, is a better strategy to guarantee higher infiltration capacity compared to the conventional tillage.

The organically managed fields had a higher soil infiltration capacity compared to the conventionally managed fields (Fig. 4.10, chapter 4.3.3). It was revealed that the higher soil infiltration capacity were associated with a higher soil aggregate stability and a higher number of macro-pores (Al-Hassoun, 2009), which associated with the work of Mapa and Gunasena (1995), who noted that the higher aggregate stability produces a higher macro-porosity in the soil, which in turn results in a higher soil infiltration capacity.

In addition, organic management is more useful for earthworm populations in comparison to conventional management. This fact was associated with Schnug et al., (2004) who stated that organic management results in a greater number and biomass of earthworms producing more "biopores" in the soil, and hence higher infiltration capacity in comparison to conventional management.

With respect to the results for the data set in 1950, the impact of the technology was investigated as shown in (Table 4.35, chapter 4.5.3). For the Schunter catchment, the total water storage capacity reveals a pronounced decreasing by 17.6 % by converting the soil management from organic to conventional. Poudel et al., (2001) demonstrated that organic management leads to a better soil structure and higher biological activity and greatly infiltration capacity of soil.

In addition, it could be deduced that with assuming the prevailing management in 1950 was organic, the cropland contributed with the half of the maximum water

storage capacity and the rest for the forest and the grassland. Otherwise, with assuming that the predominant management in 1950 was conventional tillage, the cropland contributes only one the third of the maximum water storage capacity and the contribution of the forest and the grassland increased to be 70 %.

The work of Wuest (2001), Al-Hassoun (2009) and Hartmann et al., (2009) revealed that the different soil management and tillage intensities influenced the water infiltration capacity into the soil significantly. The differences observed in the infiltration rates were a consequence of the changes in soil physical, chemical and biological properties induced by different tillage treatments (Pelegrin et al., 1990). Soil tillage intensity affects the distribution of macropores resulting in changes in the soil infiltration potential (Logsdon et al., 1990). On the other hand, it was pronounced that higher infiltration rates are due to a distinctly higher soil aggregate stability under shallow tillage, in contrast to deep tillage.
Conservation tillage produced higher infiltration capacity compared to conventional tillage (Table 4.36). This result is consistent to the data set of Al-Hassoun (2009), and convenient with Tebrügge and Düring (1999), who demonstrated that conservation tillage often, yielded more enhanced infiltration capacity compared to conventional tillage. The increase of infiltration capacity was due to greater improvement of soil properties obtained under conservation tillage in contrast to conventional tillage (Buschiazzo et al., 1998). For instance, conservation tillage produces a higher vertical connectivity and continuity of soil macropores than conventional tillage (Hangen et al., 2002). Furthermore, the ecological management with increased surface crop residues results in greater earthworm activity than conventional tillage because surface residues afford a useful food source for earthworms and provide protection to their surface environment (Hartmann et al., 2009).

However, with respect to the results of the Schunter catchment, it can be concluded that converting 10% of conventional tillage cropland to organic farming is more effective on infiltration capacity than converting the same area to conservation tillage. The maximum storage capacity of the whole watershed increased by 1 % with organic farming compared to an increase of the maximum storage capacity of the whole watershed by 0.4 % with conservation tillage.

Therefore, it can be concluded that organic farming and conservation tillage, through enhancing the infiltration capacity, could offer means as alternative strategy for flood protection. It takes place because of the mechanical stress on the soil induced by heavy machinery loads (Etana and Håkansson, 1994), and due to intensive tillage operations (Gaultney et al., 1982). Soil compaction leads to a decrease of soil macropores, an increase of the soil dry bulk density and the penetration resistance and hence causes reductions of water infiltration rates (Hillel, 1982; Oussible et al., 1992; Håkansson and Reeder, 1994; Ishaq et al., 2003).

The "silent" soil sealing can occur as well due to compaction of soil below the frequent tillage depth (Jorajuria et al., 1997). Own investigations have shown that the land-use system distribution is an important measure to guarantee high infiltration rates and to investigate the contribution of each land-use to the infiltration capacity.

It can be concluded that organic management with a high input of surface crop residues, provided a better soil physical condition, more improved soil biological properties, larger soil organic matter content, and hence higher rates of water infiltration capacity into the soil could be used as an alternative strategy for a preventive flood protection in case of loosing the grassland due to the bio-energy production.

Finally, it can be concluded that it is immensely important to avoid or minimize the "silent soil sealing" to prevent infiltration losses. This task can be achieved by a sustainable agricultural management. Crop residues on the soil surface protect the soil and in turn contribute to a greater content of organic matter and thus a higher aggregate stability. Organically managed soils support the foundation of biopores producing higher infiltration rates compared to conventional management. In addition, it could be concluded that converting conventional tillage cropland to organically managed one is more effective to maintain the soil surface and increase infiltration capacity compared to convert the same area of the cropland to the conservation tillage. Therefore, organic farming becomes as a very significant

procedure to counteract the adverse consequences of the anthropogenic sealing of soils (Schnug and Haneklaus, 2002).

Further work is proposed to fill some gaps that became clear after this work was completed. First, it is realized that the curve number CN_m varies with the crop and the land-management systems. For the future, it would be valuable to have more samples, which reflect the different land-management systems (e.g. deep ploughing, shallow tillage, no tillage) and consider the vegetation cover. In addition, more detailed land-use and different soil type are needed whereas the digital soil maps which were used performed at a scale of 1: 50.000. Some soil types were missing in the test-site, so that the predominant HSG was A. Thus, working with data of higher resolution can offer more details of different soil types, texture, different soil properties and hence distinguish between the different HSGs on the infiltration capacity.

6 Summary

Infiltration capacity is an important parameter for the hydrological properties of soil and it could be considered as a good indicator of soil quality and health. The change of the soil infiltration capacity by inadequate land-use and land-management also leads to a *silent sealing*, a deterioration of soil properties which results in negative impacts on a regional scale.

In this work the infiltration properties for several different land-use and land-management situations have been determined in the field. Based on the field measurements a modelling approach has been developed which determines the maximum water storage capacity (S_{max}) for a given land-use/soil unit. This maximum water storage capacity is closely related to the saturated hydraulic conductivity (K_s), and is also a suitable indicator to compare different land-use/land-management scenarios. S_{max} is a theoretical value describing the maximum potential of a given soil/land-use unit. Although, in reality the water storage is highly variable due to different soils and land-uses in a catchment scale, S_{max} allows the direct comparison of different soil/land-use units.

This work analyses the possibility of computing the maximum water storage capacity on a regional scale by using a new way to experimentally determine the Curve Number of the "Curve Number Model" direct from infiltration measurements.

The impact of different land-use and land-management systems on the regional scale has been evaluated for the past (1950), for the current situation (2009), and for a projected scenario (2070). Moreover, the impact of different land-management scenarios on the storage capacity has been evaluated.

The following hypotheses were tested:

1. The originally published CN values are still reliable without modifying them under different land-use and land-management situations.

The measured curve number values (CN_m) are very close to the curve number values published in the literature (NEH-4), while the computed CNs based on pedotransfer functions show much bigger differences compared to the literature values. The CN_m for different crops under conventional management showed slightly higher values for winter wheat, oilseed rape and summer barley compared to the standard reference value. Winter barley and maize fit very well to the published values. For special land-use or land-management situations, which are not covered in the handbook, the estimation of CNm by field measurements is an improvement for the description of a land-use/soil unit. In the future research on the impact of different crops on the infiltration capacity will be an interesting topic.

2. Different types of land-use and/or land-management have an impact on the water infiltration capacity of soils.

The analyses of the numerical model Hydrus-1D showed the impact of different land-uses on the cumulative infiltration. Infiltration is much higher under grassland and forest compared to cropland; these results correspond with the effects of water retention. Using Hydrus-1D for modelling the land-management impact showed that the cumulative infiltration curve under organic farming is larger than under conventional farming. The saturated hydraulic conductivity simulation under organic farming was three times higher than under conventional farming. From the temporal point of view, two hours are required for the entire top soil surface (0-30 cm) to be saturated under organic farming and the K_s values are close to the maximum saturated hydraulic conductivity, while four hours are required under conventional farming to be close to saturation. The modelling results conform to the field measurements.

3. The maximum storage capacity S_{max} is a suitable measure to compare the impact of different land-use and land-management.

The maximum storage capacity S_{max} is a suitable parameter to compare the effect of land-use change over different years, because this value takes into account the change of the infiltrating area, decreased due to urbanisation and it determines the loss of the infiltrating capacity as a result of changing the land-use and the land-management.

4. The determination of the Curve number (CN_m) by field infiltration measurements is a measure to explain the impact of different land-use and land-management on the soil infiltration capacity.

The modification of the Curve Number approach to determine the maximum water storage capacity by field measurements is a suitable tool to investigate the impact of different land-use and land-management on the infiltration properties on a region scale. The measured curve number (CN_m) can be directly determined in the field, the maximum water storage capacity S_{max} becomes a direct measure of the impact of land-use and land-management on the infiltration properties of a catchment. The saturated hydraulic conductivity was measured in this work by a tension infiltrometer. The advantage of this approach is that only the steady state infiltration rate is needed to compute the saturated hydraulic conductivity and no knowledge of the antecedent moisture conditions is required. By using the CN_m, the antecedent moisture conditions (AMC) do not have to be taken into account since the soil is water saturated. This avoids error prone conversions of the original CN according to different moisture conditions. The CN_m provides a direct measurement in *situ* for the impact of land-use and land-management on the soil infiltration characteristics.

5. Based on S_{max}, scenarios for the impact of the land-use change between 1950 and 2009 on the infiltration capacity of the Schunter catchment area can be developed.

Using S_{max} as an indicator allows the comparison of the impact of different land-use/land-management situations. The impact of cultivation of grassland in the

Schunter catchment area was pronounced, where 35.5 % of the grassland in 1950 has been converted to cropland in 2009. The view on the total catchment shows only few changes in grassland conversion, but a deeper look to the sub-catchments shows large changes. As grassland provides more infiltration capacity compared to cropland, the loss of grassland is more severe than the loss of cropland due to urbanization.

The impact of forest on the total storage capacity of the catchment increases since 1950, although the absolute area of forest has not changed very much. In addition, the infiltration capacity from 1950 to 2009 for the whole catchment reveals that the amount of the potential infiltration capacity used is reduced by 17 % with reducing the infiltrating area and increasing the urbanization impact.

The impact of the land-use change in the Schunter catchment reveals another phenomenon, whereas with increasing the urbanization activity from 1950 to 2009 by 6% and decreasing the cropland by 8%, the infiltrating area decreased from 57,527 hectares in 1950 to 53,480 hectares in 2009, and the contribution of the grassland and the forest to the infiltration capacity increased compared to the cropland impact.

The Lower Schunter sub-catchment reveals the largest increase in the urbanization activity during the past 60 years, and the total water storage capacity shows a pronounced decrease of 4 %. In addition, a small change of other land-uses has a larger impact on the total storage capacity. For instance a change of 100 ha grassland would result in a change of 1.67 % of the total storage in the sub catchment.

6. The infiltration capacity on a catchment scale can be improved by a change in the land-management.

Several impacts on the infiltration capacity have been simulated. The impact of technology (change from organic to conventional agriculture in 1950, greater use of machinery) shows a decrease by 10 % just by using a different management practice in 1950.

The effect of increased bio-fuel production showed a decrease of grassland by 10%, these result in a decrease of 1 % total storage capacity compared to the status quo. In absolute figures it is just a change of around 700 ha which have a very strong impact. The increase of organic farmland by 10 % of the total area results in an increase of 1 % total storage capacity. This can be reached by converting around 3000 ha.

The increase of conservation tillage on cropland by 10% of the total area results in an increase of 0.4 % of the total storage capacity. The area needed for conversion is around 3500 ha. Compared to the change of organic farmland, more land is needed to reach only half of the effect. In addition, the sub catchments reveal the same phenomenon.

Finally an optimized land-use with more grassland resulted in an increase of 12 mm storage capacity. But in order to reach this, around 7600 ha of conventional land have to be converted. Organic farmland has to be increased by 450 ha, conservation tillage by around 3700 ha and grassland by around 3500 ha. To reach this optimal land-use, 12.5% of the total land in the catchment needs to be converted. This is a very high effort, but just changing small amounts of cropland to organic farming is much more effective.

7. The change of the agricultural management practices can be used for a preventive flood protection.

To enhance the maximum potential water storage within the watershed, the results reveal that converting conventionally managed cropland to organic management is more effective on infiltration capacity than converting the same area to conservation tillage. The maximum storage capacity of the whole watershed increased by 1% with organic management compared to an increase of the storage capacity by 0.4 % with conservation tillage. The maintenance of a site-specific high infiltration potential is one of the important services delivered by agriculture. Choosing an adequate form of land-management can help to maintain the infiltration potential.

Zusammenfassung

Die Infiltrationskapazität ist ein wichtiger bodenhydrologischer Parameter, und ist als Indikator für Bodenqualität und Bodenfruchtbarkeit geeignet.

Die negativen Veränderungen der Infiltrationskapazität durch ungünstige Landnutzung und Bewirtschaftung führt zu einer *schleichenden Versiegelung*, einer Verschlechterung der Bodeneigenschaften, die zu großen negativen Auswirkungen auf regionalem Maßstab führen können.

Im Rahmen dieser Arbeit wurden die Infiltrationseigenschaften für verschiedene Landnutzungs- und Bewirtschaftungssituationen im Gelände bestimmt. Basierend auf Infiltrationsmessungen wurde ein Modellierungsansatz entwickelt, mit dessen Hilfe die maximale Wasser Speicherkapazität (S_{max}) für eine gegebene Landnutzungs- und Bodeneinheit bestimmt werden kann. Diese maximale Wasser Speicherfähigkeit ist eng mit der gesättigten hydraulischen Leitfähigkeit (K_s) gekoppelt, und ein geeigneter Indikator, um verschiedene Landnutzungs- und Bewirtschaftungsszenarien vergleichen zu können. S_{max} ist ein theoretischer Wert, der das maximale Speicherpotenzial einer gegebenen Landnutzung-/Bodeneinheit beschreibt. In der Realität ist die Wasserspeicherung, bedingt durch unterschiedliche Boden- und Landnutzungen, in einem Einzugsgebiet sehr variabel. Mit S_{max} wird es nun möglich, einen direkten Vergleich verschiedener Landnutzung-/Bodeneinheiten durchzuführen.

Im Rahmen dieser Arbeit wurden die Möglichkeiten der Berechnung der maximalen Wasser Speicherkapazität auf regionaler Ebene untersucht. Es wurde eine neue Methode entwickelt, um experimentell den Indexwert CN des "Curve Number Models" direkt aus Infiltrationsmessungen zu bestimmen.

Die Auswirkungen von verschiedenen Landnutzungen und Bewirtschaftungssystemen auf die regionale Wasserspeicherfähigkeit wurden in verschiedenen Szenarien untersucht. Dabei wurde unter Anderem die aktuelle Nutzungs- und Bewirtschaftungssituation (2009) einem Szenario von 1950, bzw. einem Zukunftsszenario von 2070 gegenübergestellt. Die Auswirkungen der verschiedenen Szenarien wurden bewertet.

Im Rahmen der Arbeit wurden die nachfolgenden Hypothesen untersucht:

1. Die ursprünglich veröffentlichten CN-Werte sind immer noch zuverlässig, und können ohne Veränderung für verschiedene Landnutzungs- und Bewirtschaftungssituationen verwendet werden.

Die Original *Curve Number* Werte berücksichtigen nur die Landnutzung, nicht aber die Bewirtschaftung. Die gemessenen *Curve Number* Werte (CN_m) sind den veröffentlichten Werten (NEH-4) relativ ähnlich, obwohl die Spannweiten der veröffentlichten Werte recht groß sind. Eine Berechnung der CN auf der Basis von Pedotransfer Funktionen zeigte deutliche Abweichungen.
Betrachtet man die CN_m für verschiedene Anbaukulturen unter konventioneller Bewirtschaftung, so zeigen sich leicht höhere Werte für Winterweizen, Winterraps und Sommergerste. Zukünftiger Forschungsbedarf besteht für Untersuchung über den Einfluss der angebauten Fruchtart auf die Infiltrationskapazität.

2. Unterschiedliche Landnutzungen und/oder Bewirtschaftungsmaßnahmen haben einen Einfluss auf die Infiltrationseigenschaften von Böden.

Berechnungen mit dem numerischen Modells Hydrus-1D zeigten deutlich die Auswirkungen der verschiedenen Landnutzungen auf die kumulative Infiltration. Unter Grünland und Wald sind die Infiltrationsraten deutlich höher, als im Vergleich zu Ackerland. Gleiche Ergebnisse zeigten sich auch bei der Wasserspeicherfähigkeit. Die Auswirkungen von Bewirtschaftungsänderungen lassen sich auch mit dem Modell Hydrus-1D zeigen: Die kumulative Infiltrationskurve ist bei ökologisch bewirtschafteten Flächen größer als unter konventionell bewirtschafteten Böden. Die Simulation der gesättigten hydraulischen Leitfähigkeit unter ökologischer Bewirtschaftung war dreimal höher als unter konventioneller Bewirtschaftung. Zeitlich betrachtet bedarf es zwei Stunden, bis die gesamte obere Bodenschicht (0-30 cm) unter ökologischer Bewirtschaftung gesättigt ist. Die ermittelten K_s-Werte liegen dabei nahe dem Maximum der gesättigten hydraulischen Leitfähigkeit. Im Gegensatz dazu dauert es vier Stunden unter konventioneller Bewirtschaftung, bis Werte nahe der Sättigung erreicht werden. Die Ergebnisse der Modellierung sind im Einklang mit den Feldmessungen.

3. Die maximale Speicherkapazität S_{max} ist ein geeignetes Maß, um die Auswirkungen verschiedener Landnutzungs- und Bewirtschaftungsarten zu vergleichen.

Die maximale Speicherkapazität S_{max} ist ein geeigneter Parameter, um die Auswirkung von Landnutzungsänderungen zwischen verschiedenen Jahren zu vergleichen, da dieser Wert auch den Verlust der möglichen Infiltrationsfläche berücksichtigen kann. Aufgrund von Urbanisierung kommt es zu einem irreversiblen Verlust von Böden, so dass die maximalen Speicherkapazität nicht nur durch die Veränderung der Landnutzung und der Bewirtschaftung beeinträchtig wird, sondern auch von der zur Verfügung stehenden Fläche bestimmt wird.

4. Die Bestimmung der Curve Number (CN_m) durch Feldmessungen ist geeignet, um die Auswirkungen der verschiedenen Landnutzungs- und Bewirtschaftungsformen auf die Infiltrationskapazität des Bodens zu erklären.

Die Modifizierung des *Curve Number* Ansatzes zur Bestimmung der maximalen Wasser Speicherkapazität auf der Basis von Feldmessungen ist ein geeignetes Werkzeug, um die Auswirkungen der verschiedenen Landnutzungs- und Bewirtschaftungsformen auf der Infiltrationseigenschaften im regionalen Maßstab zu untersuchen.
Die gemessene *Curve Number* (CN_m) kann direkt im Feld bestimmt werden; die maximale Wasser Speicherkapazität S_{max} liefert ein direktes Maß für den Einfluss der Landnutzungs- und Bewirtschaftungsänderungen auf die Infiltrationseigenschaften eines Einzugsgebietes. Die gesättigte hydraulische Leitfähigkeit wurde in dieser Arbeit mit einem Hauben-Infiltrometer bestimmt. Der Vorteil dieser Methode ist, dass nur die konstante Flussrate (steady state infiltration) benötigt wird, um die gesättigte hydraulische Leitfähigkeit zu berechnen. Der Feuchtezustand des Bodens (antecedent moisture conditions (AMC)) muss nicht bekannt sein, da der Boden bei der Messung wassergesättigt ist. Zur Bestimmung der CN_m wird keine fehleranfällige Korrektur der Daten an den Feuchtezustand mehr notwendig.

Die CN_m bietet somit eine direktes *in situ* Maß für die Auswirkungen von Landnutzungs- und Bewirtschaftungsänderungen auf die Infiltrationseigenschaften.

5. Basierend auf S_{max} können Szenarien über die Auswirkungen der Landnutzungsänderungen auf die Infiltrationskapazität zwischen 1950 und 2009 entwickelt werden.

Mit S_{max} steht ein Indikator zur Verfügung, der den Vergleich der Auswirkungen verschiedener Landnutzungs- und Bewirtschaftungsänderungen auf die Infiltration ermöglicht. Die bedeutendste Veränderung im Einzugsgebiet der Schunter war der Grünlandumbruch. Von den Grünlandflächen 1950 wurden bis 2009 35.5% zu Ackerland umgebrochen. Betrachtet man die absoluten Zahlen, so ist der Anteil Grünland im Einzugsgebiet über die letzten 60 Jahre relativ konstant geblieben, jedoch zeigen sich starke Veränderungen in den Teileinzugsgebieten. Gewässerbegradigungen führten einerseits zur Umwandelung von Grün- zu Ackerland, anderseits führte die Renaturierung von ehemaligen Tagbauflächen zu einem Zuwachs von Grünland, so dass in der Summe keine großen Flächenverluste auftreten. Da jedoch die Infiltrationskapazität von Grünland höher als die von Ackerland ist, ist der Verlust von Grünland zunächst kritischer einzustufen, als der Verlust von Ackerland für Bauland. Allerdings ist Bauland für die Infiltration irreversibel verloren.

Die Forstflächen nehmen seit 1950 leicht zu, was auf Aufforstungsmaßnahmen zurück zu führen ist, absolut sind die Waldflächen jedoch nahezu unverändert.

Die potentielle Infiltrationskapazität ist im Zeitraum von 1950 bis 2009 im gesamten Einzugsgebiet um 17 % zurückgegangen, ursächlich begründet durch den Verlust von infiltrierbarer Fläche durch zunehmende Bebauung. Von 1950 bis 2009 stieg der Anteil bebauter Fläche um 6 % an, bei einem gleichzeitigen Verlust von Ackerland um 8 %. Die Fläche, die für Infiltration zur Verfügung steht reduzierte sich von 57527 ha 1950 auf 53480 ha im Jahr 2009.

Das Teileinzugsgebiet der Unteren Schunter weist den höchsten Urbanisierungsgrad auf. In den vergangenen 60 Jahren nahm das Wasserspeicherfähigkeit hier um 4% ab. In diesem Teileinzugsgebiet haben damit kleine Landnutzungsänderungen bereits eine

große Auswirkung. So führt der Verlust von 100 ha Grünland bereit zu einer Reduzierung der Wasserspeicherfähigkeit um 1,67% in dem Teileinzugsgebiet.

6. Die Infiltrationskapazität auf Einzugsgebietsebene kann durch eine Veränderung in der Landbewirtschaftung verbessert werden.

Verschiedene Auswirkungen auf die Infiltrationskapazität wurden simuliert: Der Einfluss des technischen Fortschritts (Wechsel von ökologischer Bewirtschaftung 1950 zu konventioneller Bewirtschaftung 2009) führte zu einem Verlust von 10 % der Infiltrationskapazität, nur durch eine Veränderung der Bewirtschaftungsweise.
Der Umbruch von Grünland zu Ackerland durch die Ausweitung der Produktion von Biotreibstoffen führt zu einem Verlust von 1% Infiltrationskapazität, unter der Annahme das 10 % der bestehenden Grünlandflächen umgebrochen werden. In absoluten Zahlen bedeutet das für das Einzugsgebiet der Schunter, dass bereits 700 ha Grünlandumbruch zu einem Verlust von 1% Infiltrationskapazität führen.
Eine Verbesserung der Infiltrationskapazität um 1% kann erreicht werden, wenn die die Anzahl ökologisch bewirtschafteter Flächen um 10 % erhöht wird. In absoluten Zahlen bedeutet das eine Erhöhung um 3000 ha Fläche.
Würde der Anteil konservierender Bodenbearbeitung um 10 % erhöht werten, führt das nur zu einer Verbesserung von 0,4 % der gesamten Infiltrationskapazität. Dazu würden 3500 ha Fläche benötigt. Im Vergleich zur ökologischen Bewirtschaftung wird also mehr Fläche für konservierende Bodenbearbeitung benötigt, der Effekt ist jedoch nur Halb so groß.
Eine rechnerisch optimierte Landnutzung mit einem höheren Anteil Grünland kann zu einer absoluten Erhöhung der Infiltrationskapazität um maximal 12 mm führen. Dazu müssten ca. 7600 ha konventionell bewirtschaftete Fläche geändert werden. Ökologischer Landbau müsste um 450 ha, konservierende Bodenbearbeitung um ca. 3700 ha und Grünland um ca. 3500 ha vergrößert werden. Um diesen optimierten Zustand zu erreichen müssten 12,5% der Gesamtfläche des Einzugsgebietes verändert werden. Das ist ein sehr großer Aufwand; die Umwandlung zu ökologischer Bewirtschaftung ist effektiver, da bereits kleine Flächenumwandlungen große Auswirkungen erreichen können.

7. Die Veränderung der landwirtschaftlichen Bewirtschaftung kann für einen vorbeugenden Hochwasserschutz verwendet werden.

Zur Verbesserung der maximalen Wasserspeicherkapazität im Einzugsgebiet der Schunter zeigte sich, dass eine Veränderung von konventioneller Landwirtschaft zum ökologischen Landbau effektiver ist, als eine alleinige Veränderung zu konservierender Bodenbearbeitung. Eine Umwandlung zu ökologischen Landbau führte zu einer Erhöhung der Wasserspeicherfähigkeit um 1 % im Einzugsgebiet, wohingegen eine Umwandlung der gleichen Fläche zu konservierender Bodenbearbeitung nur zu einer Erhöhung um 0,4 % führte. Die Erhaltung eines standorttypischen hohen Infiltrationspotenzials ist eine der wichtigsten Leistungen der Landwirtschaft. Die Wahl einer angemessenen Wirtschaftsweise kann dabei helfen, das Infiltrationspotenzial zu erhalten.

7 Reference

Abdul-Megid AH, Schuman GE, Hart RH (1987) Soil bulk density and water infiltration as affected by grazing system. Journal of Range Management, 40, 307-309.

Al-Hassoun R (2009) Studies on factors affecting the infiltration capacity of agricultural soil. Julius Kühn-Institut. Bundesforschungsinstitut für Kulturpflanzen. ISBN 978-3-930037-54-4.

Armbruster M, Seegert J, Feger KG (2004) Effects of changes in tree species composition on water flow dynamics - Model applications and their limitations. Plant Soil, 264, 13-24.

Arnold JG, Williams JR, Nicks AD, Sammons NB (1990) SWRRB: A basin scale simulation model for soil and water resources management. Texas A&M University Press, College Station. 142pp, 10 appendices

Arnold JG, Williams JR, Srinivasan R, King KW (1996) SWAT: Soil and Water Assessment Tool. USDA-ARS, Grassland, Soil and Water Research Laboratory, Temple, TX.

Arshad MA, Lowery B, Grossman B (1996) Physical tests for monitoring soil quality.-In: J.W. Doran and A.J. Jones (eds.) Methods for assessing soil quality. SSSA Spec. Publ. 49. Soil Science Society of America, Inc., Madison, Wisconsin, USA, p.123-142.

BfN (Bundesamt für Naturschutz) (2007) Landschaftssteckbriefe. [online], Germany. To be found at <http://www.bfn.de/0311_landschaft.html?regionid=14> [cited 08.03.2010].

BKG (Bundesamt für Kartographie und Geodäsie) (2008) Digitales Basis-Landschaftsmodell, Basis-DLM [online], Germany. To be found at <http://www.geodatenzentrum.de/docpdf/basis-dlm.pdf> [cited 10.01.10].

BKG (Bundesamt für Kartographie und Geodäsie) (2009) Amtliches Topographisch-Kartographisches Informationssystem [online], Germany. To be found at <https://www.geodatenzentrum.de> [cited 10.01.10].

Boess J, Gehrt E, Müller U, Ostmann U, Sbresny J, Steininger A (2004) Erläuterungsheft zur digitalen nutzungsdifferenzierten Bodenkundlichen Übersichtskarte 1: 50.000 (BÜK50n) von Niedersachsen. Arbeitshefte Boden, Heft 2004/3.

Bouma J, Belmans CFM, Dekker LW (1982) Water infiltration and redistribution in a silt loam subsoil with vertical worm channels. Soil Sci Soc. Am. J. 46: 917-921.

Brakensiek DL, Rawls WJ, Stephenson GR (1984) Modifying SCS hydrologic soil groups and curve numbers for rangeland soils. – ASAE Paper No. PNR–84–203; St. Joseph/ Michigan.

Brocca L, Melone F, Moramarco T (2008) On the estimation of antecedent wetness conditions in rainfall-runoff modelling. Hydrol. Process., 22(5), 629-642.

Broersma K, Robertson JA, Chanasyk DS (1995) Effect of different cropping systems on soil water properties of a Boralf soil. Communication in Soil Science and Plant Analysis, 26, 1795-1811.

Bronstert A (2004) Rainfall-runoff modelling for assessing impacts of climate change. Hydrol. Proc., 18, 567-570**.**

Buschiazzo DE, Panigatti JL, Unger PW (1998) Tillage effects on soil properties and crop production in the subhumid and semiarid Argentinean Pampas. Soil and Tillage Research, Volume 49, Number 1, pp. 105-116.

Cameron DR, Shaykewich C, deJong E, Chanasyk D, Green M, Read DWL (1981) Physical aspects of soil degradation In: Agricultural land – our disappering heritage – a symposium. Proceedings of the 18th annual Alberta Soil Science workshop, pp. 186-255. Alberta Soil and Feed Testing Laboratory, Edmonton, Canada.

Campbell A (2008) Managing Australia's Soils: A Policy Discussion Paper. Prepared for the National Committee on Soil and Terrain (NCST) through the Natural Resource Management Ministerial Council (NRMMC).

Carter MR, Ball BC (1993) Soil porosity. In: Soil sampling and methods of analysis, Carter MR, Ed., Canadian Society of soil science. Lewis Publishers. ISBN 0-87371-861-5.

Chen E, Mackay DS (2004) Effects of Distribution-Based Parameter Aggregation on a Spatially Distributed Agricultural Nonpoint Source Pollution Model. Journal of Hydrology 295:211-224.

Chow VT, Maidment DR, Mays LW (1988) *Applied Hydrology*. McGraw-Hill, New York.

Cosby BJ, Hornberger GM, Clapp RB, Ginn TR (1984) A statistical exploration of the relationships of soil moisture characteristics to the physical properties of soils. Water Res. Res., 20: 682–690.

Cotter AS, Chaubey I, Costello TA, Soerens TS, Nelson MA (2003) Water Quality Model Output Uncertainty as Affected by Spatial Resolution of Input Data. Journal of the American Water Resources Association 39(4):977-986.

Dirksen C (1991) Unsaturated hydraulic conductivity. In: Smith, K.A., Mullins, C.E. (Eds.). Soil Analysis: Physical Methods. pp 209-269. Marcel Dekker, Inc., New York.

De Lange N (2006) Geoinformatik. pp 360-361. Springer, Berlin, Heidelberg.

Dexter RA (2004) Soil physical quality part I. Theory, effects of soil texture, density, and organic matter, and effects on root growth. Geoderma, 120, 201-214.

DVWK (Deutscher Verband für Wasserwirtschaft und Kulturbau e.V.) (1984) Arbeitsanleitung zur Anwendung von Niederschlags-Abfluss-Modellen in kleinen Einzugsgebieten. Teil II: Synthese. DVWK-Regeln zur Wasserwirtschaft 113, Bonn.

DWD (Deutscher Wetterdienst) (2009) Climate Data [online], Germany. To be found at <http://www.dwd.de> [cited 10.01.10].

Ernest W, Tollner PE (2002) Natural resources engineering. Iowa State Press. United States.0-8138-1847-8.

Etana A, Håkansson I (1994) Swedish experiments on the persistence of subsoil compaction caused by vehicles with high axle load. Soil Till. Res. 29 pp. 167–172.

FAO (Food and Agriculture Organisation) (2006) World reference base for soil resources 2006 (WRB), World soil resources report 103.

Fennessey, LAJ, Hawkins, RH (2001) The NRCS Curve Number, A New Look at an Old Tool. [online], USA. To be found at <www3.villanova.edu/VUSP/Outreach/pasym01/pdffiles/B32.pdf>.[cited 21.12.10].

Fetzer, KD (1986) Erläuterungen zur Standortkundlichen Bodenkarte von Bayern, München-Augsburg und Umgebung. Bayerisches Geologisches Landesamt, München.

Fu BJ, Chen LD, Ma KM, Zhou HF, Wang J (2000) The relationships between land use and soil conditions in hilly area of the Loess Plateau in northern Shaanxi, China. Catena, 36, 69-79.

Gardner WR (1958) Some steady-state solutions to the unsaturated flow equation with application to the evaporation from a water table. Soil Sci. 85:228–232.

Gaultney L, Krutz GW, Steinhardt GC, Liljedahl JB (1982) Effects of subsoil compaction on corn yields, Trans. Am. Soc. Agric. Eng. 25 pp. 563–569.

Gifford GF, Hawkins RH (1978) Hydrological impact of grazing on infiltration. Water Resources Research, 14, 305-313.

Green WH, Ampt GA (1911) Studies on soil physics: 1. Flow of air and water through soils. Journal Agric. Science 4, 1-124.

Håkansson I, Reeder RC (1994) Subsoil compaction by vehicles with high axle load- extent, persistence and crop response. Soil Till. Res. 29 pp. 277–304.

Hangen E, Buczko U, Bens O, Brunotte J, Hüttl RF (2002) Infiltration patterns into two soils under conventional and conservation tillage: influence of the spatial distribution of plant root structures and soil animal activity. Soil and Tillage Research, Volume 63, Number 3, pp. 181-186.

Halbfaß S (2005) Entwicklung eines GIS-gestützten Modells zur Quantifizierung diffuser Phosphoreinträge in Oberflächengewässer im mittleren Massstab unter Berücksichtigung geoökologisch wirksamer Raumstrukturen. Diss., Beiträge zur Landschaftsforschung, Bd. 1, Rhombos-Verlag, Berlin.

Hartge HK (1988) The problem of compaction on agricultural lands. Applied Geography and Development 32. 44-50.

Hartmann K, Lilienthal H, Abu Hashim M, Al-Hassoun R, Schnug E (2009) Vergleichende Untersuchungen der Infiltrationseigenschaften von konventionell und ökologisch bewirtschafteten Böden. Eine Fallstudie aus dem Main-Tauber Kreis, Baden-Württemberg, Julius Kühn-Institut. Bundenforschungsinstitut für Kulturpflanzen.

Hawkins RH (1993) Asymptotic determination of runoff curve numbers from data. J. Irrg. Drain. ASCE; 119(2), 334-345.

Hawkins RH, Ward TJ, Woodward DE, Van Mullem JA (2009) Curve Number Hydrology: State of the practice. Rev. Ed., U.S.D.A., Washington D.C., U.S.A.

Heermann D, Duke HR (1983) Applications in dryland agriculture. In: Advances in Infiltration. Proc. of National Conference on Advances in Infiltration. American Society of Agriculture Engineers, St. Joseph, MI, pp. 254-263.

Hermawan B, Cameron KC (1993) Structural changes in a silt loam under long-term conventional or minimum tillage. Soil and Tillage Research, 26: 139-150.

Hernanz JL, López R, Navarrete L, Sánchez-Girón V (2002) Long-term effects of tillage systems and rotations on soil structural stability and organic carbon stratification in semiarid central Spain, Soil Till. Res. 66 pp. 129–141.

Hillel D (1982) Introduction to soil physics. Academic Press Inc., New York, USA.

Hillel D (2004) Introduction to environmental soil physics. Elsevier, London, UK.

Horten RE (1940) An approach towards a physical interpretation of infiltration capacity. Soil Sci. Soc. Am. Proc. 5, 399-417.

Ishaq M, Ibrahim M, Lal R (2003) Persistence of subsoil compaction effects on soil properties and growth of wheat and cotton in Pakistan. Expl Agric. volume 39, pp. 341-348.

ISO (International Standard) 11277 (1998) Soil quality-Determination of particle size distribution in mineral soil material- Method by sieving and sedimentation.

Jain MK, Mishra SK, Suresh Babu P, Venugopal K, Singh VP (2006) Enhanced runoff curve number model incorporating storm duration and a nonlinear ia-S relation. J. Hydrol. Eng.-ASCE, 11(6), 631-635.

Jorajuria D, Draghi L, Aragon A (1997) The effect of vehicle weight on the distribution of compaction with depth and the yield of Lolium/Trifolium grassland, Soil Till. Res. 41, pp. 1–12.

KA 5 (Ad-hoc-ARBEITSGRUPPE BODEN der Geologischen Landesämter und der Bundesanstalt für Geowissenschaften und Rohstoffe der Bundesrepublik Deutschland) (2005) Bundesanstalt für Geowissenschaften und Rohstoffe. Schweitzerbart´sche Verlagsbuchhandlung. Stuttgart. S. 438.

Kalin L,Govindaraju RS, Hantush MM (2003) Effect of Geomorphologic Resolution on Modeling of Runoff Hydrograph and Sedimentograph Over Small Watersheds. Journal of Hydrology 276:89-111.

Kannan N, Santhi C, Williams JR, Arnold JG (2008) Development of a continuous soil moisture accounting procedure for curve number methodolgy and its behaviour with different evapotranspiration methods. Hydrol. Process., 22(13), 2114-2121.

King KW, Balogh JC (2008) Curve numbers for golf course watersheds. T. ASAE, 51(3), 987-996.

Klute A (1986) Water retention: Laboratory methods. In: Klute, A. (Ed). Methods of soil analysis. Part 1. 2nd edition. Agronomy Monograph 9, pp 635-662. ASA and SSSA, Madison, WI.

Kosugi K (1999) General model for unsaturated hydraulic conductivity for soils with lognormal pore size distribution. Soil Sci. Soc. Am. J. 63:270-277.

Kouwenhoven JK, Perdok UD, Boer J, Oomen GJM (2002) Soil management by shallow mouldboard ploughing in The Netherlands. Soil and Tillage Research. Volume 65, Issue 2, Pages 125-139.

Laurance, WF (2007) Environmental science: Forests and floods. Nature, 499, 409-410, online at <http://www.nature.com/nature/Journal/v449/n7161/full/.html> [cited 26.09.07].

Le Bissonnais Y, Arrouays D (1997) Aggregate stability and assessment of soil crustability and erodibility:II. Application to humic loamy soils with various organic carbon contents. Eur. J. Soil Sci. 48: 39-48.

Lilienthal H, Abu Hashim M, Schnug E (2009) Preventative Flood protection - Adaption of land management to improve soil infiltration. In: Proceeding of the International conference in Dimensions of ecology from global change to molecular ecology: September, 14th to 18th 2009. Bayreuth, Germany.

Logsdon SD, Allmaras RR, Wu L, Swan JB, Randall GW (1990) Macroporosity and its relation to saturated hydraulic conductivity under different tillage practices. Soil Sci. Soc. J. 54: 1096-1101.

Man T., Alexe M., (2006) Modelare hidrologica in GIS. Implementarea modelului SCS-CN pentru evaluarea scurgerii, Geographia Technica Nr.1/2006, pp.121-126, ISSN 1842-5135.

Mann L, Tolbert V (2000) Soil Sustainability in Renewable Biomass Plantings. AMBIO: A Journal of the Human Environment. Volume 29. Issue 8. Article: pp. 492–498.

Mapa RB (1995) Effect of reforestation using Tectona grandis on infiltration and soil water retention. Forest Ecology and Management 77 (1995) 119-125.

Mapa RB, Gunasena HPM (1995) Effect of alley cropping on soil aggregate stability of a tropical Alfisol. Kluwer Academic Publishers. Printed in the Netherlands. Agroforestry Systems 32: 237-245.

Mc Calla GR, Backburn WH, Merrill LB (1984) Effects of livestock grazing on infiltration rate. Edwards Plateau of Texas. Journal of Range Management, 37, 265-269.

Michel C, Andreassian V, Perrin C (2005) Soil Conservation Service Curve Number method: How to mend a wrong soil moisture accounting procedure? Water Resour. Res., 41, W02011, doi:10.1029/2004WR003191.

Mishra SK, Singh VP (1999) Another look at SCS-CN method, J. Hydrol. Eng. ASCE, 4(3), 257-264.

Mishra SK, Singh VP (2006) Arelook st NEH-4 vurve number data and antecedent moisture condition criteria. Hydrol. Process., 20(13), 2755-2768.

Mishra SK, Jain MK, Pandey RP, Singh VP (2005) Catchment area-based evaluation of the AMC-dependent SCS-CN-based rainfall-runoff models. Hydrol. Process., 19(14), 2701-2718.

Mishra SK, Pandey RP, Jain MK, Singh VP (2008) A rain duration and modified AMC dependent SCS-CN based rainfall-runoff events. Water Resour. Manag., 22(7), 861-876.

Mualem Y (1976) A new model predicting the hydraulic conductivity of unsaturated porous media. Water Resour. Res. 12:513-522.

National Insitute of Hydrology (1997) Determination of SCS runoff curve number and land use changes for Hamidnagar sub basin of Punpun basin by NIH (1996-97). [online], India. To be found at http://www.indiawaterportal.org/node/10752 [cited 21.12.10].

NLWKN (Niedersächsischer Landesbetrieb für Wasserwirtschaft, Küsten- und Naturschutz) (2005) Deutsches Gewässerkundliches Jahrbuch 2002, Weser- und Emsgebiet. Norden.

NLWKN (Niedersächsischer Landesbetrieb für Wasserwirtschaft, Küsten- und Naturschutz) (2010) Deutsches Gewässerkundliches Jahrbuch 2006, Weser- und Emsgebiet. Norden.

Oussible M, Crookston PK, Larson WE (1992) Subsurface compaction reduces the root and shoot growth and grain yield of wheat. Agronomy Journal 84:34–38.

Pelegrin F, Moreno F, Martin-Aranda J, Camps M, (1990) The influence of tillage methods on soil physical properties and water balance for a typical crop rotation in SW Spain, Soil Till. Res. 16 pp. 345–358.

Ponce VM, Hawkins RH (1996) Runoff curve number: Has it reached maturity?. J. Hydrol. E.-ASCE, 1(1), 11-18.

Poudel DD, Ferris H, Klonsky H, Horwath WR, Scow KM, Van Brugen AHC, Lanini WT, Mitchell JP, Temple SR (2001) The sustainable agriculture farming system project in California,s Sacramento vally. Outlook on Agriculture, 30: 159-160.

Reynolds WD, Bowman BT, Brunke RR, Drury CF, Tan CH (2000) Comparison of tension infiltrometer, pressure infiltrometer, and soil core estimates of saturated hydraulic conductivity. Soil Sci. Soc. Am. J. 64:478-484.

Reynolds WD, Elrick DE (1991) Determination of hydraulic conductivity using a tension infiltrometer. Soil Sci. Soc. Am. J. 55:633–639.

Rogasik J, Panten K, Schnug E, Rogasik H (2004) Infiltration Management Factors. Encyclopedia of Soil Science DOI:10.1081 /E-ESS-120019048.

Romero P, Castro G, Gomez JA, Fereres (2007) Curve number values for olive orchards under different soil moisture management. Soil Sci. Soc. Am. J., 71(6), 1758-1769.

Sahu RK, Mishra SK, Eldho TI, Jain MK (2007) An advanced soil moisture accounting procedure for SCS curve number method, Hydrol. Process., 21(21), 2872-2881.

Saxton KE, Rawls WJ, Romberger JS, Papendick RI (1986) Estimating generalized soil-water characteristics from texture. Soil Sci. Soc. Am. J., 50: 1031–1036.

Schaap MG, Bouten W (1996) Modeling water retention curves of sandy soils using neural networks. Water Resour. Res. 32:3033-3040.

Schaap MG, Leij FJ (1998) Database Related Accuracy and Uncertainty of Pedotransfer Functions, Soil Science 163:765-779.

Schaap MG, Leij FJ, Van Genuchten MTh (1999) A bootstrap-neural network approach to predict soil hydraulic parameters. In: Van Genuchten, M.Th., F.J. Leij, and L. Wu (eds.), Proc. Int. Workshop, Characterization and Measurements of the Hydraulic Properties of Unsaturated Porous Media, pp 1237-1250, University of California, Riverside, CA.

Schaap MG, Leij FJ, Van Genuchten MTh (2001) ROSETTA: a computer program for estimating soil hydraulic parameters with hierarchical pedotransfer functions. Journal of Hydrology, 251:163-176.

Schaap MG, Leij FJ, Van Genuchten MTh (1998) Neural network analysis for hierarchical prediction of soil water retention and saturated hydraulic conductivity. Soil Sci. Soc. Am. J. 62:847-855.

Schäuble H (2003) HydroTools 1.0 for ArcView 3.x, Institute of Applied Geosciences, Technical University of Darmstadt, www.terracs.de

Schnug E, Haneklaus S (2002) Agricultural production techniques and infiltration significance of organic farming for preventive flood protection. Landbauforschung Völkenrode 52: 197-203.

Schnug E, Rogasik J, Panten K, Paulsen HM, Haneklaus S (2004) Ökologischer Landbau erhöht die Versickerungsleistung von Böden – ein unverzichtbarer Beitrag zum vorbeugenden Hochwasserschutz. Ökologie & Landbau 32 (132): 53-55.

Schüler G (2006) Identification of Flood-generating Forest Areas and Forestry Measures for Water Retention. Forest, Snow Landscape Res., 80, 99-114.

Schwärzel K, Punzel J (2007) Hood Infiltrometer. A new type of tension infiltrometer. Soil Sci Soc. Am. J. 71,1438-1447.

SCS – Soil Conservation Service (1986) National Engineering Handbook, section 4, Hydrology, Rev. Ed., U.S.D.A., Washington D.C., U.S.A.

Shukla MK, Lal R, Owens LB, Unkefer P (2003) Land use and management impacts on structure and infiltration characteristics of soils in North Appalachian region of Ohio. Soil Science, 168, 167-177.

Simanton JR, Hawkins RH, Mohseni-Saravi M, Renard KG (1996) Runoff curve number variation with drainage area, walnut gulch, Arizons, T. ASAE, 39(4), 1391-1394.

Šimůnek J, Van Genuchten MTH, Šejna M (2008) Development and applications of the HYDRUS and STANMOD software packages, and related codes, Vadose Zone Journal, doi:10.2136/VZJ2007.0077, Special Issue "Vadose Zone Modeling", 7(2), 587-600.

Siriri D, Tenywa MM, Ong CK, Black CR, Bekunda MA (2006) Water infiltration, conductivity and runoff under fallow agroforestry on sloping terraces. African Crop Science Journal, 14, 59-71.

Soulis KX, Valiantzas JD, Dercas N, Londra (2009) Analysis of the runoff generation mechanism for the investigation of the SCS-CN method applicability to a partial area experimental watershed. Hydrol. Earth Syst. Sci. Discuss., 6, 373-400.

Spohrer K, Herrmann L, Ingwersen J, Stahr K (2006) Applicability of uni-and bimodal retention functions for water flow modelling in a tropical Acrisol. Vadose zone J. 5,48-58.

Statistisches Bundesamt (2010) Statistik Portal - Land-use [online], Germany. To be found at http://www.statistik-portal.de/Statistik-Portal/en/en_jb09_jahrtabf1.asp [cited 10.01.10].

Tebrügge F, Düring RA (1999) Reducing tillage intensity- a review of results from a longterm study in Germany. Soil and Tillage Research 53: 15-28.

Tisdall JM, Oades JM (1980) The effect of crop rotation on aggregation in a red-brown earth. Aust. J. Soil Res. 18:423–434.

Tollner EW, Calvert GV, Langdale G (1990) Animal trampling effects on soil physical properties of two Southeastern U.S. Ultisols. Agriculture, Ecosystem and Environment, 33, 75-87.

Tripathi MP, Raghuwanshi NS, Rao GP (2006) Effect of Watershed Subdivision on Simulation of Water Balance Components. Hydrological Processes 20:1137-1156.

UGT (Umwelt-Geräte-Technik) (2004) Hood Infiltrometer. Müncheberg, Germany.

Unger PW (1992) Infiltration of simulated rainfall: Tillage system and crop residue effects. Soil Sci. Soc. Am. J. 56: 283-289.

USDA, Natural Resource Conservation Service (2003) National Engineering Handbook, Part 630, Hydrology. [online], USA. To be found at <www.wcc.nrcs.usda.gov/hydro/hydro-techref-neh-630.html> [cited 10.01.10].

USDA, Soil Conservation Service (1954 et seq) National Engineering Handbook, Section 4 Hydrology. 400pp.

USDA, Natural Resource Conservation service (1998) Soil quality indicators: Infiltration [online], USA. To be found at <http://soils.usda.gov/sqi/publications/files/Infiltration.pdf> [cited 10.12.10].

Van Genuchten MTH (1980) A closed-form equation for predicting the hydraulic conductivity of unsaturated soils. Soil Sci. Am. J. 44:892-898.

Vereecken H, Maes J, Feyen J (1990) Estimating unsaturated hydraulic conductivity from easily measured soil properties. Soil Sci., 149: 1–12.

Voges J (1999) Empirisches Modell für die mittlere Maßstabsebene zur GIS-gestützen Bestimmung der Anbindung erosiongefährdeter Ackerflächen an Fließgewässer. Diss. Univ. Hannover.

Wahl NA, Bens O, Schäfer B, Hüttl RF (2003) Impact of change in land-use management on soil hydrulic properties: Hydrulic conductivity, water repellency and water retention. Physics and Chemistry of the Earth, 28, 1377-1387.

Wahren A, Feger KH, Schwärzel K, Münch A (2009) Land-use effects on flood generation-considering soil hydraulic conductivity measurements in modeling. Advances in Geosciences, 21, 99-107.

Wienhold BJ, Tanaka DL (2000) Haying, tillage, and nitrogen fertilization influences on infiltration rates at a conservation reserve program site. Soil Science Society of America Journal 64:379-381.

Williams JR (1995) The EPIC model. In: Singh, V.P. (Ed.), Computer Models of Watershed Hydrology. Water Resources Publications, Highlands Ranch, CO, pp. 909-1000.

Wood HB (1971) Land use effects on the hydrologic characteristics of some Hawaii soils. Journal of Soil and Water Conservation, 26, 158-160.

Wood MK and Blackburn W (1981) Grazing systems: their influence on infiltration rates in the rolling Plains of Texas. Journal of Range Management, 34,331-335

Wooding RA (1968) Steady infiltration from a shallow circular pond. Water Resour. Res. 4:1259–1273.

Wuest SB (2001) Earthworm, infiltration, and tillage relationships in a dry land pea–wheat rotation. Applied Soil Ecology 18 187–192.

Young A (1997) Agroforestry for soil management. Second edition. CAB International, New York, USA.

Young RA, Onstad CA, Bosch DD, Anderson WP (1987) AGNPS, Agricultural Non-Point Source Pollution Model: A Watershed Analysis Tool. USDA Conservation Report 35. USDA-ARS, Washington, DC.

8 Appendix

Tab. A1: Soil texture and sample location for the additional data set used in this work.

Field ID	X_COORD	Y_COORD	Land mangement	Sand %	Silt %	Clay %	Soil class KA 5
B-C1	3540421.732	5492031.128	Ecological	2.10	52.10	45.80	Tu 2
B-C2	3540453.000	5491992.614	Conventional	2.20	51.50	46.30	Tu 2
B-C3	3541037.447	5491719.658	Conventional	11.30	58.50	30.30	Tu3
B-C4	3541030.114	5491780.968	Ecological	11.30	52.10	36.50	Tu3
B-C5	3539854.086	5491287.900	Ecological	3.30	44.60	52.00	Tu 2
B-C6	3539829.607	5491334.309	Conventional	3.00	60.80	36.20	Tu3
B-C7	3539806.453	5492396.078	Ecological	3.30	63.00	33.70	Tu3
B-C8	3539765.706	5492365.518	Conventional	6.10	56.60	37.40	Tu3
B-C9	3539646.393	5492707.655	Ecological	1.20	60.90	37.80	Tu3
B-C10	3539602.002	5492739.126	Conventional	1.90	54.90	43.50	Tu3
FV36-C1	3597621.613	5795970.705	Conventional	36.25	56.62	7.13	Us
FV36-C2	3597618.370	5795959.715	Conventional	37.34	55.09	7.58	Us
FV4	3597549.717	5795990.567	Conservation	34.69	58.58	6.73	Us
FV4	3597565.230	5795985.610	Conventional	34.73	58.33	6.93	Us
FV4	3597532.418	5795986.973	Grassland	35.60	57.30	7.10	Us
FV10	3597912.633	5795912.710	Conventional	41.97	50.78	7.26	Us
FV10	3597878.807	5795938.430	Conventional	43.30	49.78	6.92	Us
FV7	3597733.480	5795990.140	Conventional	37.60	54.92	7.43	Us
FV7	3597725.030	5795959.810	Conventional	40.28	52.73	7.00	Us
FV7	3597721.990	5795996.800	Conventional	39.59	53.27	7.15	Us
FV7	3597708.810	5795929.305	Conventional	41.41	51.76	6.83	Us
Bs-F	3597520.045	5795885.595	Forest	48.47	41.69	9.85	Slu
T-K-C1	3600743.511	5960926.211	Ecological	39.60	42.02	18.38	Ls2
T-K-C2	3601139.094	5961031.573	Ecological	45.71	42.66	11.63	Slu
T-G1	3599828.770	5960288.592	Grassland	47.55	35.52	16.94	Sl4
T-e-C3	3601318.571	5961471.359	Conservation	39.23	41.22	19.54	Ls2
T-K-C4	3600743.511	5960926.211	Ecological	39.60	42.02	18.38	Ls2
T-G2	3601139.094	5961031.573	Grassland	45.71	42.66	11.63	Slu

Tab. A1: Continued.

Field ID	X_COORD	Y_COORD	Land mangement	Sand %	Silt %	Clay %	Soil class KA 5
T-G3	3599828.770	5960288.592	Grassland	47.55	35.52	16.94	Sl4
T-e-C5	3601318.571	5961471.359	Conservation	39.23	41.22	19.54	Ls2
M-C1	3533811.210	5824093.778	Conventional	28.28	49.26	22.47	Ls2
M-C2	3533775.958	5824151.013	Conventional	27.54	49.18	23.27	Ls2
M-G1	3533815.273	5823963.038	Grassland	11.12	58.71	30.16	Tu3
M-G2	3532542.165	5826327.978	Grassland	57.53	36.68	5.79	Su3
M-C3	3532269.533	5826138.510	Conventional	50.53	40.40	9.07	Slu
M-C4	3531932.130	5827231.863	Conventional	66.94	27.31	5.74	Su3
FV36-C	3597622.315	5795949.848	Conventional	37.85	54.95	7.53	Us
FV36-C	3597618.370	5795959.715	Conventional	37.34	55.09	7.58	Us
FV4-C	3597549.717	5795990.567	Conventional	34.69	58.58	6.73	Us
FV4-C	3597565.230	5795985.610	Conventional	34.73	58.33	6.93	Us
FV36-C	3597621.613	5795970.705	Conventional	36.25	56.62	7.13	Us

Land-use: C: Cropland, F: Forest, G: Grassland

Location: B: Brehmen, FV: Braunschweig experimental farm, M: Mariensee, T: Trenthorst

Tab. A2: Soil physical characteristics for the data set used in this work

Field ID	Land-use	C_{org} [%]	Effective bulk density	Infiltration capacity mm/hr
B-C1	C	2.01	1.65	1103.54
B-C2	C	1.90	1.73	667.37
B-C3	C	2.10	1.53	200.30
B-C4	C	2.01	1.71	401.54
B-C5	C	2.78	1.48	667.37
B-C6	C	2.13	1.38	204.00
B-C7	C	2.50	1.50	287.35
B-C8	C	2.64	1.66	174.10
B-C9	C	1.50	1.77	372.00
B-C10	C	2.31	1.59	204.00
FV36-C1	C	1.35	1.48	301.86
FV36-C2	C	1.48	1.38	411.84
FV4	C	0.82	1.58	624.00
FV4	C	0.90	1.47	174.72
FV4	G	1.14	1.53	264.42
FV10	C	0.76	1.59	21.84
FV10	C	0.94	1.59	43.68
FV7	C	0.60	1.67	23.40
FV7	C	0.87	1.56	32.76
FV7	C	0.77	1.60	28.08
FV7	C	0.85	1.60	56.16
Bs-F	F	1.96	1.49	404.82
T-K-C1	C	1.39	1.58	1528.80
T-K-C2	C	1.12	1.52	586.56
T-G1	G	2.77	1.60	486.72
T-e-C3	C	1.57	1.61	873.60
T-K-C4	C	1.39	1.58	611.52
T-G2	G	1.12	1.52	430.56
T-G3	G	2.77	1.60	561.60
T-e-C5	C	1.57	1.61	954.72

Tab. A2: Continued

Field ID	Land-use	C_{org} [%]	Effective bulk density	Infiltration capacity mm/hr
M-C1	C	1.24	1.70	892.32
M-C2	C	1.28	1.61	566.28
M-G1	G	4.03	1.69	393.12
M-G2	G	2.04	1.47	453.96
M-C3	C	3.85	1.63	280.80
M-C4	C	1.31	1.55	212.16
FV36-C	C	1.40	1.43	376.74
FV36-C	C	1.35	1.48	175.50
FV4-C	C	0.82	1.58	413.40
FV4-C	C	0.90	1.47	152.88
FV36-C	C	1.35	1.48	107.64

Land-use: C: Cropland, F: Forest, G: Grassland

Location: B: Brehmen, FV: Braunschweig experimental farm, M: Mariensee, T: Trenthorst

Tab. A3: Predicted saturated hydraulic conductivity (K_s [cm d^{-1}]) from PTFs compared to measured results of the data set used in this work.

Field ID	Measured	Rosetta	Cosby	Saxton	Vereecken	Brakensiek
B-C1	28.26	1.75	8.29	7.88	7.10	2.43
B-C2	17.81	1.17	8.25	7.76	3.69	2.24
B-C3	3.34	5.13	13.60	13.48	9.17	43.47
B-C4	9.28	1.68	12.41	9.19	1.81	18.96
B-C5	19.19	4.58	7.83	6.83	17.41	0.85
B-C6	3.98	8.67	9.80	11.28	66.64	11.78
B-C7	5.21	4.84	10.26	12.87	23.89	17.01
B-C8	3.74	2.00	10.53	9.87	3.39	12.16
B-C9	8.44	1.03	9.08	10.86	5.40	8.23
B-C10	4.87	2.41	8.52	8.48	12.20	3.54
FV36-C1	5.79	28.65	39.46	88.07	33.27	510.79
FV36-C2	6.73	40.32	40.46	84.47	65.72	496.59
FV4	14.65	20.56	37.94	91.13	19.58	525.72
FV4	3.15	30.76	37.87	89.69	45.81	522.33
FV4	5.57	23.86	38.74	88.35	23.02	515.15
FV10	0.75	18.26	46.49	86.91	15.89	455.35
FV10	1.40	19.18	48.57	89.89	13.92	441.65
FV7	0.78	13.36	40.86	85.63	9.33	496.85
FV7	0.82	20.61	44.44	89.00	19.13	477.57
FV7	0.88	17.62	43.46	87.78	14.13	482.96
FV7	1.72	18.25	46.04	90.45	14.07	466.52
Bs-F	12.48	23.78	54.04	64.85	16.04	347.72
T-K-C1	37.69	7.41	36.84	25.00	5.22	291.90
T-K-C2	16.72	17.44	48.59	52.59	14.18	363.63
T-G1	16.85	9.81	47.40	27.37	3.22	279.32
T-e-C3	22.76	6.09	35.83	22.13	3.78	270.83
T-K-C4	15.08	7.41	36.84	25.00	5.22	291.90
T-G2	12.29	17.44	48.59	52.59	14.18	363.63

Tab. A3: Continued

Field ID	Measured	Rosetta	Cosby	Saxton	Vereecken	Brakensiek
T-G3	19.55	9.81	47.40	27.37	3.22	279.32
T-e-C5	24.79	6.09	35.83	22.13	3.78	270.83
M-C1	20.11	3.26	24.98	18.99	2.07	195.61
M-C2	10.77	4.50	24.16	17.81	4.40	178.94
M-G1	7.49	2.31	13.56	13.66	1.84	43.79
M-G2	22.11	44.73	74.62	107.16	26.37	221.43
M-C3	12.99	16.75	58.03	71.23	3.63	323.94
M-C4	14.62	46.16	98.12	117.55	15.09	104.33
FV36-C	6.84	33.40	41.09	84.82	46.45	493.46
FV36-C	3.46	27.22	40.46	84.47	29.73	496.59
FV4-C	9.72	20.56	37.94	91.13	19.58	525.72
FV4-C	2.71	30.76	37.87	89.69	45.81	522.33
FV36-C	2.09	28.65	39.46	88.07	33.27	510.79

Land-use: A: Cropland, F: Forest, G: Grassland

Location: B: Brehmen, FV: Braunschweig experimental farm, M: Mariensee, T: Trenthorst

Tab. A4: Infiltration capacity scenarios for the Wabe sub-catchment and the contribution of each land-use and land-management attributed to the infiltrating area.

Scenario	Land-use	S [mm]	%	% /100ha	Infiltrating area [ha]	Total S [mm]	S [%]
Scenario I	Crop conv.	0.00	0.00	0.00	0.00		
100% Org. (1950)	Crop org.	126.85	48.77	0.73	6652.29		
	Crop n/l till	0.00	0.00	0.00	0.00		
	Pasture	25.38	9.76	0.93	1046.23		
	Forest	107.88	41.47	1.59	2603.59		
	Total area				10302.12	260.11	60.94
Scenario II	Crop conv.	76.36	36.43	0.55	6652.29		
100% conv. (1950)	Crop org.	0.00	0.00	0.00	0.00		
	Crop n/l till	0.00	0.00	0.00	0.00		
	Pasture	25.38	12.11	1.16	1046.23		
	Forest	107.88	51.46	1.98	2603.59		
	Total area				10302.12	209.62	49.11
Scenario III	Crop conv.	0.00	0.00	0.00	0.00		
No agric., No grass	Crop org.	0.00	0.00	0.00	0.00		
(1950)	Crop n/l till	0.00	0.00	0.00	0.00		
	Pasture	0.00	0.00	0.00	0.00		
	Forest	426.81	100.00	0.97	10301.03		
	Total area				10301.03	426.81	100.00
Scenario IV	Crop conv.	47.88	23.09	0.55	4171.33		
Status quo (2009)	Crop org.	3.31	1.60	0.92	173.81		
	Crop n/l till	20.69	9.98	0.69	1448.38		
	Pasture	21.94	10.58	1.17	904.55		
	Forest	113.52	54.75	2.00	2739.82		
	Total area				9437.88	207.35	53.02
Scenario V	Crop conv.	48.63	23.58	0.56	4236.45		
Reduction of	Crop org.	3.37	1.63	0.92	176.52		
grassland by 10 %	Crop n/l till	21.01	10.19	0.69	1470.99		
	Pasture	19.75	9.57	1.18	814.10		
	Forest	113.52	55.03	2.01	2739.82		
	Total area				9437.88	206.28	52.74
Scenario VI	Crop conv.	41.23	19.47	0.54	3591.98		
Increase of org.	Crop org.	14.36	6.78	0.90	753.16		
by 10 %	Crop n/l till	20.69	9.77	0.67	1448.38		
	Pasture	21.94	10.36	1.15	904.55		
	Forest	113.52	53.61	1.96	2739.82		
	Total area				9437.88	211.75	54.14
Scenario VII	Crop conv.	41.23	19.73	0.55	3591.98		
Increase of	Crop org.	3.31	1.59	0.91	173.81		
Conserv. by 10%	Crop n/l till	28.97	13.86	0.68	2027.73		
	Pasture	21.94	10.50	1.16	904.55		
	Forest	113.52	54.32	1.98	2739.82		
	Total area				9437.88	208.98	53.43

Tab. A4 Continued

Scenario		S [mm]	%	% /100ha	Infiltrating area [ha]	Total S [mm]	S [%]
Scenario IX	Crop conv.	0.00	0.00	0.00	0.00		
No agric., No grass	Crop org.	0.00	0.00	0.00	0.00		
(2009)	Crop n/l till	0.00	0.00	0.00	0.00		
	Pasture	0.00	0.00	0.00	0.00		
	Forest	391.09	100.00	1.06	9438.97		
	Total area				9438.97	391.09	100.00
Scenario X	Crop conv.	40.80	20.50	0.58	3553.79		
Urban growth	Crop org	2.82	1.42	0.96	148.07		
(2070)	Crop n/l till	17.63	8.86	0.72	1233.95		
	Pasture	18.53	9.31	1.22	763.97		
	Forest	119.21	59.91	2.08	2877.14		
	Total area				8576.92	198.99	56.00
Scenario XI	Crop conv.	0.00	0.00	0.00	0.00		
No agric., No grass	Crop org	0.00	0.00	0.00	0.00		
(2070)	Crop n/l till	0.00	0.00	0.00	0.00		
	Pasture	0.00	0.00	0.00	0.00		
	Forest	355.33	100.00	1.17	8575.83		
	Total area				8575.83	355.33	100.00

Tab. A5: Infiltration capacity scenarios for Uhrau sub-catchment and the contribution of each land-use and land-management attributed to the infiltrating area.

Scenario	Land-use	S [mm]	%	%/100ha	Infiltrating area [ha]	Total S [mm]	S [%]
Scenario I	Crop conv.	0.00	0.00	0.00	0.00		
100% Org. (1950)	Crop org.	118.14	43.42	1.84	2365.59		
	Crop n/l till	0.00	0.00	0.00	0.00		
	Pasture	36.80	13.52	2.33	579.23		
	Forest	117.18	43.06	3.99	1079.81		
	Total area				4024.62	272.12	62.31
Scenario II	Crop conv.	71.12	31.60	1.34	2365.59		
100% conv. (1950)	Crop org.	0.00	0.00	0.00	0.00		
	Crop n/l till	0.00	0.00	0.00	0.00		
	Pasture	36.80	16.35	2.82	579.23		
	Forest	117.18	52.06	4.82	1079.81		
	Total area				4024.62	225.10	51.54
Scenario III	Crop conv.	0.00	0.00	0.00	0.00		
No agric., No grass	Crop org.	0.00	0.00	0.00	0.00		
(1950)	Crop n/l till	0.00	0.00	0.00	0.00		
	Pasture	0.00	0.00	0.00	0.00		
	Forest	436.74	100.00	2.48	4024.62		
	Total area				4024.62	436.74	100.00
Scenario IV	Crop conv.	42.88	18.35	1.29	1426.09		
Status quo (2009)	Crop org.	2.97	1.27	2.14	59.42		
	Crop n/l till	18.53	7.93	1.60	495.17		
	Pasture	49.09	21.01	2.72	772.72		
	Forest	120.16	51.43	4.65	1107.27		
	Total area				3860.67	233.62	55.76
Scenario V	Crop conv.	44.55	19.27	1.30	1481.73		
Reduction of	Crop org.	3.08	1.33	2.16	61.74		
grassland by 10 %	Crop n/l till	19.25	8.32	1.62	514.49		
	Pasture	44.18	19.11	2.75	695.44		
	Forest	120.16	51.97	4.69	1107.27		
	Total area				3860.67	231.22	55.19
Scenario VI	Crop conv.	36.92	15.54	1.27	1228.02		
Increase of org.	Crop org.	12.86	5.41	2.10	257.49		
by 10 %	Crop n/l till	18.53	7.80	1.57	495.17		
	Pasture	49.09	20.67	2.67	772.72		
	Forest	120.16	50.58	4.57	1107.27		
	Total area				3860.67	237.56	56.70
Scenario VII	Crop conv.	36.92	15.71	1.28	1228.02		
Increase of	Crop org.	2.97	1.26	2.12	59.42		
Conserv. by 10%	Crop n/l till	25.94	11.03	1.59	693.24		
	Pasture	49.09	20.88	2.70	772.72		
	Forest	120.16	51.11	4.62	1107.27		
	Total area				3860.67	235.08	56.11

Tab. A.5: continued

Scenario	Land-use	S [mm]	%	%/100ha	Infiltrating area [ha]	Total S [mm]	S [%]
Scenario IX	Crop conv.	0.00	0.00	0.00	0.00		
No agric., No grass	Crop org.	0.00	0.00	0.00	0.00		
2009	Crop n/l till	0.00	0.00	0.00	0.00		
	Pasture	0.00	0.00	0.00	0.00		
	Forest	418.95	100.00	2.59	3860.67		
	Total area				3860.67	418.95	100.00
Scenario X	Crop conv.	34.54	14.61	1.27	1148.96		
Urban growth 2070	Crop org.	2.39	1.01	2.11	47.87		
	Crop n/l till	14.93	6.31	1.58	398.95		
	Pasture	61.39	25.97	2.69	966.21		
	Forest	123.14	52.09	4.59	1134.73		
	Total area				3696.72	236.39	58.93
Scenario XI	Crop conv.	0.00	0.00	0.00	0.00		
No agric., No grass	Crop org.	0.00	0.00	0.00	0.00		
	Crop n/l till	0.00	0.00	0.00	0.00		
	Pasture	0.00	0.00	0.00	0.00		
	Forest	401.12	100.00	2.71	3696.31		
	Total area				3696.31	401.12	100.00

Tab. A6: Infiltration capacity scenarios for Sandbach sub-catchment and the contribution of each land-use and land-management attributed to the infiltrating area.

Scenario	Land-use	S [mm]	%	%/100ha	Infiltrating area [ha]	Total S [mm]	S %
Scenario I	Crop conv.	0.00	0.00	0.00	0.00		
100% Org. (1950)	Crop org.	117.06	42.37	2.12	2000.91		
	Crop n/l till	0.00	0.00	0.00	0.00		
	Pasture	35.43	12.82	2.69	475.98		
	Forest	123.82	44.81	4.60	973.99		
	Total area				3450.88	276.31	62.98
Scenario II	Crop conv.	70.47	30.68	1.53	2000.91		
100% conv. (1950)	Crop org.	0.00	0.00	0.00	0.00		
	Crop n/l till	0.00	0.00	0.00	0.00		
	Pasture	35.43	15.42	3.24	475.98		
	Forest	123.82	53.90	5.53	973.99		
	Total area				3450.88	229.71	52.36
Scenario III	Crop conv.	0.00	0.00	0.00	0.00		
No agric., No grass	Crop org.	0.00	0.00	0.00	0.00		
(1950)	Crop n/l till	0.00	0.00	0.00	0.00		
	Pasture	0.00	0.00	0.00	0.00		
	Forest	438.69	100.00	2.90	3450.88		
	Total area				3450.88	438.69	100.00
Scenario IV	Crop conv.	44.14	18.83	1.50	1253.19		
Status quo (2009)	Crop org.	3.05	1.30	2.50	52.22		
	Crop n/l till	19.07	8.14	1.87	435.13		
	Pasture	37.14	15.85	3.18	499.07		
	Forest	131.00	55.89	5.42	1030.47		
	Total area				3270.08	234.40	56.39
Scenario V	Crop conv.	45.40	19.52	1.51	1288.99		
Reduction of	Crop org.	3.14	1.35	2.52	53.71		
grassland by 10 %	Crop n/l till	19.62	8.43	1.88	447.57		
	Pasture	33.44	14.38	3.20	449.34		
	Forest	131.00	56.32	5.47	1030.47		
	Total area				3270.08	232.59	55.95
Scenario VI	Crop conv.	38.01	15.94	1.48	1079.13		
Increase of org.	Crop org.	13.24	5.55	2.45	226.27		
by 10 %	Crop n/l till	19.07	8.00	1.84	435.13		
	Pasture	37.14	15.58	3.12	499.07		
	Forest	131.00	54.94	5.33	1030.47		
	Total area				3270.08	238.46	57.36
Scenario VII	Crop conv.	38.01	16.11	1.49	1079.13		
Increase of	Crop org.	3.05	1.30	2.48	52.22		
Conserv. by 10%	Crop n/l till	26.70	11.32	1.86	609.19		
	Pasture	37.14	15.75	3.15	499.07		
	Forest	131.00	55.53	5.39	1030.47		
	Total area				3270.08	235.90	56.75

Tab. A6: continued

Scenario	Land-use	S [mm]	%	%/100ha	Infiltrating area [ha]	Total S [mm]	S [%]
Scenario IX	Crop conv.	0.00	0.00	0.00	0.00		
No agric., No grass	Crop org.	0.00	0.00	0.00	0.00		
(2009)	Crop n/l till	0.00	0.00	0.00	0.00		
	Pasture	0.00	0.00	0.00	0.00		
	Forest	415.70	100.00	3.06	3270.08		
	Total area				3270.08	415.70	100.00
Scenario X	Crop conv.	37.53	16.08	1.51	1065.72		
Urban growth	Crop org.	2.60	1.11	2.51	44.41		
(2070)	Crop n/l till	16.22	6.95	1.88	370.04		
	Pasture	38.89	16.66	3.19	522.52		
	Forest	138.18	59.20	5.45	1086.95		
	Total area				3089.63	233.41	59.42
Scenario XI	Crop conv.	0.00	0.00	0.00	0.00		
No agric., No grass	Crop org.	0.00	0.00	0.00	0.00		
(2070)	Crop n/l till	0.00	0.00	0.00	0.00		
	Pasture	0.00	0.00	0.00	0.00		
	Forest	392.81	100.00	3.24	3089.99		
	Total area				3089.99	392.81	100.00

Tab. A7: Infiltration capacity scenarios for Upper Schunter sub-catchment and the contribution of each land-use and land-management attributed to the infiltrating area.

Scenario	Land-use	S[mm]	%	%/100ha	Infiltrating area [ha]	Total S [mm]	S [%]
Scenario I	Crop conv.	0.00	0.00	0.00	0.00		
100% Org. (1950)	Crop org.	114.05	41.43	0.37	11110.06		
	Crop n/l till	0.00	0.00	0.00	0.00		
	Pasture	19.11	6.94	0.47	1463.66		
	Forest	142.15	51.63	0.81	6372.90		
	Total area				18946.62	275.31	65.15
Scenario II	Crop conv.	68.66	29.86	0.27	11110.06		
100% conv. (1950)	Crop org.	0.00	0.00	0.00	0.00		
	Crop n/l till	0.00	0.00	0.00	0.00		
	Pasture	19.11	8.31	0.57	1463.66		
	Forest	142.15	61.83	0.97	6372.90		
	Total area				18946.62	229.92	54.40
Scenario III	Crop conv.	0.00	0.00	0.00	0.00		
No agric., No grass	Crop org.	0.00	0.00	0.00	0.00		
(1950)	Crop n/l till	0.00	0.00	0.00	0.00		
	Pasture	0.00	0.00	0.00	0.00		
	Forest	422.61	100.00	0.53	18946.62		
	Total area				18946.62	422.61	100.00
Scenario IV	Crop conv.	46.21	20.00	0.27	7477.43		
Status quo (2009)	Crop org.	3.20	1.38	0.44	311.56		
	Crop n/l till	19.97	8.64	0.33	2596.33		
	Pasture	15.91	6.89	0.57	1218.71		
	Forest	145.72	63.08	0.97	6532.83		
	Total area				18136.85	231.00	57.10
Scenario V	Crop conv.	46.75	20.31	0.27	7564.88		
Reduction of	Crop org.	3.24	1.41	0.45	315.20		
grassland by 10 %	Crop n/l till	20.20	8.77	0.33	2626.70		
	Pasture	14.33	6.22	0.57	1097.24		
	Forest	145.72	63.29	0.97	6532.83		
	Total area				18136.85	230.23	56.91
Scenario VI	Crop conv.	39.79	16.91	0.26	6438.90		
Increase of org.	Crop org.	13.86	5.89	0.44	1350.09		
by 10 %	Crop n/l till	19.97	8.49	0.33	2596.33		
	Pasture	15.91	6.77	0.56	1218.71		
	Forest	145.72	61.94	0.95	6532.83		
	Total area				18136.85	235.25	58.15
Scenario VII	Crop conv.	39.79	17.11	0.27	6438.90		
Increase of	Crop org.	3.20	1.38	0.44	311.56		
Conserv. by 10%	Crop n/l till	27.95	12.02	0.33	3634.86		
	Pasture	15.91	6.84	0.56	1218.71		
	Forest	145.72	62.65	0.96	6532.83		
	Total area				18136.85	232.57	57.49

Tab. A7: continued

Scenario	Land-use	S [mm]	%	%/100ha	Infiltrating area [ha]	Total S [mm]	S [%]
Scenario IX	Crop conv.	0.00	0.00	0.00	0.00		
No agric., No grass	Crop org	0.00	0.00	0.00	0.00		
(2009)	Crop n/l till	0.00	0.00	0.00	0.00		
	Pasture	0.00	0.00	0.00	0.00		
	Forest	404.55	100.00	0.00	18136.85		
	Total area				18136.85	404.55	100.00
Scenario X	Crop conv.	42.97	18.97	0.27	6954.15		
Urban growth	Crop org	2.97	1.31	0.45	289.76		
(2070)	Crop n/l till	18.57	8.20	0.34	2414.64		
	Pasture	12.72	5.61	0.58	973.75		
	Forest	149.28	65.90	0.98	6692.76		
	Total area				17325.05	226.52	58.61
Scenario XI	Crop conv.	0.00	0.00	0.00	0.00		
No agric., No grass	Crop org	0.00	0.00	0.00	0.00		
(2070)	Crop n/l till	0.00	0.00	0.00	0.00		
	Pasture	0.00	0.00	0.00	0.00		
	Forest	386.49	100.00	0.58	17327.08		
	Total area				17327.08	386.49	100.00

Abflüsse — Wesergebiet — 2002

A_{Eo} : 592 km²
PNP: NN + 60.92 m
Lage: 3.6 km oberhalb der Mündung rechts

Q
m³/s

Pegel : Harxbüttel Nr. 4828140
Gewässer : Schunter
Gebiet : Aller

Tageswerte

Tag	2001 Nov	2001 Dez	2002 Jan	Feb	Mrz	Apr	Mai	Jun	Jul	Aug	Sep	Okt	Nov	Dez
1.	1.19	2.69	7.65	5.74	16.1	3.09	6.03	1.66	1.28	5.15	2.69	1.66	4.24	17.4
2.	1.41	3.68	7.62	5.02	16.9	3.02	4.71	1.66	1.41	8.35	2.50	1.65	6.64	14.5
3.	1.40	4.93	9.88	4.19	13.4	2.96	4.59	1.67	1.42	6.39	2.33	1.64	11.1	10.3
4.	1.28	3.69	5.96	3.69	9.73	2.60	12.2	1.59	1.34	4.95	2.25	1.64	12.2	8.28
5.	1.28	4.63	4.09	3.31	8.29	2.44	18.2	1.68	1.50	4.85	2.26	1.88	9.69	7.06
6.	1.16	9.21	3.64	3.14	6.92	2.37	20.7	2.27	1.34	6.08	2.26	2.38	6.83	6.20
7.	1.15	9.22	2.92	2.86	7.18	2.30	13.6	4.05	1.34	4.66	2.10	2.20	5.58	5.41
8.	1.57	5.73	3.18	2.61	7.09	2.24	8.52	3.24	1.29	4.03	2.02	2.11	5.34	4.67
9.	2.61	3.92	2.86	2.63	6.20	2.27	6.66	3.34	1.29	4.46	1.94	1.85	10.8	3.84
10.	2.06	3.32	2.45	4.27	5.99	2.29	5.52	2.67	1.60	5.31	1.86	1.68	14.5	3.95
11.	1.47	2.93	2.42	5.17	5.66	2.23	4.97	1.97	2.27	9.76	1.86	1.50	13.6	4.79
12.	1.41	2.62	2.29	10.9	5.00	2.23	5.74	1.89	2.46	14.5	1.70	1.49	12.2	4.80
13.	1.79	2.69	2.26	12.7	4.68	2.39	4.01	2.06	1.77	20.7	1.62	1.43	9.97	3.66
14.	1.87	2.37	2.23	7.95	5.35	3.06	3.80	2.07	1.60	22.9	1.62	1.42	7.78	2.40
15.	1.78	1.91	1.94	5.39	5.24	3.86	3.29	2.70	1.69	18.3	1.71	1.81	7.19	1.94
16.	1.60	1.64	1.56	4.43	4.70	7.84	3.18	2.81	1.61	15.4	1.72	1.80	6.61	1.85
17.	1.51	1.61	1.27	3.73	4.40	9.77	3.00	2.09	5.21	9.69	1.72	1.71	11.2	1.95
18.	1.42	1.59	1.42	3.85	4.19	8.65	2.82	1.67	21.9	6.84	1.81	1.62	16.2	1.59
19.	1.36	1.73	1.74	3.99	4.51	7.12	2.82	1.67	51.7	5.49	1.82	1.53	13.4	1.50
20.	1.25	3.46	3.21	6.85	4.42	7.12	2.35	1.93	64.8	4.74	1.82	1.43	8.66	1.41
21.	1.19	3.63	10.7	8.28	4.95	5.20	2.18	2.59	48.0	4.32	1.91	1.76	6.79	1.33
22.	1.35	5.95	14.5	5.91	6.19	4.66	2.27	1.77	24.0	4.02	2.26	2.25	5.76	1.67
23.	2.41	4.39	12.3	9.82	5.55	4.13	2.56	1.73	23.3	4.23	2.63	2.62	6.43	3.07
24.	2.05	3.24	8.59	14.8	4.70	4.32	2.95	1.52	18.6	4.98	2.54	3.49	6.75	1.84
25.	1.79	4.43	6.57	15.8	4.31	4.85	2.29	1.34	12.7	4.99	2.11	2.80	5.73	1.65
26.	2.20	14.0	5.76	17.3	4.03	4.31	2.12	1.31	9.14	4.89	2.00	4.40	5.23	2.67
27.	2.76	14.7	10.3	19.6	3.85	4.73	1.96	1.27	7.97	4.58	1.90	5.57	4.21	11.3
28.	2.58	13.2	16.2	19.2	3.58	4.94	2.05	1.32	6.37	3.86	1.80	8.66	4.26	14.4
29.	2.77	18.2	15.9		3.51	6.38	2.06	1.33	5.58	3.35	1.61	8.65	4.84	14.8
30.	3.06	19.3	10.2		3.13	7.06	1.81	1.33	4.82	3.16	1.67	6.67	12.7	14.5
31.		13.8	7.06		3.26		1.74		4.40	2.88		5.31		19.7

Hauptwerte

	2001 Nov	2001 Dez	2002 Jan	Feb	Mrz	Apr	Mai	Jun	Jul	Aug	Sep	Okt	Nov	Dez
Tag	7.	18.	17.	8.	30.	11.+	31.	27.	1.	31.	29.	14.	27.	21.
NQ	1.15	1.59	1.27	2.61	3.13	2.23	1.74	1.27	1.28	2.88	1.61	1.42	4.21	1.33
MQ	1.76	6.08	6.09	7.60	6.23	4.35	5.18	2.01	10.8	7.35	2.00	2.79	8.55	6.27
HQ	3.77	19.9	17.8	19.8	17.6	10.1	22.4	5.99	70.0	23.9	2.79	12.6	16.6	26.3
Tag	30.	29.	28.	28.	1.	17.	6.	7.	20.	14.	1.	28.	18.	31.
h_N mm	44	91	41	75	33	64	53	68	190	98	23	80	103	70
h_A mm	8	28	28	31	28	19	23	9	49	33	9	13	37	28

	1960/2001		1961/2002 (42 Jahre)											
Jahr	1964	1969	1970	1963	1963	1991	1991	2000	2000	1989	1995	1964	1964	1969
NQ	0.380	0.160	0.140	0.480	0.490	0.976	0.725	0.525	0.465	0.317	0.278	0.430	0.380	0.160
MNQ	1.17	1.57	2.00	2.40	2.67	2.62	1.61	1.22	0.986	0.866	0.875	0.979	1.23	1.49
MQ	2.33	4.09	5.11	5.44	6.36	5.02	2.94	2.27	1.74	1.54	1.29	1.48	2.40	3.97
MHQ	7.82	13.6	15.4	15.7	19.5	12.4	9.48	8.34	6.17	5.79	3.53	4.52	7.76	13.5
HQ	26.9	50.3	53.9	47.2	61.7	50.9	32.4	44.4	70.0	23.9	13.0	37.0	26.9	50.3
Jahr	1998	1986	1987	1970	1979	1994	1961	1961	2002	2002	1981	1998	1998	1986
Mh_N mm	51	60	49	43	51	50	57	71	67	67	47	46	52	59
Mh_A mm	10	19	23	22	29	22	13	10	8	7	6	7	11	18

	Abflußjahr (*) 2002 Jahr	Datum	Winter	Sommer	Kalenderjahr 2002 Jahr	Datum
NQ m³/s	1.15	am 07.11.2001	1.15	1.27	1.27	am 17.01.2002
MQ m³/s	5.19		5.34	5.05	5.77	
HQ m³/s	70.0	am 20.07.2002 bei W= 374 cm	19.9	70.0	70.0	am 20.07.2002 bei W= 374 cm
Nq l/(s km²)	1.94		1.94	2.15	2.15	
Mq l/(s km²)	8.77		9.02	8.53	9.75	
Hq l/(s km²)	118		33.6	118	118	
h_N mm	860		348	512	898	
h_A mm	276		141	136	307	

	1961/2002 (*) 42 Jahre				1961/2002	
NQ m³/s	0.140	am 10.01.1970	0.140	0.278	0.140	am 10.01.1970
MNQ m³/s	0.645		1.02	0.733	0.675	
MQ m³/s	3.29		4.73	1.88	3.29	
MHQ m³/s	29.2		27.1	14.2	30.2	
HQ m³/s	70.0	am 20.07.2002 bei W= 374 cm	61.7	70.0	70.0	am 20.07.2002 bei W= 374 cm
HQ_1 m³/s						
HQ_5 m³/s						
MNq l/(s km²)	1.09		1.72	1.24	1.14	
Mq l/(s km²)	5.56		7.99	3.18	5.56	
MHq l/(s km²)	49.3		45.8	24.0	51.0	
Mh_N mm	658		303	354	658	
Mh_A mm	175		125	50	175	

Dauertabelle

Unterschreitungsdauer in Tagen	Unterschrittene Abflüsse m³/s: Abflußjahr (*) 2002	Kalenderjahr 2002	1961/2002 42 Kalenderjahre: Obere Hüllwerte	Mittlere Werte	Untere Hüllwerte
(365)					
364	64.8	64.8	64.8	30.3	6.44
363	51.7	51.7	51.7	24.5	6.00
362	48.0	48.0	49.0	22.0	5.62
361	24.0	24.0	49.0	20.6	4.70
360	23.3	23.3	43.2	18.9	4.66
359	22.9	22.9	43.1	17.8	4.63
358	21.9	21.9	43.0	16.9	4.62
357	21.9	21.9	40.7	16.1	4.34
356	21.9	21.9	40.6	15.6	4.25
350	18.3	18.2	31.5	12.4	3.65
340	14.7	15.4	23.0	9.24	3.04
330	12.3	13.6	18.3	7.31	2.46
320	9.73	11.2	17.7	6.21	2.15
300	7.18	8.66	13.6	4.70	1.71
270	5.49	6.61	9.28	3.47	1.44
240	4.68	5.34	7.21	2.71	1.20
210	3.92	4.67	5.66	2.18	1.02
183	3.14	4.02	4.50	1.85	0.867
150	2.58	3.00	3.80	1.54	0.781
130	2.29	2.59	3.51	1.40	0.739
120	2.24	2.38	3.42	1.33	0.714
110	2.09	2.29	3.25	1.26	0.698
100	1.96	2.24	3.16	1.19	0.679
90	1.87	2.07	3.02	1.12	0.660
80	1.80	1.95	2.90	1.05	0.632
70	1.73	1.84	2.82	0.981	0.616
60	1.68	1.76	2.65	0.921	0.588
50	1.64	1.69	2.50	0.861	0.551
40	1.57	1.66	2.46	0.796	0.518
30	1.47	1.61	2.30	0.731	0.465
25	1.42	1.52	2.26	0.694	0.461
20	1.35	1.49	2.22	0.661	0.452
15	1.34	1.42	2.22	0.624	0.415
10	1.31	1.41	2.17	0.571	0.260
9	1.29	1.34	2.16	0.560	0.260
8	1.29	1.34	2.16	0.546	0.260
7	1.29	1.34	2.13	0.531	0.200
6	1.28	1.32	2.10	0.514	0.200
5	1.28	1.31	2.07	0.501	0.190
4	1.25	1.31	2.06	0.481	0.190
3	1.25	1.31	2.03	0.463	0.190
2	1.25	1.28	2.00	0.445	0.160
1	1.16	1.28	1.99	0.372	0.160
0	1.15	1.27	1.95	0.140	0.140

Extremwerte

	Niedrigwasser m³/s	l/(s km²)	Datum	Hochwasser m³/s	l/(s km²)	cm	Datum
1	0.140	0.236	10.01.1970	70.0	118	374	20.07.2002
2	0.278	0.470	01.09.1995	61.7	104	335	04.03.1979
3	0.317	0.535	22.08.1989	60.8	103	326	13.03.1981
4	0.330	0.557	02.08.1974	53.9	91.0	316	01.01.1987
5	0.335	0.566	07.09.2001	52.5	88.7	307	28.01.1994
6	0.340	0.574	09.09.1973	52.4	88.5	325	20.03.1970
7	0.350	0.591	15.09.1964	50.9	86.0	308	15.04.1994
8	0.374	0.632	13.08.1999	50.7	85.6	326	16.01.1968
9	0.375	0.633	22.09.1991	47.2	79.7	314	24.02.1970
10	0.420	0.709	22.08.1996	45.5	76.9	293	20.03.1994

(*) Abflußjahr: 1.11. des Vorjahres bis 31.10.
Repräsentativ für die Hydrologische Landschaft Ost-Braunschweig

NLWKN

Fig. A1: Primary values for the Harxbüttel gauge, hydrological year 2002 (NLWKN 2005, P.181).

Abflüsse — Wesergebiet — 2006

A_{Eo} : 592 km²
PNP: NN + 60.92 m
Lage: 3.6 km oberhalb der Mündung rechts

Q m³/s

Pegel : Harxbüttel Nr. 4828140
Gewässer : Schunter
Gebiet : Aller

Tageswerte

Tag	2005 Nov	2005 Dez	2006 Jan	Feb	Mrz	Apr	Mai	Jun	Jul	Aug	Sep	Okt	Nov	Dez
1.	0.919	1.04	3.21	1.66	3.25	8.31	3.43	3.65	0.854	0.591	0.860	0.696	0.892	0.784
2.	0.920	1.03	4.14	1.66	3.19	7.70	2.85	3.28	0.825	0.614	0.669	0.820	0.762	0.789
3.	0.980	0.964	3.83	1.66	2.87	6.82	2.48	2.33	0.796	0.674	0.742	0.742	0.722	0.794
4.	0.952	0.969	3.65	1.66	2.82	7.22	2.17	1.96	0.750	0.652	0.838	0.718	0.721	0.798
5.	0.926	1.26	3.09	1.59	2.64	6.51	1.92	1.78	0.730	0.643	0.857	0.717	0.720	0.921
6.	0.924	1.70	2.76	1.45	2.58	5.92	1.72	1.61	0.755	0.630	0.820	0.718	0.705	0.986
7.	0.908	1.46	2.44	2.59	2.65	4.76	1.72	1.57	0.659	0.614	0.743	0.726	0.692	1.03
8.	0.895	1.37	2.22	12.8	2.68	4.47	1.69	1.43	1.20	0.614	0.713	0.728	0.691	0.948
9.	0.878	1.33	1.98	9.63	2.93	4.22	1.64	1.31	0.931	0.628	0.685	0.714	0.691	0.898
10.	0.866	1.32	1.92	5.40	4.49	3.88	1.63	1.23	0.846	0.640	0.678	0.701	0.675	0.868
11.	0.862	1.25	1.85	5.10	12.1	3.47	1.57	1.13	0.840	0.639	0.678	0.667	0.662	0.864
12.	0.837	1.23	1.80	3.96	6.89	3.45	1.54	1.03	0.793	0.638	0.661	0.656	0.740	0.886
13.	0.838	1.23	1.77	3.30	4.82	3.77	1.48	0.999	0.762	0.625	0.648	0.656	1.06	0.939
14.	0.839	1.24	1.70	2.88	3.95	3.65	1.44	1.01	0.737	0.630	0.635	0.655	1.19	0.945
15.	0.840	1.24	1.64	2.90	3.63	3.52	1.43	0.993	0.718	0.728	0.617	0.654	0.958	0.932
16.	0.937	3.19	1.86	7.32	3.33	3.41	1.43	2.10	0.710	0.759	0.617	0.654	0.802	0.921
17.	1.15	7.22	1.62	7.60	3.12	3.80	1.38	2.09	0.685	0.839	0.616	0.653	0.770	0.925
18.	1.19	3.91	2.11	9.36	3.13	3.72	1.33	1.44	0.685	0.765	0.616	0.652	0.765	0.974
19.	1.06	3.00	2.40	8.55	3.17	3.36	1.82	1.16	0.684	0.749	0.632	0.652	0.753	0.988
20.	1.01	4.77	2.08	7.59	3.96	3.06	1.67	1.48	0.662	0.733	0.643	0.651	0.758	0.971
21.	1.95	5.88	4.71	8.62	5.81	2.81	1.77	1.34	0.652	0.752	0.642	0.650	0.763	0.975
22.	2.12	4.62	11.2	10.2	4.86	2.70	1.40	1.12	0.677	0.794	0.623	0.649	0.768	0.979
23.	1.47	3.96	5.01	7.29	4.11	2.72	1.36	1.01	0.633	0.824	0.629	0.649	0.773	0.984
24.	1.25	3.69	3.87	5.64	3.65	2.72	1.34	0.959	0.606	0.777	0.640	0.648	0.814	0.988
25.	1.21	3.44	3.61	4.77	3.92	2.60	1.72	0.931	0.595	0.761	0.620	0.748	0.976	0.992
26.	1.19	3.28	2.81	4.04	7.08	2.51	1.76	0.929	0.594	0.791	0.566	0.736	0.886	0.996
27.	1.11	2.71	2.47	3.49	13.6	2.39	1.75	0.926	0.599	0.977	0.578	0.700	0.843	1.00
28.	1.07	2.45	2.09	3.29	14.0	2.40	2.68	0.891	0.593	1.11	0.622	0.672	0.823	1.02
29.	1.04	2.23	1.74		9.71	2.55	2.56	0.863	0.592	1.35	0.672	0.950	0.774	1.14
30.	1.04	2.05	1.63		7.72	3.62	2.83	0.854	0.592	1.32	0.693	1.39	0.779	1.17
31.		1.94	1.66		8.17		2.37		0.591	1.21		1.09		1.08

Hauptwerte

	1960/2005		1961/2006 (46 Jahre)											
Tag	12.	3.	17.	6.	6.	27.	18.	30.	31.	1.	26.	24.	11.	1.
NQ	0.837	0.964	1.62	1.45	2.58	2.39	1.33	0.854	0.591	0.591	0.566	0.648	0.662	0.784
MQ	1.07	2.47	2.87	5.22	5.19	4.05	1.87	1.45	0.727	0.776	0.675	0.732	0.798	0.951
HQ	2.40	11.0	14.6	16.8	17.7	8.41	3.88	4.56	1.32	1.48	1.09	1.49	1.39	2.31
Tag	22.	17.	22.	8.	11.	1.	1.	1.	7.	31.	1.	30.	13.	18.
h_N mm	44	66	27	43	50	41	62	32	21	97	14	39	36	31
h_A mm	5	11	13	21	23	18	8	6	3	4	3	3	3	4

	1961/2006 (46 Jahre)													
Jahr	1964	1969	1970	1983	1963	1991	1991	2000	2000	1989	1995	1964	1964	1969
NQ	0.380	0.160	0.140	0.480	0.490	0.976	0.725	0.525	0.465	0.317	0.278	0.430	0.380	0.160
MNQ	1.22	1.56	2.01	2.43	2.68	2.55	1.58	1.19	0.962	0.845	0.853	0.960	1.19	1.47
MQ	2.43	4.05	5.31	5.54	6.20	4.84	2.86	2.18	1.63	1.48	1.26	1.44	2.33	3.82
MHQ	7.81	13.6	16.5	15.8	19.1	12.0	9.29	7.83	5.31	5.42	3.55	4.32	7.43	13.0
HQ	28.9	50.3	60.3	47.2	61.7	50.9	32.4	44.4	42.7	23.9	13.0	37.0	28.9	50.3
Jahr	1998	1986	2003	1970	1979	1994	1961	1961	2002	2002	1981	1998	1998	1986
Mh_N mm	52	59	51	42	50	48	56	68	66	67	48	46	52	57
Mh_A mm	11	18	24	23	28	21	13	10	7	7	6	7	10	17

Abflußjahr (*) 2006

	Jahr	Datum	Winter	Sommer
NQ m³/s	0.566	am 26.09.2006	0.837	0.566
MQ m³/s	2.24		3.46	1.04
HQ m³/s	17.7	am 11.03.2006 bei W= 210 cm	17.7	4.56
Nq l/(skm²)	0.956		1.41	0.956
Mq l/(skm²)	3.78		5.84	1.76
Hq l/(skm²)	29.9		29.9	7.70
h_N mm	536		271	265
h_A mm	119		91	28

Kalenderjahr 2006

	Jahr	Datum
NQ m³/s	0.566	am 26.09.2006
MQ m³/s	2.09	
HQ m³/s	17.7	am 11.03.2006 bei W= 210 cm
Nq l/(skm²)	0.956	
Mq l/(skm²)	3.53	
Hq l/(skm²)	29.9	
h_N mm	493	
h_A mm	111	

	1961/2006 (*) 46 Jahre				1961/2006	
	Jahr	Datum	Winter	Sommer	Jahr	Datum
NQ m³/s	0.140	am 10.01.1970	0.140	0.278	0.140	am 10.01.1970
MNQ m³/s	0.640		1.02	0.721	0.668	
MQ m³/s	3.26		4.73	1.81	3.23	
MHQ m³/s	28.6		27.3	13.2	29.5	
HQ m³/s	61.7	am 04.03.1979 bei W= 335 cm	61.7	44.4	61.7	am 04.03.1979 bei W= 335 cm
HQ_1 m³/s						
HQ_5 m³/s						
MNq l/(skm²)	1.08		1.72	1.22	1.13	
Mq l/(skm²)	5.51		7.99	3.06	5.46	
MHq l/(skm²)	48.3		46.1	22.3	49.8	
Mh_N mm	652		302	350	650	
Mh_A mm	174		125	49	172	

Dauertabelle

Unterschreitungsdauer in Tagen	Abflußjahr (*) 2006	Kalenderjahr 2006	1961/2006 (46 Kalenderjahre) Obere Hüllwerte	Mittlere Werte	Untere Hüllwerte
	Unterschrittene Abflüsse m³/s				
(365)					
364	14.0	14.0	57.9	29.2	6.44
363	13.6	13.6	51.3	24.2	6.00
362	12.8	12.8	49.0	21.6	5.62
361	12.1	12.1	49.0	20.2	4.70
360	11.2	11.2	43.2	18.6	4.66
359	10.2	10.2	43.1	17.6	4.63
358	9.71	9.71	43.0	16.6	4.62
357	9.63	9.63	40.7	16.0	4.34
356	9.36	9.36	40.6	15.3	4.25
350	7.70	7.70	31.5	12.2	3.65
340	6.51	5.81	23.0	9.07	3.04
330	4.82	4.71	18.3	7.21	2.46
320	4.04	3.92	17.7	6.10	2.15
300	3.61	3.36	13.6	4.61	1.71
270	2.82	2.60	9.28	3.42	1.44
240	2.12	1.78	7.21	2.68	1.20
210	1.67	1.45	5.66	2.15	1.02
183	1.38	1.06	4.50	1.81	0.867
150	1.06	0.925	3.80	1.51	0.781
130	0.929	0.824	3.51	1.36	0.739
120	0.866	0.793	3.42	1.30	0.714
110	0.846	0.768	3.25	1.22	0.698
100	0.796	0.752	3.16	1.16	0.679
90	0.752	0.733	3.02	1.09	0.660
80	0.730	0.717	2.90	1.02	0.632
70	0.710	0.692	2.82	0.952	0.616
60	0.684	0.675	2.65	0.895	0.588
50	0.661	0.661	2.50	0.841	0.551
40	0.650	0.650	2.46	0.781	0.518
30	0.639	0.639	2.30	0.721	0.465
25	0.632	0.632	2.26	0.689	0.461
20	0.623	0.623	2.22	0.656	0.452
15	0.617	0.617	2.22	0.622	0.415
10	0.606	0.606	2.17	0.570	0.260
9	0.599	0.599	2.16	0.558	0.260
8	0.595	0.595	2.16	0.542	0.260
7	0.594	0.594	2.13	0.529	0.200
6	0.593	0.593	2.10	0.511	0.200
5	0.593	0.593	2.07	0.495	0.190
4	0.593	0.593	2.06	0.481	0.190
3	0.592	0.592	2.03	0.461	0.190
2	0.592	0.592	2.00	0.442	0.160
1	0.578	0.578	1.99	0.376	0.160
0	0.566	0.566	1.95	0.140	0.140

Extremwerte

	Niedrigwasser m³/s	Niedrigwasser l/(skm²)	Niedrigwasser Datum	Hochwasser m³/s	Hochwasser l/(skm²)	Hochwasser cm	Hochwasser Datum
1	0.140	0.236	10.01.1970	61.7	104	335	04.03.1979
2	0.278	0.470	01.09.1995	60.8	103	326	13.03.1981
3	0.317	0.535	22.08.1989	60.3	102	339	04.01.2003
4	0.330	0.557	02.08.1974	53.9	91.0	316	01.01.1987
5	0.335	0.566	07.09.2001	52.5	88.7	307	28.01.1994
6	0.340	0.574	09.09.1973	52.4	88.5	325	20.03.1970
7	0.350	0.591	15.09.1964	50.9	86.0	308	15.04.1994
8	0.369	0.623	06.09.2003	50.7	85.6	326	16.01.1968
9	0.374	0.632	13.08.1999	47.2	79.7	314	24.02.1970
10	0.375	0.633	22.09.1991	45.5	76.9	293	20.03.1994

(*) Abflußjahr: 1.11. des Vorjahres bis 31.10.
Repräsentativ für die Hydrologische Landschaft Ost-Braunschweig

NLWKN

Fig. A2: Primary values for the Harxbüttel gauge, hydrological year 2006 (NLWKN 2010, P.181).

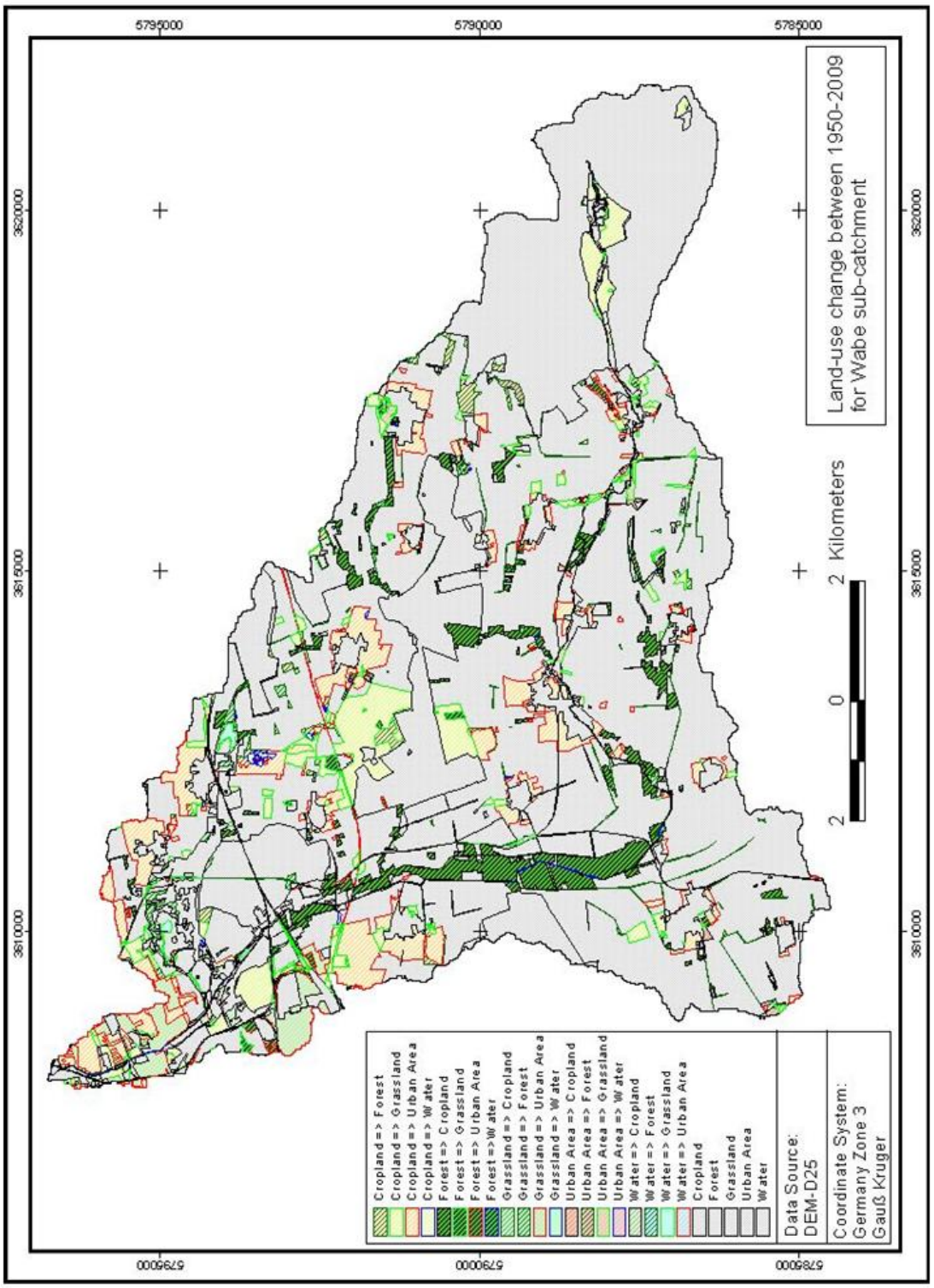

Fig. A 3: Land-use change between 1950-2009 for Wabe sub-catchment.

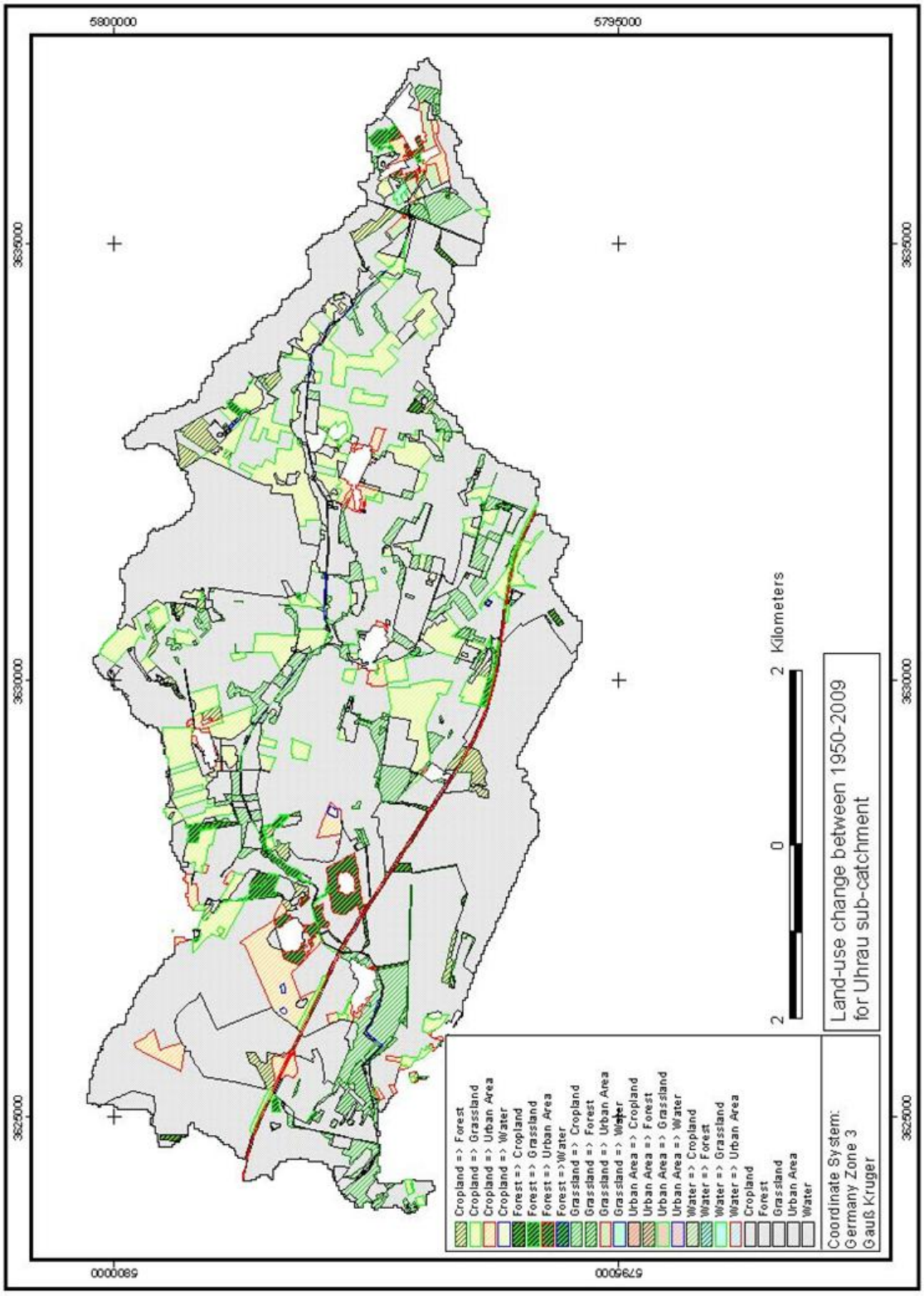

Fig. A4:Land-use change between 1950-2009 for Uhrau sub-catchment.

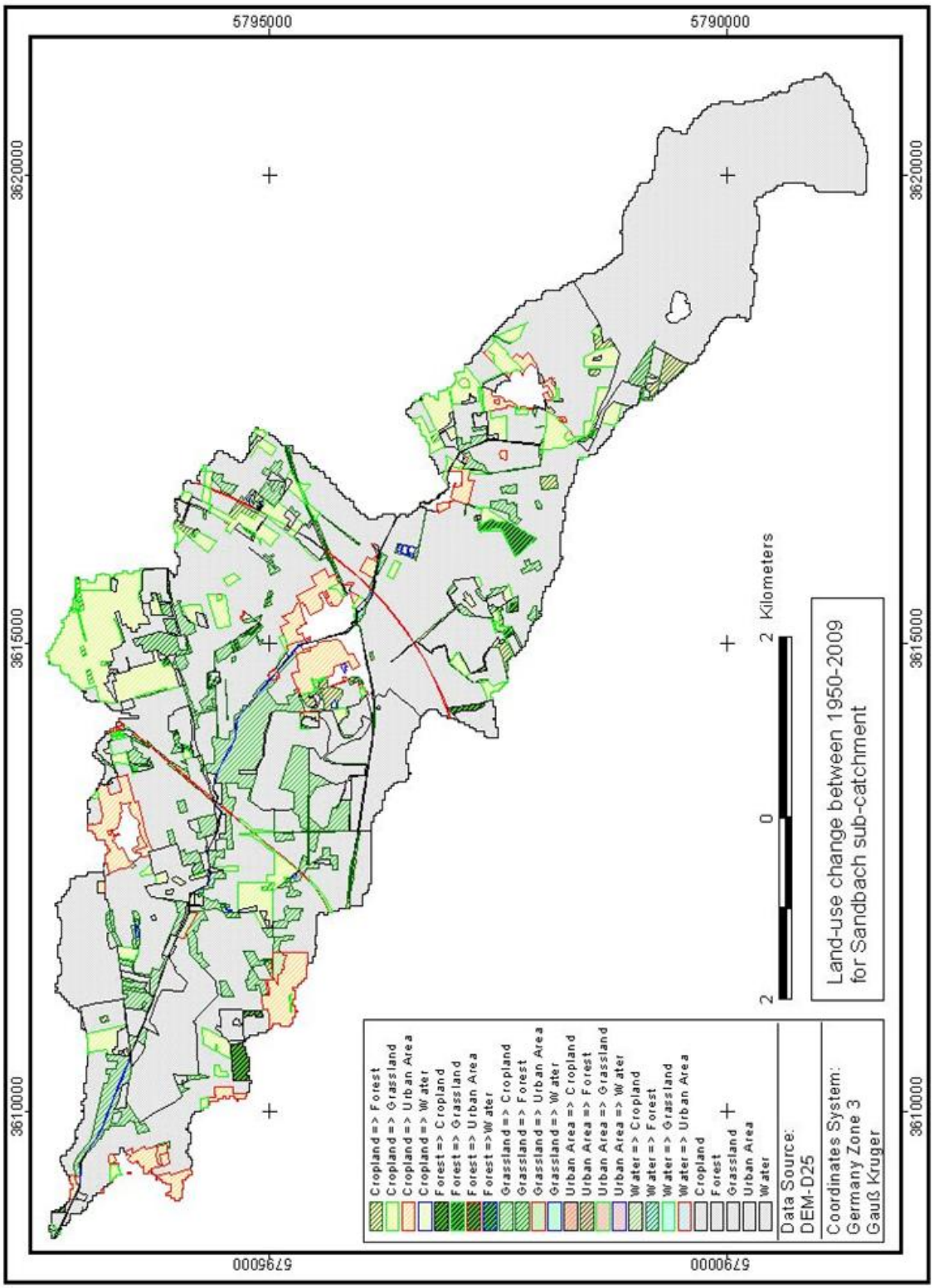

Fig. A5: Land-use change between 1950-2009 for the Sandbach Sub-catchment.

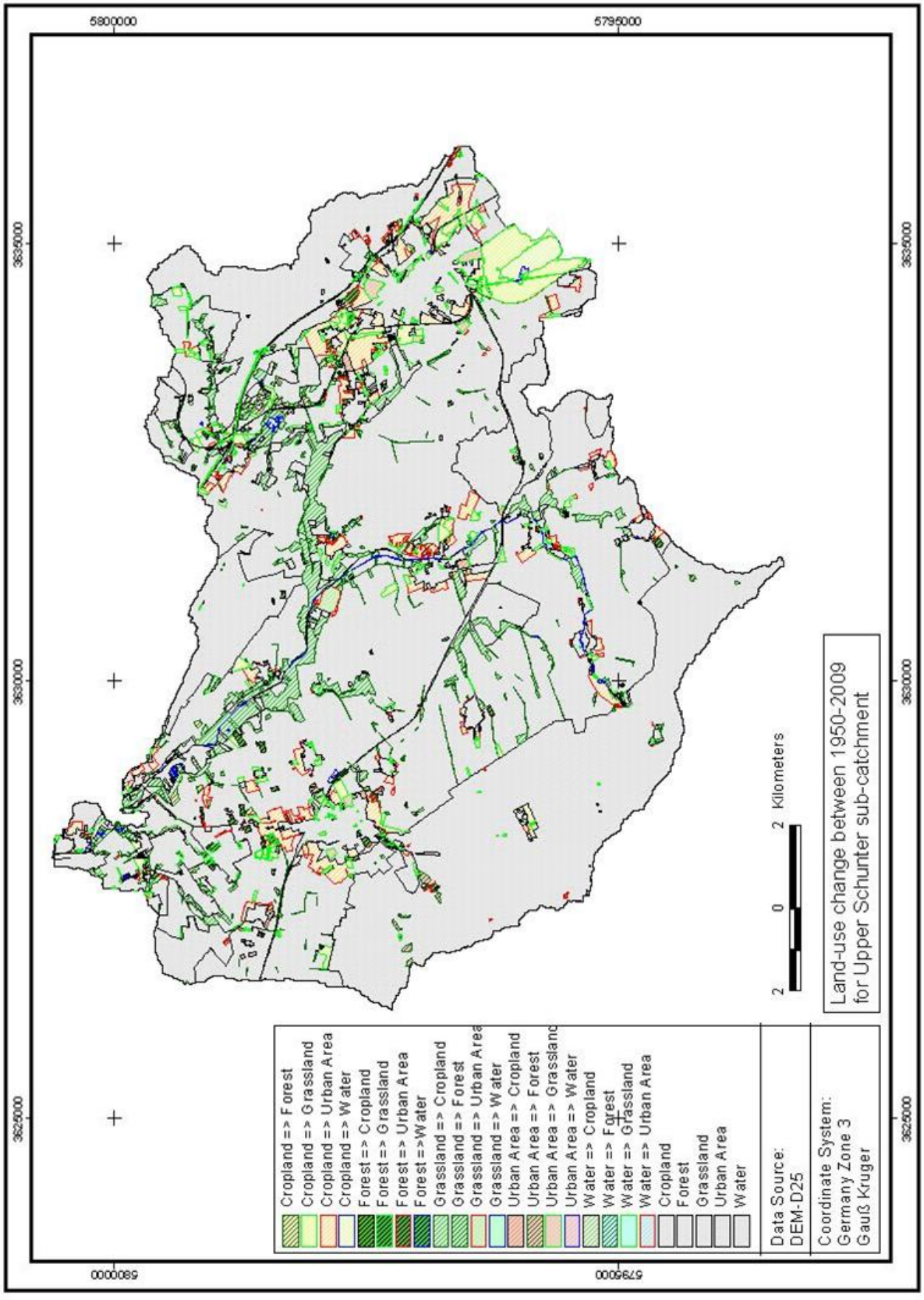

Fig. A6: Land-use change between 1950-2009 for Upper Schunter sub-catchment.

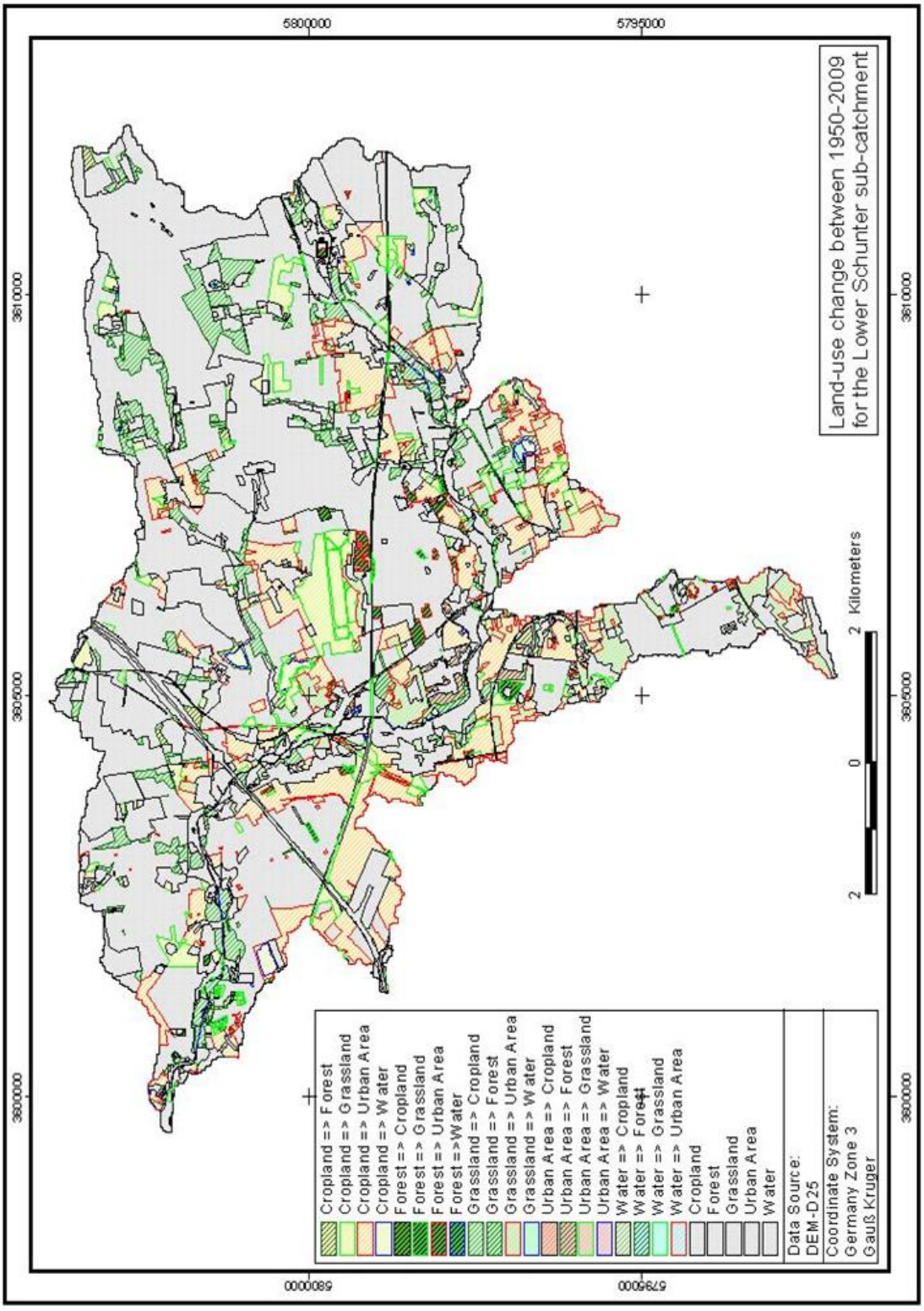

Fig. A7: Land-use change between 1950-2009 for the lower Schunter sub-catchment.

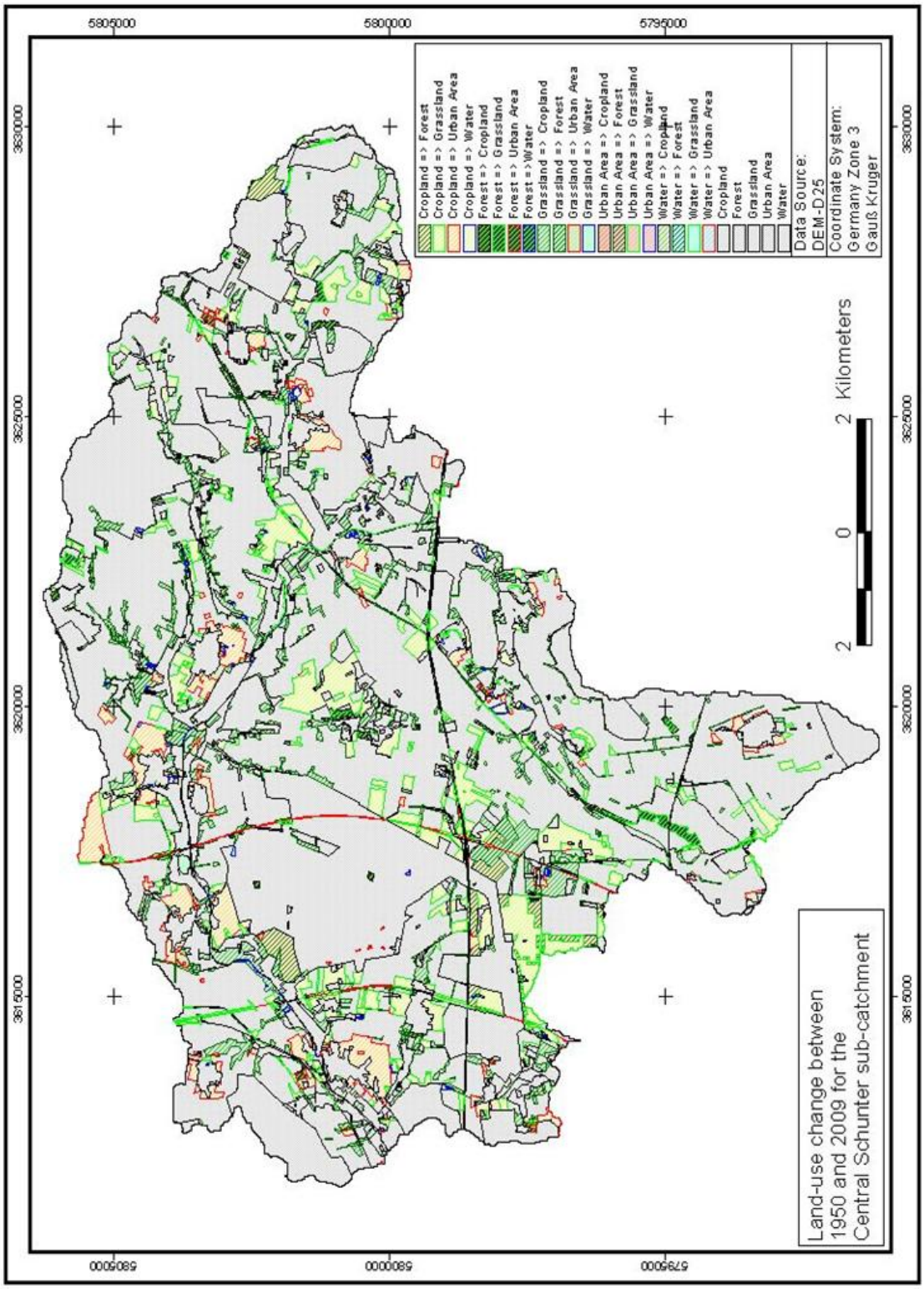

Fig. A8: Land-use change between 1950-2009 for the Central Schunter sub-catchment.

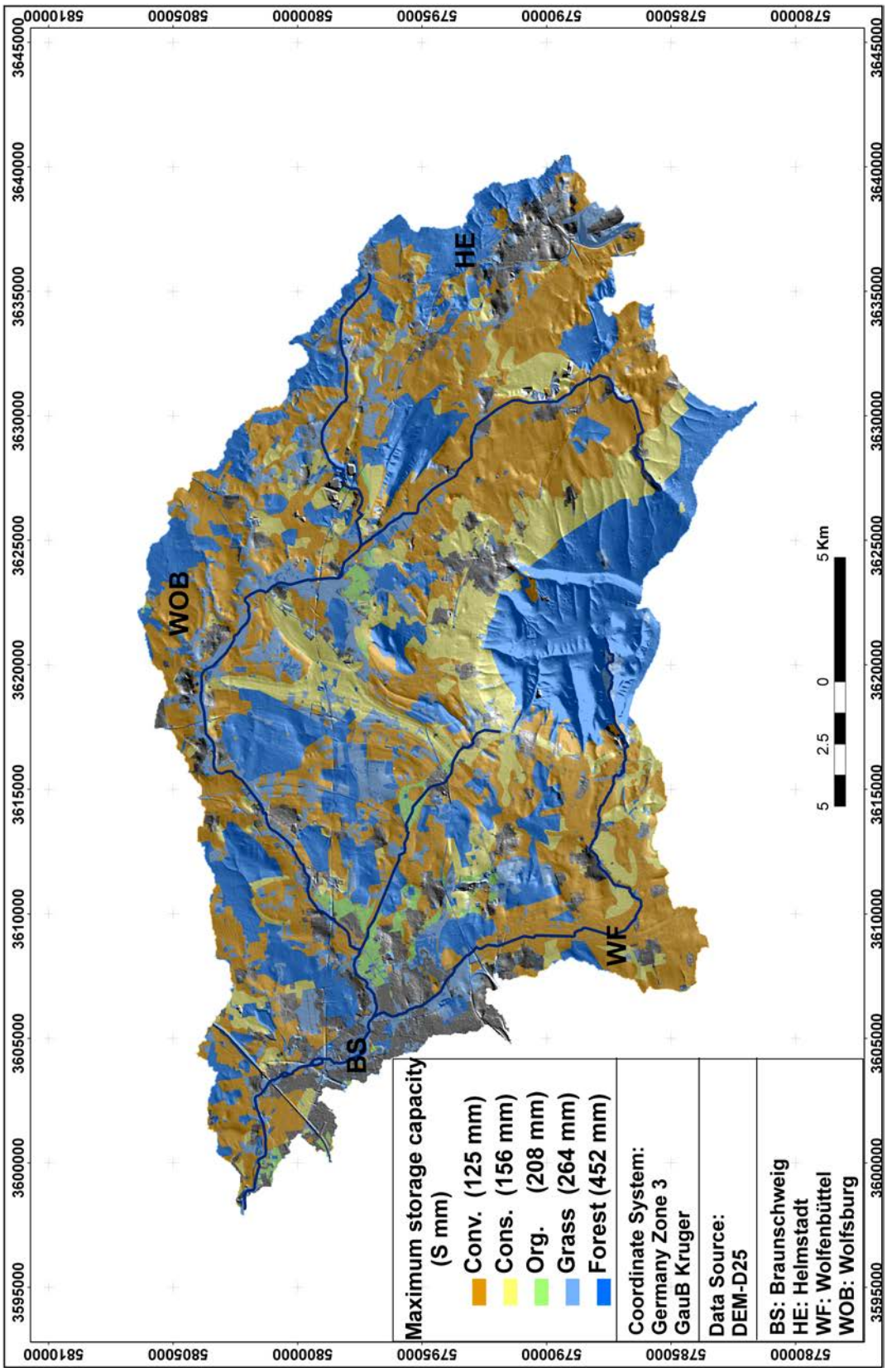

Fig. A9: The contribution of each land-use and land-management for the maximum storage capacity for the whole Schunter catchment.